Development of Methods allowing Correlation of *Dothistroma* and Dothistromin *In Planta*

A thesis presented in partial fulfilment of the
requirements for the degree of

Master of Science

in

Biochemistry

at Massey University, Manawatu,
New Zealand

Timothy J. Owen

2010

Abstract

Dothistroma septosporum is a fungal pathogen of pines with a worldwide distribution. It is responsible for the disease red band needle blight, in which necrotic lesions appear on infected needles. The red colour of the disease is due to the presence of the mycotoxin dothistromin. This toxin is structurally related to the better characterised mycotoxins aflatoxin and sterigmatocystin. The function of these toxins is unknown, but dothistromin is hypothesised to act as a competition factor. While much work has been done on *D. septosporum* and dothistromin in broth culture, *in planta* work has been limited by the methods available.

This work focused first on the development of a method for the reliable and high yield extraction of DNA from infected lesions, as previously used methods were found to be inadequate. It was found that the addition of an enzyme lysis step to the Qiagen DNeasy protocol and the replacement of its column purification with chloroform purification gave a greatly increased yield of DNA with an acceptable loss of purity.

To allow quantification of dothistromin from the same lesion samples, previously used assay systems were optimised and compared in their accuracy and sensitivity. An HPLC-fluorescence method was found most effective, and was able to accurately quantify dothistromin at single lesion quantities.

The developed methods were used to give a correlation between *Dothistroma* biomass and dothistromin in lesions at various stages of development. While this correlation was not found to be statistically significant, continuation of this work should allow valid conclusions to be drawn.

To give insight into the evolution of dothistromin biosynthesis, the genomes of other dothideomycetes were examined for the presence of dothistromin biosynthesis gene homologs. While no homologs were conclusively identified, a number of genes were shown to have similarity to known toxin biosynthesis genes.

In summary, while not all research hypotheses were able to be proven or disproven, this work sets a firm basis for future investigation in these areas using the methods developed, and strongly suggests the direction continued study should take.

Acknowledgements

First and foremost, my sincere thanks to my supervisor, Rosie Bradshaw, not only for giving so much guidance and support in my work, but also for putting up with my constant misuse of the word ‘significantly’.

Thank you to Rose Motion, for giving up so much of your time to help me with the chemistry side of things, of which I still know far too little about.

Thank you to the past and present members of the Fungal Jungle who have been so helpful; Carole, for always knowing where everything is, especially if it’s right in front of me; Arne, for pointing me in the right direction; Rebecca, for running the real time PCR and always having such good advice; Shuguang, for showing me through the methods; Melissa, for showing that there is light at the end of the tunnel; Kabir, for all his help with the pine seedling work; and to Adam, Shuiying, Yanfei, and Pranav for answering my mostly inane questions.

Thank you to everyone from IMBS for being so friendly and so willing to give up your time to help someone else. Unfortunately there is no way I can name all of you!

Thanks to Robert and Rex for giving me excellent advice on working with dothistromin. It was a privilege to have benefit of such experience. Thanks to Karl and Scott of AgResearch for the MS work.

More personally, thanks Kerry for being amazing, and thanks Mum and Dad for all the support.

Table of Contents

List of figures

List of tables

Chapter 1: Introduction

1.1 History, hosts, and geographic range

Dothistroma species are fungal pathogens of pines with a worldwide distribution. Infection results in development of red band needle blight, in which needles develop red necrotic lesions. This red colour is caused by the presence of the toxic secondary metabolite dothistromin. Red band needle blight can cause needle loss, growth retardation, and, in severe cases, the death of affected trees (Woods, Coates et al. 2005). While *Dothistroma* blight was initially identified in Europe in 1911, it was first recognised as a serious disease of pines in 1957, when plantations in the region now known as Tanzania (then Tanganyika) were affected. The disease was not initially attributed to *Dothistroma*, and only after later, more significant, incidents was *Dothistroma* identified as the cause (Gibson 1972). In 1964 *Dothistroma* blight symptoms were identified in plants located in Chile and New Zealand, both countries having a sizeable forestry industry. It is thought that the disease had most likely been occurring at lower levels for several years prior to this (Gibson 1972). Subsequent to these initial outbreaks, the disease has been successfully controlled in New Zealand by the use of copper based antifungal agents. Control using antifungal agents is a cost effective solution since the fungus does not usually affect mature *Pinus radiata* plants, meaning only immature plants require spraying (*P. radiata* being the most widely grown commercial species in New Zealand). Resistance to the disease varies between host species, but *P. radiata* is considered to be highly susceptible when compared to other pine species (Watt, Kriticos et al. 2009).

Recently, the disease has begun to affect pines in their native ranges, such as the lodgepole pines found in North America. Woods et al (2005) hypothesise that this is due to changes in weather conditions favourable to the spread of the disease, and that these changes are related to climate change. By mapping disease outbreaks against recorded weather patterns, increased rainfall was found to play a significant part in the increased occurrence of red band needle blight (Woods, Coates et al. 2005). Recent climate modelling has shown that the outbreaks of *Dothistroma* needle blight are limited in location more by the climate specificity of host species than that of the pathogen. While large areas around the world possess optimal climates for disease outbreak, some areas

have not seen any serious occurence of red band needle blight. The authors suggest that this may be due to disease resistance of potential host species in these areas. While it is possible that these areas have not been exposed to *Dothistroma* species, the ability of the disease to disperse over long distances through a variety of mechanisms makes this unlikely (Watt, Kriticos et al. 2009).

1.2 Identification, differentiation, and DNA extraction

Initial classification of *Dothistroma* species was complicated (Gibson 1972), and the current division into species *D. pini* and *D. septosporum* based on phylogenetics is relatively recent (Barnes, Crous et al. 2004). The two species mostly vary in geographic range, but show very little physical difference, with only a small variation in conidial width differentiating them. Molecular methods are usually required to distinguish the species (Barnes, Kirisits et al. 2008). A method developed by Barnes et al. (2004) allows differentiation based on PCR-RFLP patterns, caused by the presence of an *Alu*I restriction enzyme site in *D. pini* which is absent in *D. septosporum*. Other methods include PCR using species specific primers, or Real Time PCR differentiation based on melting curve analysis (McDougal, unpublished). Real time PCR can also be used to specifically quantify DNA from different *Dothistroma* species (Ioos, Fabre et al. 2010), and has been used to quantify biomass in related species (Keon, Antoniw et al. 2007).

The genetic material used in these tests can be extracted from infected plant tissue or from fungal cultures. Isolation of DNA requires, sequentially, the disruption of target cells, removal of contaminating compounds, and isolation of extracted DNA. While DNA extraction from fungal mycelia is relatively straightforward, the reliable extraction of DNA from infected needles is hampered by the presence of host tissue. Plant tissues in general are resistant to chemical disruption without prior physical breakdown. Because of this, most methods involve an initial physical disruption step, such as grinding with mortar and pestle under liquid nitrogen, which is designed to break down tissue and expose target cells. A chemical or enzymatic lysis step follows, mostly involving a strong detergent such as sodium dodecyl sulfate. Removal or vitiation of contaminants is accomplished by the addition of chemicals such as 2-mercaptoethanol (to disrupt enzymes) and polyvinylpyrrolidone (to adsorb polyphenols). Precipitated contaminants can be removed through centrifugation, and

further contaminants are mostly removed by extraction into chloroform or phenol, leaving relatively pure DNA. This can be precipitated, pelleted, and resuspended to a suitable concentration (Tsumura and Ohba 1993; Al-Samarrai and Schmid 2000; Barnes, Crous et al. 2004; Bearchell, Fraaije et al. 2005; Bradshaw 2006). Because plant material is generally plentiful, available plant extraction methods mostly concentrate on extraction from large (over one gram) samples, and sacrifice yield to obtain high purity DNA. This limits their effectiveness in extracting PCR-quality DNA from smaller samples.

1.3 The chemistry and biosynthesis of dothistromin

Dothistromin is a bright red difuroanthraquinone produced by species of *Dothisotroma* and *Cercospora* (Stoessl 1984). It was first identified as a secondary metabolite of *Dothistroma* species in 1970 (Bassett, Buchanan et al. 1970). The structure of dothistromin was found to be similar to that of mycotoxins produced by other fungi. It bears a particular resemblance to versicolorin B, a precursor to both sterigmatocystin and aflatoxin (Fig. 1.1).

Fig. 1.1: Dothistromin and related secondary metabolites

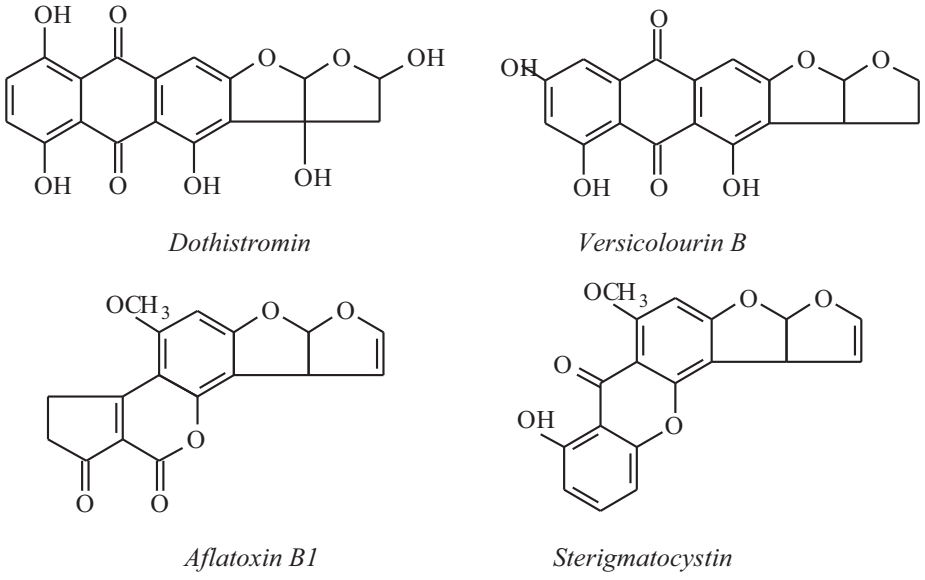

These compounds are both toxic and carcinogenic; aflatoxin being well known for its potent carcinogenicity. Due to the ecological niches of their producer organisms (for example infection of peanuts (*Arachis hypogaea)* by *Aspergillus flavus* (Hesseltine,

Shotwell et al. 1966)) aflatoxin and sterigmatocystin are potential commercial and consumer hazards. Consequently, these toxins are relatively well characterised in comparison to dothistromin. This has enabled the characterisation of dothistromin biosynthesis based on shared characteristics with these toxins.

The genes encoding aflatoxin and sterigmatocystin biosynthetic pathways occur in clusters, centred on a polyketide synthase gene. A polyketide synthase is involved in the initial formation of norsolorinic acid from acetate. A further 11 steps are required to synthesize sterigmatocystin, and a further 14 to synthesize aflatoxin (Yu, Chang et al. 2004; Weissman 2008). Gene clustering is a common feature of fungal secondary metabolite biosynthesis pathways (Keller and Hohn 1997). Sterigmatocystin biosynthesis genes in *Aspergillus nidulans* and aflatoxin biosynthesis genes in *Aspergillus parasiticus* are found in single clusters of around 70 kb (Ehrlich, Yu et al. 2005). The transfer of these biosynthesis clusters is thought to be vertical, as opposed to horizontal. This is indicated by the presence of gene duplicates throughout genomes of sequenced *Aspergillus* species (Carbone, Ramirez-Prado et al. 2007).

Because of both its similarity to versicolorin B and early work showing similar backbone carbon incorporation (Shaw, Chick et al. 1978), the biosynthetic pathway of dothistromin was predicted to share components with those of aflatoxin and sterigmatocystin. Dothistromin biosynthesis genes were initially located by hybridisation of probes based on aflatoxin synthesis genes (Bradshaw, Bhatnagar et al. 2002). In contrast to the large, single clusters found in *A. parasiticus* and *A. nidulans*, dothistromin biosynthesis genes in *D. septosporum* were found to reside in three separate mini-clusters (Zhang, Schwelm et al. 2007). Genes located within these clusters show significant sequence similarity to those found in *A. nidulans* and *A. parasiticus* sterigmatocystin and aflatoxin clusters. Some gene function has been confirmed by gene knockouts (Bradshaw, Bhatnagar et al. 2002; Bradshaw, Jin et al. 2006; Zhang, Schwelm et al. 2007). More recently, preliminary genomic data has allowed the tentative identification of further biosynthesis gene homologs in *D. septosporum*. These homologs are distributed in several ‘mini-clusters’ dispersed over the length of a 1.3 Mb chromosome. It is not known if the dothistromin biosynthesis genes are conserved within the Dothideomycetes class of fungi, but investigation of this could shed light on the evolutionary history of dothistromin biosynthesis.

1.4 Dothistromin as a mycotoxin

Dothistromin is both toxic and mutagenic. It acts as a catalyst in the production of harmful radicals from oxygen, leading to oxidative stress in affected organisms. This is thought to be achieved by the diaphorase enzyme NADPH-cytochrome c-(ferredoxin)-oxidoreductase, which reduces the ketone groups of the quinone moiety of dothistromin to hydroxyl groups, yielding a hydroquinone moiety. This is known as the activated form. In the presence of oxygen this activated intermediate autoxidates, producing superoxide and returning the dothistromin molecule to its original state. The superoxide produced is able to dismutate to hydrogen peroxide.

Fig. 1.2 Production of oxygen radicals by dothistromin

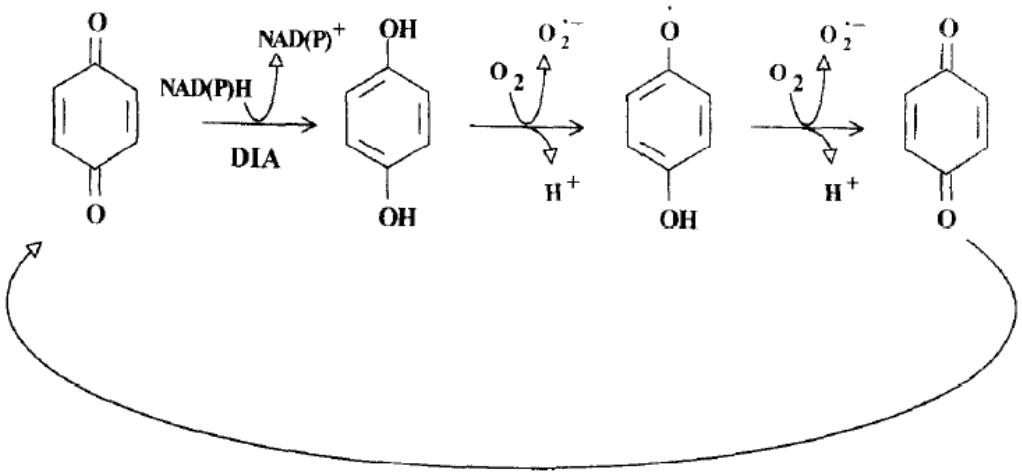

Oxidation of NAD(P)H by a diaphorase (DIA) drives reduction of dothistromin ketone groups, allowing production of oxygen radicals.
(Reproduced from Heiser, Osswald et al. 1998)

While harmful on its own, hydrogen peroxide can be further reduced by activated dothistromin, producing hydroxyl radicals (Youngman and Elstner 1984; Heiser, Osswald et al. 1998). While many cells have mechanisms to deal with oxygen radicals, which are routinely produced as a by-product of oxidative metabolism, these mechanisms can become overloaded, resulting in the oxidation of cellular components. This is known as oxidative stress.

Diaphorases are ubiquitous, giving dothistromin a broad toxicity. This toxicity has been demonstrated on a number of organisms, including *P. radiata*, brine shrimp, molluscs, beetroot, and a variety of microorganisms (Stoessl, Abramowski et al. 1990;

Jones, Harvey et al. 1995). Mutagenic effects of dothistromin have been shown in human cells. Chromosome damage caused by dothistromin was found to be less severe than that caused by aflatoxin B_1, but is sufficient for weak carcinogenic activity. The level of dothistromin required for mutagenesis was found to be very close to that which results in cell death. Because of this it has been suggested that any mutagenic effects of dothistromin would be masked by its toxicity (Ferguson, Parslow et al. 1986). Toxicity in some organisms displays a strong dependency on light. This could indicate that dothistromin possesses photosensitising properties, however a mechanism of light dependent toxicity has not been determined (Youngman and Elstner 1984; Stoessl, Abramowski et al. 1990). Despite this, *Dothistroma* infection has been shown to be positively influenced by increased light intensity.

Of lesser concern are the toxic properties of other *Dothistroma* metabolites. Because of dothistromin's chemical similarity to versicolorin B, its synthesis pathway is thought to be similar to that of these mycotoxins. Precursors of aflatoxin and sterigmatocystin include norsolorinic acid, averantin, and averufin. Of these compounds only averantin displays mutagenicity, and none demonstrate toxicity at levels comparable to aflatoxin or sterigmatocystin (Dunn, Lee et al. 1982). Based on this, the toxicity and mutagenicity of dothistromin precursors are also likely to be negligible.

1.5 The biological role of dothistromin

The role dothistromin plays *in vivo* has not been conclusively resolved. A time course of dothistromin production by *D. septosporum* in broth culture (Schwelm, Barron et al. 2008) shows production of dothistromin to be highest during early logarithmic phase (as seen in Fig 1.3).

Fig. 1.3: Early production of dothistromin

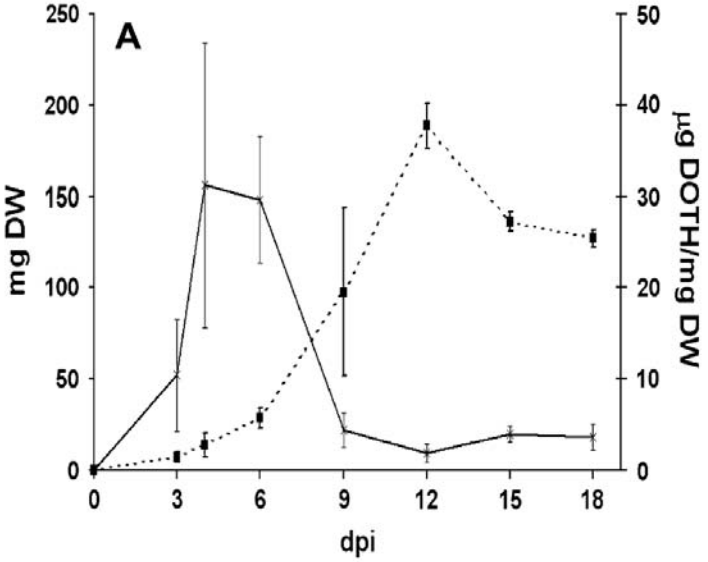

Solid-line: Graph of dothistromin per Dothistroma weight in broth culture, showing peak production during early log. phase. Dashed-line: Growth curve of Dothistroma culture, measured by dry weight of mycelia.

(Reproduced from Schwelm, Barron et al, 2008)

In contrast, aflatoxin and sterigmatocystin are produced during the late exponential and stationary phase (Park and Bullerman 1981; Schwelm, Barron et al. 2008). The biological roles of these mycotoxins are also unknown, though it has been hypothesized that they are produced as a response to oxidative stress (Reverberi, Ricelli et al. 2010).

It was originally thought that dothistromin acts as a pathogenicity factor, and was responsible for disease symptoms. This hypothesis was supported by the observation that the injection of purified dothistromin into pine needles induces the formation of the necrotic lesions characteristic of red-band needle blight (Shain and Franich 1981). Despite its ability to induce lesion formation, subsequent experiments showed that the majority of injected dothistromin was degraded prior to full lesion extension. Additionally, more recent work has shown that dothistromin-deficient mutants retain their pathogenicity. Seedlings inoculated with dothistromin-producing and dothistromin-null strains of *D. septosporum* showed no statistically significant difference in the percentage of needles infected (Schwelm, Barron et al. 2009). Therefore, dothistromin is not required for pathogenicity. Lesion formation is now thought to occur as a result of benzoic acid production by the plant host, possibly in

response to the presence of some elicitor derived from *Dothistroma* (Franich, Carson et al. 1986).

Dothistromin was also shown to inhibit the growth of several potential fungal competitors (Schwelm, Barron et al. 2009). This has led to the current hypothesis that dothistromin is produced as a competition factor. The biosynthesis of dothistromin during early log phase may inhibit the growth of competing microorganisms in the necrotic needle lesion environment. The closely related fungus *Mycosphaerella graminicola* undergoes a latent phase prior to rapid growth and concomitant programmed cell death of the plant host cells (PCD). Induction of PCD, presumably by elicitors from the fungus, causes localised cell death, creating a nutrient rich environment for fungal growth (Keon, Antoniw et al. 2007). It is thought that *D. septosporum* may follow a similar mode of growth; this would correspond well with the competition factor hypothesis. Investigation of this hypothesis and the mode of growth of *D. septosorum* requires more *in planta* study.

1.6 Purification and quantification of dothistromin

Determining the role of dothistromin *in planta* requires measuring its production in the needle. To do this a sensitive and reliable assay technique is needed, but currently available methods have limitations in this regard. Previous work on purification and quantification of dothistromin was attempted for a multitude of other reasons for which sensitivity at low concentrations was not so critical. Dothistromin's interesting chemistry initially inspired investigation into its structure, and later its similarity to aflatoxin provoked inquiry into its toxicity and biochemistry. More recently work has been carried out on the genes and regulatory aspects responsible for its production. A range of increasingly refined purification and quantification protocols have been developed to support this work.

Most quantitative assays involve an initial crude extraction of the toxin, followed by the use of a more selective resolution method before quantification can be made. Prior to running through most separation systems crude samples must undergo one or more pre-purification steps to remove dissimilar contaminating compounds. Solvent extraction is a simple and reliable technique (Zhang, personal communication; Franich personal communication), although other methods such as column

chromatography can be used (Schuster, Marx et al. 1992). Solvent extraction involves the mixture of a liquid sample with a non-miscible solvent in which the molecule of interest is more soluble. Ethyl acetate is a common solvent for extraction of dothistromin, but other solvents such as chloroform have been used successfully (Zhang, personal communication). Extraction solvents are usually acidified to prevent ionisation of the dothistromin molecule (Franich 1981).

Separation of dothistromin from more closely related secondary metabolites of *Dothistroma* and contaminating plant compounds has historically proven difficult. These metabolites can be very similar in structure; for example deoxydothistromin differs from dothistromin by a single hydroxyl group. These two molecules were initially separated using a counter current distribution system (Gallagher 1971). This method was time consuming, and has since been superseded by thin layer chromatography (TLC) and high performance liquid chromatography (HPLC). TLC and HPLC can be either normal phase, where the stationary phase is more polar than the mobile phase, or reversed phase, where the stationary phase is less polar than the mobile phase. Reversed phase methods are more commonly used both in separation of dothistromin and in general.

TLC methods have been mostly superseded by HPLC, but are capable of providing comparable results. The ability of TLC systems to separate dothistromin from contaminants varies, with plant-derived chlorophyllic and phenolic contaminants being particularly problematic. One example of a normal-phase TLC system used for dothistromin uses silica as the stationary phase and a mobile phase of 1:1 ethyl acetate-dichloromethane acidified with 4% formic acid (Franich 1981). An example of a reverse-phase system is that developed by R. F. Franich, which uses the same silica stationary phase, but a 2:1 methanol:water mobile phase. This system was developed because of inadequate resolution when using the previous method with green plant tissue (Franich 1981). Because of the fluorescent properties of the dothistromin molecule fluorescence densitometry is often used to quantify dothistromin from TLC separated samples. Fluorescence densitometry allows quantification of a compound based on the size and intensity of fluorescence of a TLC spot. Detection of as little as 10 ng of dothistromin has been achieved, but this is unlikely to represent the lower limit. The error in quantification by this method has been calculated at around 10% (Franich 1981).

HPLC is a more modern technique than TLC, and is able to give far better resolution with shorter separation times than TLC (Frisvad and Thrane 1987; Schuster, Marx et al. 1992). HPLC results are also less operator dependent, meaning that quantification will be more consistent between assays. For these reasons HPLC has become the more widely used system for quantification of aflatoxins, especially for routine testing (Frisvad and Thrane 1987; Schuster, Marx et al. 1992; Chiavaro, Dall'Asta et al. 2001; Takino and Tanaka 2008; Senyuva, Gilbert et al. 2010). HPLC does have the disadvantage of being more expensive than TLC, and HPLC methods have not been extensively used for dothistromin separation or quantification (Debnam and Quach).

Quantification in liquid chromatography systems is simplified by the fact that they can connect directly to inline assay instruments. This allows quantification of the toxin to be performed in real time. Assay systems which can be used inline include fluorescence detection, ultra violet-visible absorption (UV-VIS), and electrospray ionisation mass spectrometry (ESI-MS). Using mass spectrometry, extremely small quantities of a specific metabolite can be detected (Schuster, Marx et al. 1992). Takino and Tanaka were able to detect as little as 20 picograms of aflatoxin B_1 or G_1 resuspended in 1 mL of solvent (Takino and Tanaka 2008). Despite these benefits, the expensive equipment required limits its availability and therefore its usefulness as a routine quantification technique. Fluorescence detection and UV-VIS absorption have lower sensitivity, but equipment is more readily available. Fluorescence is more sensitive than UV-VIS absorbance, with fluorescence based assays for aflatoxins able to detect as little as 1 ng (Schuster, Marx et al. 1992). While not as selective as ESI-MS, fluorescence detection is more selective than UV-VIS, meaning that incomplete separation is less likely to affect quantification.

Enzyme-linked immunosorbent assay (ELISA) is a quantification technique which does not require prior separation of the target molecule. These assays involve the use of antibodies which bind specifically to the dothistromin molecule. Because of this specificity they require less preparatory separation than spectrometry-based assays (Bradshaw, Ganley et al. 2000). ELISA based methods give higher sensitivity than fluorescence densitometry, with considerably lower limits of detection. Lower limits of quantification have been estimated to be around 300 pg (Jones, Harvey et al. 1993). Additionally, the range of detection given by use of this method is slightly greater than that seen with fluorescence densitometry. Unfortunately the labelled anti-dothistromin

antibodies currently used for dothistromin ELISA were donated by HortResearch, and once these stocks have been depleted obtaining more will not be cost effective. Previous work using a competitive ELISA for dothistromin has encountered difficulties, including high variability (see Fig 1.3) and the time consuming nature of the assay.

While these methods can be compared on paper, determining the practical differences between them will require hands-on testing. Most have mainly been used for quantification of dothistromin from broth culture, and are untested on single lesion quantities of dothistromin. Additionally, improvement and modernisation of the equipment used may have rendered much of the quantitative testing previously performed invalid. Whether these methods are sensitive and accurate enough to give a reliable picture of dothistromin production *in planta* remains to be determined.

1.7 Research hypotheses

1) Methods can be developed to allow high yield extraction of PCR-amplifiable *Dothistroma* DNA from single needle lesions.
2) Systems can be developed to allow accurate quantification of dothistromin from the same *Dothistroma* lesions.
3) Dothistromin levels relative to *Dothistroma* biomass will be highest in early stage lesions.
4) Dothideomycete fungi closely related to *D. septosporum* contain homologs of dothistromin biosynthesis genes.

1.8 Aims and Objectives

1) Develop DNA extraction methods to allow reliable extraction of PCR-amplifiable DNA from single lesions.
    a. Develop a high yield DNA extraction system using larger uninfected pine needle samples.
    b. Optimize previously developed system for lesion size samples.
    c. Test system on single *Dothistroma* needle lesions, herbarium specimens, and fungal mycelia.
2) Develop methods to allow quantification of dothistrom from single *Dothistroma* lesions.
    a. Optimize dothistromin solvent extraction protocols.
    b. Optimize, then compare, previously developed methods for dothistromin quantification to find the most effective technique for quantification of dothistromin from single lesions.
3) Use developed methods to compare *Dothistroma* biomass with dothistromin production *in planta*.
    a. Run a time course of *Dothistroma* lesion development using secondary infection of an inoculated seedling.
    b. Extract and quantify DNA from needle lesions using previously developed systems and quantitative real time PCR.
    c. Extract and quantify dothistromin from needle lesions using previously developed systems.
    d. Correlate dothistromin levels with *Dothistroma* biomass.

4) Use bioinformatic methods to search for dothistromin biosynthesis gene homologs in closely related organisms with sequenced genomes.
    a. Locate potential homologs of the *Dothistroma* PksA gene in other dothideomycete genomes.
    b. Narrow PksA homolog selection by proximity of other potential polyketide toxin biosynthesis gene homologs.
    c. Compare genes in selected putative clusters with known toxin biosynthesis genes.
    d. Use previously developed methods to assay *M. graminicola* for dothistromin production.

Chapter 2: Materials and Methods

2.1 DNA Extraction and Purification

2.1.1 DNA extraction; needles and fungal mycelia

Infected and uninfected pine needles used in DNA extraction experiments were harvested from Gordon Kear Forest (Linton, Palmerston North) in 2008, and stored in sealed bags at -20^{o}C until required. Dry herbarium specimen needles were kindly supplied by M. A. Dick and R. Tetenburg of Scion (Rotorua, New Zealand), and were stored at room temperature. Fungal mycelia (*Dothistroma septosporum NZE10)* for extraction were harvested from broth (methods 2.2.1) using vacuum filtration, freeze dried on Dura-Dry MP (FTS Systems, Stone Ridge, New York, USA), then stored at -20^{o}C until required.

2.1.2 Sampling and freeze drying

Infected needle samples were identified visually using an Olympus VMZ stereo microscope (Olympus Corporation, Tokyo, Japan), and cut with a scapel to measured 3 mm sections centered on a lesion. Measured lengths of uninfected needle were cut to the lengths required with scissors from the central needle section of green needles. Wet weights measured using a Mettler AC100 five-figure balance (Mettler-Toledo, Columbus, Ohio, USA). Needle samples were then placed in labelled, unsealed microcentrifuge tubes and freeze dried for 24 hours on a Dura-Dry MP at -85^{o}C and <100 mT. Dry weights of samples were then measured, if accurate measurement was possible. It has been noted in the text where accurate measurement was limited by the sensitivity of the scales. Microcentrifuge tubes containing dried samples were sealed and stored in a dessicator until required.

2.1.3 Grinding

Prior to extraction, samples were ground in microcentrifuge tubes using sterile micropestles. All grinding was done at low temperature by placing tubes in a rack immersed in a small ‘bath’ of liquid nitrogen. The evaporation rate of liquid nitrogen

was reduced by keeping the liquid nitrogen bath on ice. Samples were ground into as fine a powder as possible before any lysis buffer was added. For samples where glass beads were used, approximately 30 mg of sterile 40 mesh glass beads were added after initial grinding, and samples were further ground until homogenous. Lysis buffer from the initial DNA extraction step was then added, and grinding was continued if any large particles of sample were visible.

2.1.4 Qiagen DNeasy DNA extraction (Qiagen, Duesseldorf, Germany)

(As per steps 7-19 of Mini Protocol, paraphrased) For Qiagen DNeasy lysis, 400 µL of Qiagen Buffer AP1 and 4 µL RNase A (Invitrogen, Carlsbad, California, USA) were transferred into sample tubes after grinding, and mixed thoroughly. The sample tubes were then placed in a 65^{o}C waterbath and incubated for 10 minutes, mixing by inversion several times. 130 µL of Qiagen Buffer AP2 was added, and samples were mixed then kept on ice for 5 minutes. Samples were then centrifuged at 20,000 g for 5 minutes in a Heraeus Pico 17 microcentrifuge (Thermo-Fisher Scientific, Waltham, Massachusetts, USA) to remove cell debris (and glass beads, if used).

For Qiagen DNeasy purification the supernatant, including non-pelleted cell debris, was then transferred to labelled Qiagen QIAshredder Mini columns and centrifuged for 2 minutes at 20,000 g. The supernatant of the flow-through fraction was transferred to a new, labelled microcentrifuge tube, with care taken not to disturb the pellets. Qiagen Buffer AP3/E was added at 1.5 times the volume of supernatant and samples were mixed by pipetting. 650 µL of each sample mixture was added to a Qiagen DNeasy Mini spin column and centrifuged at 6000 g for one minute. The flow through fraction was discarded and the process was repeated with the remaining sample mixture. The columns were then placed in new collection tubes, 500 µL of Qiagen Buffer AW was added, and they were centrifuged for 1 minute at 6000 g. Another 500 µL of Buffer AW was added and they were spun at 20,000 g for a further 2 minutes. The columns were then placed in a new microcentrifuge tube, and 100 µL of Buffer AE was added to each membrane, incubated for 5 minutes, then centrifuged for 1 minute at 6000 g. This was repeated to elute a complete volume of 200 µL. Samples were then stored at 4^{o}C. For 1 cm needle samples volumes used were 200 µL AP1, 90 µL AP2, and for 3 mm samples volumes were 100 µL AP1, 45 µL AP2.

2.1.5 Nucleon Phytopure DNA extraction (GE Healthcare, Little Chalfont, United Kingdom)

*(As per steps 4-22 of Nucleon Phytopure small sample protocol, paraphrased, and with modifications in **bold**)* For Phytopure lysis, 600 µL of Reagent 1 **and 4 µL of RNase A (Invitrogen)** was added to samples after grinding, and mixed thoroughly. 200 µL of Reagent 2 was then added to the samples, which were mixed until homogenous. The tubes were then incubated at 65°C for 10 minutes with regular mixing, before placing them on ice for 20 minutes. The samples were then removed from the ice and **centrifuged at 20,000 g for 5 minutes** in a Heraeus Pico 17 microcentrifuge (Thermo-Fisher Scientific, Waltham, Massachusetts, USA) to remove cell debris (and glass beads, if used).

For Phytopure purification, 500 µL of ice cold chloroform was added to samples following extraction, followed by 100 µL of Nucleon Phytopure resin suspension. The samples were placed on a shaker for 10 minutes, then centrifuged at 1300 g for a further 10 minutes. The upper layer was transferred to a fresh tube, while avoiding disturbing the resin layer. An equal volume of cold isopropanol was added this tube and mixed by inversion. The samples were then centrifuged at 4000 g for 5 minutes to pellet DNA, and pellets were washed with cold 70% ethanol. The DNA was repelleted with an additional 4000 g, 5 minute centrifugation. The pellets were then air dried, resuspended in 20 µL of TE buffer, and stored at 4°C.

2.1.6 Combined DNA extraction method

For DNA extraction using a combination of Qiagen lysis and Phytopure chloroform purifcation, the supernatant of the first centrifugation in the Qiagen protocol was added to 500 µL of chloroform and 100 µL Phytopure resin suspension, and the Phytopure purification was continued from that point (steps 1-4 above of the original Qiagen DNeasy Mini protocol, and then steps 5-10 of the original Phytopure protocol). Chloroform extraction only was the same as that for use of the Phytopure kit, except without the addition of resin suspension. For the final method 100 µL 5x TE buffer was added instead of 100 µL Phytopure resin.

2.1.7 Glucanex enzyme incubation

Glucanex enzyme was prepared from Glucanex (Novozymes A/S, Bagsvaerd, Denmark) at 10 mg/mL in CTAB buffer (2% CTAB, 1% PVP40, 1.4 M NaCl, 20 mM

EDTA, 0.1 M Tris/HCl, pH adjusted to 8). Glucanex enzyme solution was added to samples immediately after 65°C incubation. For 3 cm needle sections 130 µL was added, for 1 cm sections 70 µL, and for 3 mm sections 35 µL. Samples were then incubated for 30 minutes in a 37°C waterbath.

2.1.8 Fastprep bead beater

For tests involving bead beating, this was run immediately after manual grinding (2.1.3), but prior to 65°C incubation. Samples and glass beads were transferred to compatible microcentrifuge tubes and placed on a Thermo-Savant Fastprep FP120 (Thermo Scientific) at maximum speed for one minute.

2.1.9 DNA Quantification

Purified DNA was quantified by absorbance at 260 nm. 1 µL of resuspended DNA was placed on a Nanodrop 1000 (Nanodrop Products, Wilmington, Delaware, USA). The $A_{260:280}$ ratio was recorded to give an estimate of DNA purity.

2.1.10 PCR Conditions

25 µL PCR reactions were used and contained 1 µL primer 1, 1 µL primer 2 (at 10 µM), 1 µL dNTP's (at 1.25 mM), 0.75 µL $MgCl_2$ (at 50 mM), 2.5 µL 10x PCR Buffer (Invitrogen), 0.2 µL Taq polymerase (Invitrogen), and 2 µL template, made up to 25 µL with MilliQ water. Target sequences were amplified using 34 cycles of 30 seconds denaturation at 94°C, 20 seconds annealing at 56°C, and 30 seconds extension at 72°C. This was preceded by 2 minutes at 94°C and followed by 2 minutes at 72°C. Thermal cycling was performed on an Eppendorf Mastercycler Gradient (Eppendorf, Hamburg, Germany) or a Corbett PC-960G (Corbett Research Pty Ltd, Sydney, Australia). For PCR trials with BSA, 1 µL of water in the reaction mix was substituted with a 5% w/v solution of BSA in MilliQ water.

Table 2.1: PCR Primers

Primer name	Sequence (5' to 3')	Target	Product (bp)
CAD 793	GGGATTGTAACAGAGATTGGTAG	*P. radiata*, CAD gene	200
CAD 973	ATACTGCTTGCAAATCCTCC		
ITS1	TCCGTAGGTGAACCTGCGG	Fungal ITS	~500
ITS4	TCCTCCGCTTATTGATATGC		
DPS ITS spec fwd	CTGAGTGAGGGCGAAAG	*D. septosporum* ITS (nested)	406
DPS ITS spec rev2	CTCTTCAGCGAAATATATG		
DPS pksA fwd2	GCCTCTGGGAAGCG	*D. septosporum* pksA	219
DPS pksA rev2	GACTGAGCTCCCAAGG		
DPS pksA fwd3	GCGAAAGATTCGTTGATTGT	*D. septosporum* pksA (nested)	142
DPS pksA rev3	CCAAGGCTCCTCAAGTC		

CAD 793/973 developed by Dr Rebecca McDougal based on Moyle et al (1998).

ITS1/4 from White et al (1990).

PksA primers developed by Dr Arne Scwelm (unpublished).

2.1.11 Surface sterilisation

Surface sterilisation of samples was carried out as per Ganley and Newcombe (Ganley and Newcombe 2006): Prior to freeze drying, needle sections were immersed in 96% ethanol for 1 minute, then 6% sodium hypochlorite for 5 minutes, and then 96% ethanol for a further 30 seconds.

2.1.12 Nested PCR

Each stage of nested PCR was run as per the PCR method in 2.1.10. Primer combinations used were ITS1/4 then DPS ITS spec fwd/rev2, and DPS pksA fwd2/rev2 then DPS pksA fwd3/rev3. The template for the nested amplification was 2 µL taken directly from the previous reaction. To avoid contamination, Neptune Barriertips (Continental Lab Products, San Diego, California, USA) were used for all pipetting, and the reactions were setup in a UV-sterilised Laminar Flow Workstation (Email Airhandling, Ingleburn, New South Wales, Australia).

2.1.13 DNA gels

All PCR amplifications were visualised by agarose gel electrophoresis. Agarose gels were made up using 2% w/v Agarose Low EEO (AppliChem GmbH, Gatersleben, Saxony-Anhalt, Germany) in 1x TBE buffer (Appendix 8.1). Ten µL from each completed PCR reaction was mixed with 1 µL bromophenol blue loading dye (Appendix 8.1) and added to a gel in 1x TBE buffer. Samples were run alongside 5 µL of 1 kb+ ladder (Invitrogen). Gels were run at 70V until the dye front had moved through approximately 80% of the gel, then immersed in ethidium bromide solution for ten minutes. Following this, gels were immersed in MilliQ water, then visualised under UV light on a Bio Rad Gel Doc (Bio-Rad Laboratories, Hercules, California, USA).

2.2 Dothistromin Extraction and Quantification

2.2.1 Broth cultures

Dothistroma septosporum NZE10 broth cultures were grown in Dothistroma Broth (DB; 2.5% malt extract (Oxoid, Cambridge, United Kingdom), 2% nutrient broth (Oxoid)). NZE10 is a wild-type strain isolated from infected needles (West 2004). Broths were inoculated using ground mycelia from ~1 cm colonies grown on Dothistroma Medium (DM; 5% malt extract (Oxoid), 2.8% nutrient agar (Oxoid)). *Mycosphaerella graminicola* broth cultures were grown in potato dextrose broth (PDB; 24 g potato dextrose broth (Difco) in 1 L MilliQ), and were inoculated using ground mycelia from ~1 cm colonies grown on PDA (39 g potato dextrose agar (Merck) in 1 L MilliQ). *M. graminicola* broth cultures were grown at 22^{o}C on shaker tables for 14 days, and were tested for contamination by streaking on PDA and incubating at 22^{o}C or 30^{o}C for four days. *M. graminicola* was a wild-type strain isolated on the 17th of January 2003 in Christchurch (Consort Wheat).

2.2.2 Solvent extraction

For non-quantitative extraction of metabolites from broth cultures, an equal volume of ethyl acetate was added, acidified with 1%/5% acetic acid or 1% formic acid, as specified. Flasks were then sealed, covered in tinfoil to minimise exposure to light, and placed on a shaker table for at least 24 hours (or up to 72 hours as specified in

results) at room temperature. After extraction, the mixture was transferred into 50 mL tubes and centrifuged at 4000 g for 5 minutes. The ethyl acetate supernatant was then transferred to a rotary evaporator and concentrated to an appropriate volume for storage (approximately 10 mL).

For extraction from needles and needle lesions 1 mL of acidified ethyl acetate was added to ground samples in microcentrifuge tubes. The tubes were then covered with tinfoil and placed on a shaker table for 72 hours. Following extraction the tubes were centrifuged at 8000g for 5 minutes, and the ethyl acetate supernatant transferred to new tubes. The ethyl acetate was then evaporated, and the samples were resuspended using a solvent and volume appropriate for their purpose (i.e. 200 μL for HPLC).

For extraction of dothistromin and DNA from the same lesion sample acidified ethyl acetate was added to DNA extraction by-products. 500 μL of ethyl acetate acidifed with 1% formic acid was added to the beads and cell debris pelleted as described in the DNeasy extraction centrifugation, and an additional 500 μL was added to the chloroform layer left over from Phytopure purification. These tubes were then covered with tinfoil and placed on a shaker for 72 hours at room temperature. After 72 hours the tubes were centrifuged for five minutes at 8000 g, and the ethyl acetate layers from each sample collated in new tubes. The ethyl acetate was then evaporated off in a fume hood and the samples were resuspended in acetonitrile with 1% formic acid for HPLC.

2.2.3 Dothistromin

Purified and bulk crude dothistromin for TLC, HPLC, and ELISA standards and testing was kindly provided by Dr Robert Franich of Scion (Rotorua, New Zealand). Additional crude dothistromin was prepared from cultures as above (2.2.1 and 2.2.2). For quantification, dothistromin samples were weighed on a Mettler AC100 five-figure balance. A single, weighed standard, resuspended in DMSO, was used for comparative quantification.

2.2.4 ELISA

ELISA was carried out as per Barron (Barron 2006), which was originally based on Jones et al (Jones, Harvey et al. 1993).

To make Doth-MSA conjugate plates, first 5 μL Doth-MSA and 15 mL 1× PBS (Appendix 8.2) were mixed, and 100 μL added to each well of a Nunc Immuno 96-well microtitre plate (Thermo-Fisher Scientific). The plate was then wrapped in gladwrap

and incubated at 37°C for 3 hours. After this incubation, each well was washed 5 times with PBST (Appendix 8.2), and 400 µL blocking solution (Appendix 8.2) was added. The plate was then covered with gladwrap and incubated at 37°C for a further 3 hours. Following this second incubation the plate was washed once with PBST and stored at 4°C until required for the assay.

Samples were prepared in Costar 96-well vinyl pre-incubation plates (Corning Incorporated, Corning, New York, USA). One µL of standard solution (weighed dothistromin standards in DMSO; 1 mg – 3.9 µg in a 2× dilution series, and a blank) was added to 1 mL of dilution buffer (Appendix 8.2). For test samples, 120 µL of sample was added to 860 µL of 50:50 dilution buffer and MilliQ. One hundred µL of sample and 100 µL of labelled peroxidise (Appendix 8.2) was added to each plate, then plates were covered with gladwrap and incubated at 37°C for 1 hour. Standards and samples were loaded in triplicate.

For the dothistromin assay, wells in Doth-MSA conjugate plates were washed once with PBST, and 100 µL of sample from the pre-incubation plate transferred into the wells. The plates were then covered with gladwrap and incubated for 3 hours at 37°C. The plates were then washed six times with PBST, 200 µL of substrate added to each well (Appendix 8.2), covered with tinfoil, and placed on a shaker table for 30 minutes. To stop the reaction, 50 µL of 4 M H_2SO_4 was added to each well. The plates were then read on a BioTek Powerwave XS plate reader (BioTek, Winooski, Vermont, USA) using a measurement wavelength of 490 nm and a reference wavelength of 595 nm. Measurements were subtracted from the blank, then given as a percentage of the blank value. Dothistromin concentration of samples was determined from a standard curve.

2.2.5 Thin Layer Chromatography

TLC separations were assessed using aluminium-backed, 200 µm silica analytical plates (Merck TLC Silica Gel 60; Merck & Co., Inc., Whitehouse Station, New Jersey, USA). The aluminium-backed TLC plates were cut into 2 x 10 cm strips and 25 µL of crude dothistromin in ethyl acetate was spotted 2 cm from the end of each strip, at 1, 10, or 250-fold dilutions. The strips were air dried under tinfoil, then were suspended vertically in a 500 mL Schott bottle (Schott AG, Mainz, Germany) containing 1 cm depth of mobile phase (50:3 chloroform:methanol, 1:1 ethyl acetate:dichloromethane, or 2:1 methanol:water, all acidified with 1% formic acid), so

that the bottom 1 cm of the strip was immersed in the mobile phase. TLC strips were allowed to run until the mobile phase had travelled approximately 80% of the distance. They were then removed from the mobile phase and the solvent front was marked with pencil. The strips and plates were then covered with tinfoil and allowed to air dry before imaging. TLC strips were illuminated in a dark room with a Camag Dual-wavelength UV lamp (Camag, Muttenz, Switzerland), and photographed with a Canon 20D camera (Canon, Tokyo, Japan) mounted on a vertical stand.

Quantitative TLC comparisons were made using glass-backed, 200 μm analytical plates (Merck TLC Silica Gel 60). Standards were added as 1 μL spots, with the exception of the 10 μg standard, which had to be added as 10 μL. They were then air dried under tinfoil and placed in a glass TLC-chamber containing 1 cm of 50:3 chloroform:methanol acidified with 1% formic acid. As with TLC strips, plates were allowed to run until the mobile phase had travelled approximately 80% of the way up the plate, removed from the mobile phase, and the solvent front was marked with pencil. The plates were then covered with tinfoil and allowed to air dry before imaging. Glass-backed TLC plates were imaged under UV illumination using a Bio-Rad Gel Doc. TLC quantification of standards was performed by measurement of integrated optical density in images using ImageJ (http://rsbweb.nih.gov/ij/).

Dothistromin bands were identified by comparison of Rf values to both previously determined values (Debnam and Quach) and values of a dothistromin standard.

2.2.6 HPLC

The HPLC method used was based on Debnam and Quach (unpublished), and modified to suit the needs of the project. Dothistromin-containing samples were resuspended in 200 μL acetonitrile with 1% formic acid and filtered through Minisart RC4 0.2 μm syringe filters (Sartorius Stedim Biotech, Aubagne Cedex, France) into labelled septum vials. The HPLC system was comprised of a Phenomenex Luna C18 4.7x150mm (Phenomenex, Torrance, California, USA) column, Dionex UltiMate 3000 pump (1 mL/min) (Dionex, Sunnyvale, California, USA) , Dionex ASI-100 autosampler (50 μL injection volume), and Dionex STH-585 column oven maintained at 40^{o}C . The final gradient used involved five minutes at 5% acetonitrile, then a rise to 75% over the next 30 minutes, followed by a rise to 100% at 38 minutes, dropping back to 5% between 42 and 45 minutes, and a 15 minute equilibration. UV spectra were measured

by a Dionex UVD340U diode array detector, and fluorescence response (excitation wavelength 470 nm, emission wavelength 545 nm) was taken by a Dionex RF2000. Data were recorded and processed using Dionex Chromeleon software (http://www.dionex.com/en-us/products/chromatography-software/chromeleon6/lp-72985.html). Dothistromin was quantified by fluorescence peak area at 23.1±0.05 minutes. A dothistromin response standard curve was determined from a 10-fold dilution series of the purified dothistromin standard, and concentrations of unknowns were determined from this standard curve.

2.2.7 Mass Spectrometry

Mass spectrometry (MS) was carried out on contract by Karl Fraser and Scott Harrison of Agresearch Grasslands (Grasslands Research Centre, Palmerston North, New Zealand). Work was performed using a Jasco XLC UHPLC pump (Jasco Inc., Easton, Maryland, USA), PAL autosampler, C18 column, Thermo-Fisher Surveyor PDA (Thermo-Fisher Scientific), Shimadzu RF-10A fluorescence detector (Shimadzu Corporation, Kyoto, Japan), and Thermo-Fisher LTQ linear ion trap MS.

2.3 *Dothistroma* lesion sampling

2.3.1 Seedling inoculation

The inoculated *Pinus radiata* seedling used to obtain lesion samples for chapter 5 was graciously provided and watered by Md. Shahjahan Kabir. The seedling was grown from a cutting, and was approximately 1 year old at the time of inoculation. The seedling was sprayed with a suspension of *Dothistroma septosporum* spores in water (10^6 spores/mL) using a hand-sprayer, then enclosed for 48 hours. Continuous misting was started at 4 hours. After 48 hours the seedling was stored in an enclosure within a greenhouse, with continuous misting.

2.3.2 Labelling

Time course labelling was started at 42 days after seedling inoculation. Needles were inspected visually for signs of infection every two days. Those showing what appeared to be initial stage *D. septosporum* infection were labelled with the date of

symptom appearance. Labels were made using masking tape, and were wrapped around the tip of the needle. Needles with multiple lesions were not labelled.

2.3.3 Quantification

All infected needles were cut from the seedling at 103 days post inoculation, and placed in labelled microcentrifuge tubes. Needles were photographed at 1.6× magnification using a Leica MZ12 stereomicroscope (Leica Microsystems GmbH, Wetzlar, Germany). Needle samples were stored at -20^{o}C until needed. To quantify both dothistromin toxin and *Dothistroma* DNA, both were extracted as per the dual extraction method (methods 2.2.2). Dothistromin for the needle lesion was quantified using HPLC-fluorescence, as per methods 2.2.6.

Dothistroma DNA was kindly quantified by Dr. Rebecca McDougal, using a quantitative real time PCR method. Real-time PCR was performed using a LightCycler® 480 instrument (Roche Applied Sciences). Ten µL reactions were set up using a LightCycler® 480 Probes Master kit (Roche Applied Sciences) and consisted of 1.2 µL PCR-grade water, 5 µL 2× Master mix, 1 µL 10× primer/probe mix, and 2 µL template or standard DNA. The 10× primer/probe mix consisted of primers pksA64, pksA164, CAD918, and CAD1019 at 4 µM, and hydrolysis probes Probe88 and Probe945 at 2 µM (final concentrations in PCR were 0.4 µM and 0.2 µM for primers and probes respectively; primers and probes listed in Table 2.2 below). Concentrations of primers and probes had been previously optimised for quantification using this assay. Standard curves were prepared using a 10-fold dilution series of genomic DNA in a ratio of 1:1000 *D. septosporum:P. radiata*, giving 5 standards with pine DNA concentrations between 1000-0.1 ng and *Dothistroma* DNA concentrations between 1000-0.1 pg. Thermal cycling conditions consisted of 45 cycles of denaturation at 95^{o}C for 10 seconds and annealing at 59^{o}C for 30 seconds. Extension was not required. The amplification cycles were preceded by a hotstart at 95^{o}C for 10 minutes, and followed by cooling at 40^{o}C for 10 seconds. PCR reactions were performed in duplicate for each sample. Sample DNA concentration was quantified from the standard curves based on crossing point values, using the LightCycler® 480 software.

Table 2.2: Realtime PCR primers and probes

Primer name	Sequence (5' to 3')	Target	Product (bp)
pksA64	CTGTCTTCCTCGACCTGTT		
pksA164	AAGCACACCTGGAAAGAATGA	*D. septosporum* pksA	102
Probe88	6FAM-CCATCGATCCCAGCACCGCT-BHQ1		
CAD918	CAGCAAGAGGATTTGGACCTA		
CAD1019	TTCAATACCCACATCTGATCAAC	*P. radiata* CAD	101
Probe945	HEX-TGTGAACCATGACGGCACCC-BHQ1		

Primers and probes designed by Dr. Rebecca McDougal.

2.4 Bioinformatics

2.4.1 Cluster location

Initial location of polyketide synthase genes in *Alternaria brassicola, Cochliobolus heterostrophus, Mycosphaerella fijiensis, M. graminicola,* and *Stagonospora nodorum* genomes was by BLASTP of *D. septosporum* pksA (NCBI AAZ95017) against gene models using JGI genome analysis tools (http://genome.jgi-psf.org/, Joint Genome Institute, Walnut Creek, California, USA). Hits with E-value below e-50 were targeted for further investigation. Gene models located within 35 kilobases of these low E-value hits were aligned against the NCBI database (http://www.ncbi.nlm.nih.gov/, National Center for Biotechnology Information, National Library of Medicine, Bethesda, Maryland, USA) using BLASTP through the JGI genome tools. Hits against known toxin biosynthesis genes from *D. septosporum, A. nidulans*, and *A. parasiticus* were recorded. For each genome, the pksA match showing the highest concentration of toxin gene blast hits within 35 kb was selected for further investigation. The approximate area within which putative toxin biosynthetic gene hits were contained was selected, and predicted domains of gene models within the area were recorded (automatically predicted domains by JGI genome tools).

2.4.2 Alignment

Based on similarity between predicted domains in gene models and known toxin biosynthesis gene domains, the protein sequences of gene models in the potential cluster areas (obtained from JGI) were aligned against those of toxin biosynthesis genes (obtained from NCBI) from *D. septosporum, A. nidulans* and *A. parasiticus* (Yu, Chang

et al. 2004; Zhang, Schwelm et al. 2007). A full list of compared genes is shown in appendix 8.3. Alignments were performed using MacVector (MacVector Inc., Cary, North Carolina, USA).

Chapter 3: Development of DNA Extraction Methods

3.1 Introduction

The correlation of dothistromin production with *D. septosporum* growth *in vivo* requires the use of a sensitive and specific assay for fungal biomass. Real time PCR allows quantification of biomass with specificity determined by the primers used, and has been used to determine biomass in the related fungus *M. graminicola* (Keon, Antoniw et al. 2007). Quantitative real time PCR has been used to assay expression of dothistromin biosynthesis genes in *D. septosporum* (Schwelm, Barron et al. 2008; Ioos, Fabre et al. 2010), and to quantify DNA from *Dothistroma* species (McDougal, unpublished). While real time PCR quantification is sensitive, high yield extraction of *Dothistroma* DNA from individual lesions would increase consistency and accuracy in the quantification of early stage infection, where fungal biomass levels are likely to be very low.

Previously used DNA extraction methods (Qiagen DNeasy) were found to give low DNA yields from pine needle tissue, leading to unreliable PCR (Schwelm, personal communication). It was hypothesised that one reason for this was the fibrous nature of the needles that restricts the extent of cell lysis. Additionally, the membrane filters used by the Qiagen DNeasy kit, while removing the vast majority of DNA contaminants, may also retain some DNA. This could reduce yield below an acceptable threshold when used with samples much smaller than the weight recommended in the manufacturers protocol, such as single lesions. It was thought possible that a method which sacrificed DNA purity to obtain a higher yield could give better results for small samples. A number of modifications to the protocol were proposed, with the aim of increasing cell lysis and reducing DNA loss. Comparison of these methods required a consistent amount of DNA in the starting tissue. Because *D. septosporum* biomass, and therefore DNA, is highly variable between lesions *P. radiata* DNA from uninfected needles was used instead.

A major part of this project was developing a method to correlate the biomass of *D. septosporum* with its dothistromin production *in planta.* To determine the DNA and dothistromin content of a single lesion, extraction of both from the same lesion is required. To allow correlation of early stage growth and dothistromin production, extraction of both components must have high yield and consistency. The ability to extract dothistromin along with DNA was taken into account when developing DNA extraction protocols.

3.2 Results

3.2.1 DNA extraction optimization

Starting with the Qiagen DNeasy Plant extraction protocol as a baseline, modifications with the potential to alleviate perceived deficiencies in the DNeasy method were tested to determine their effect on yield. These modifications were made in a stepwise fashion, with the method giving the highest yield in the previous comparison being used as the standard against which further modifications were compared. In addition, the protocols were split into tissue lysis and DNA purification sections, to enable testing of combinations of methods or kits. Tested modifications to the original Qiagen DNeasy protocol were freeze drying of needle tissue prior to extraction, use of alternative lysis and precipitation buffers, use of a Fastprep bead beater, the addition of an enzymatic lysis step, and use of chloroform or GE Healthcare Phytopure DNA purification steps to replace the Qiagen DNeasy column purification. These modifications to the Qiagen protocol were tested on 3 cm uninfected *P. radiata* needle sections to determine their effect on yield.

Preliminary testing showed that freeze dried samples, ground with glass beads, lysed with Qiagen DNeasy buffers, and purified with a GE Healthcare Phytopure DNA purification protocol gave the highest yield, so this modified method was used as the initial standard for further work. Replacement of the Qiagen DNeasy column DNA purification with a chloroform-based DNA purification method also allowed for dothistromin extraction from the same lesion samples (methods 2.2.2).

Yields were measured with a Nanodrop 1000 spectrophotometer as per methods 2.1.9, and test PCRs were run using *P. radiata* CAD primers (methods 2.1.10; Table

2.1) to check for the presence of amplifiable DNA. Results are shown in Fig 3.1, and a summary of the effects of altering key steps is shown below, with comparisons made between pairs of extractions differing only by the one variable in question.

Freeze drying: Comparison of needles freeze dried prior to extraction (Figure 3.1, lane 1) and fresh (not freeze dried) needles (lane 2) showed that the former yielded significantly more DNA than the latter ($P_{2=1}$ = 0.006). Freeze-dried needles were therefore used for all further comparisons. Both methods gave acceptable amplification with CAD primers.

Lysis and purification: Comparison of DNeasy (column purification, lane 3) and Phytopure (chloroform purification, lane 5) kits with the 'standard' method (combining DNeasy lysis and Phytopure purification, lane 1) showed a significantly higher yield with the standard ($P_{3=1}$ = 0.011, $P_{5=1}$ = 0.005). Yields from the Phytopure kit were highly variable, and showed unreliable PCR amplification. This was hypothesised to be due to poor performance of the lysis buffer, as Phytopure lysis buffer containing ground samples was relatively clear after incubation, whereas samples in Qiagen lysis buffer were considerably cloudier. The cloudiness was thought to indicate the release and denaturing of cellular proteins.

Glucanex lysis: The addition of an incubation step with Glucanex, an enzyme preparation that contains β-chitinase, (methods 2.1.7, lane 7) was shown to significantly increase yield when compared to the standard ($P_{7=1}$ = 0.001), and to a 'mock incubation' control lacking Glucanex (lane 8, $P_{8=7}$ = 0.003).

Fastprep bead beater: The used of a Fastprep bead beater (methods 2.1.8) in addition to manual grinding (lane 9) gave a small increase in yield compared to manual grinding alone ($P_{9=7}$ = 0.068). The small increase in yield provided by an additional bead beating step was not considered worth the additional time and complexity. PCR amplification from Fastprep samples was also found to be unreliable, indicating that some degradation of DNA may occur, possibly due to shearing. Complete replacement of manual needle grinding with agitation in a Fastprep bead beater gave very low average yield (lane 10, $P_{10=7} = 1.42 \times 10^{-8}$), and was not able to be amplified by PCR.

Kit alternatives: The cost of buying two commercial DNA extraction kits from which only a fraction of the components were to be used (as in the 'standard' method) was considered wasteful and expensive. Therefore extensive testing was done using alternative buffers in an effort to replicate the success of the AP1 lysis and AP2

precipitation buffers from the Qiagen DNeasy kit. Buffers tested were either based on previously published methods or alternatives using known lysis and precipitation components (full list of buffers trialled in appendix 8.4). None of the buffers tested gave comparable performance to the Qiagen DNeasy combination (results not shown), and since the DNeasy buffers were able to be purchased separately from the rest of the DNeasy kit the cost was considered justifiable.

Replacement of the Phytopure kit extraction steps was more successful. While removing the Phytopure resin step gave a large reduction in DNA yield (lane 11, compared to lane 7; $P_{11=7} = 1.72x10^{-8}$), replacement of the Phytopure resin suspension with 5x TE buffer gave comparable yield (compare lane 12 with lane 7, $P_{12=7} = 0.65$) and purity (estimated by $A_{260:280}$ ratio). Because of the cost savings associated with removal of the Phytopure kit this method was used for all future work. Both of these methods gave PCR amplifiable DNA. The increase in standard deviation between 7 and 12 is most likely caused by the decreased sample size.

Fig 3.1: Yields obtained from different DNA extraction protocols

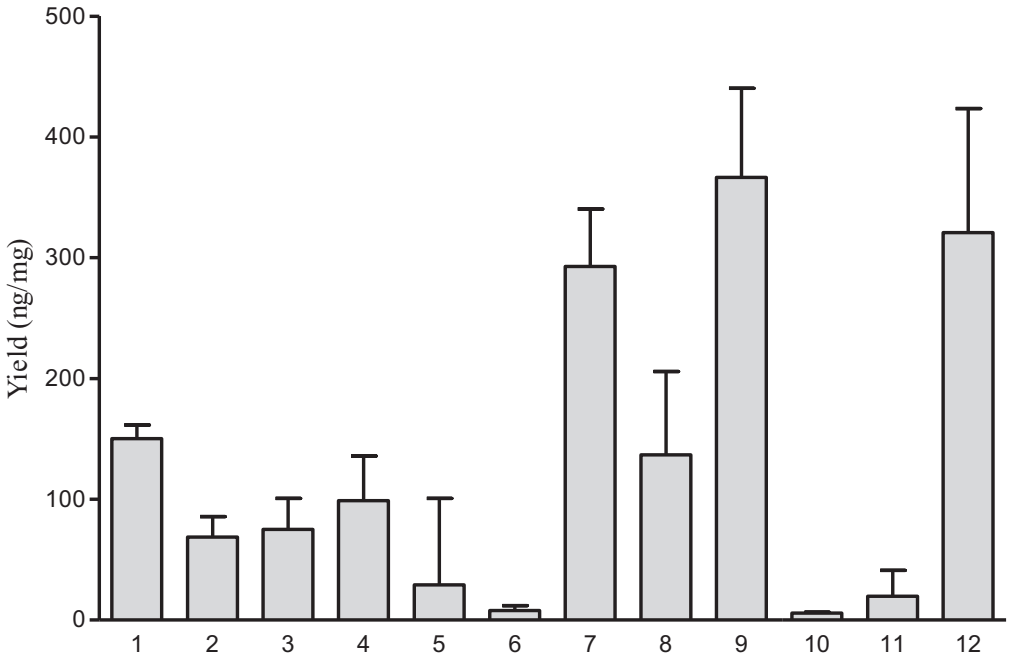

Mean yields of different DNA extraction techniques on 3 cm uninfected needle sections. Numbers correspond to method summaries in Table 3.1, with error bars showing the 95% confidence interval.

Table 3.1: Summary of method modifications

Mod.	1	2	3	4	5	6	7	8	9	10	11	12
Yield	150.1	69.6	75	98.9	29	7.8	292.8	136.8	366.6	5.7	19.6	320.8
95% CI	11.4	17.1	25.7	37	71.7	4	47.6	69	73.6	0.7	21.5	102.7
Fresh	-	+	-	-	-	-	-	-	-	-	-	-
Glnx.	-	-	-	+	-	+	+	N	+	+	+	+
Grnd.	+	+	+	+	+	+	+	+	+	-	+	+
Btr.	-	-	-	-	-	-	-	-	+	+	-	-
Lysis	Q	Q	Q	Q	P	P	Q	Q	Q	Q	Q	Q
Pcn.	P	P	Q	Q	P	P	P	P	P	P	C	M
n	18	3	3	3	3	3	18	6	3	3	3	6
PCR	++	++	++	++	+	-	++	++	-	-	++	++
$A_{260/280}$	1.74	1.87	1.71	1.94	1.22	1.51	1.77	1.71	1.84	1.13	1.44	1.83

Yield is given as ng DNA/mg fresh weight of green needle tissue.

Key to Table 3.1		
Fresh:	+	Needles not freeze-dried before extraction.
Glnx.:	+	Ground needles incubated 30 minutes with Glucanex enzyme.
	N	Ground needles incubated with CTAB buffer (negative control for Glucanex).
Grnd	+	Needles were not manually ground (to test if Fastprep was sufficient by itself).
Btr	+	Needles ground using a Fastprep bead beater.
Lysis		Kit used for lysis of ground pine needle sections, Qiagen (Q) or Phytopure (P).
Pcn		Kit or method used for purification of DNA, Qiagen (Q), Phytopure (P), chloroform (C), or modified chloroform (M).
n		Number of samples tested.
PCR		Amplification from purified product; ++ consistently good, + poor/variable, - no amplification

3.2.2 Extraction from small pine needle samples

Following optimization of methods on larger needle sections, the final extraction method (column 12 in Table 3.1) was tested on intermediate (10 mm length) and 'single lesion' size (3 mm length) sections of uninfected *P. radiata* needle samples, using modified buffer volumes (methods 2.1.4). The difference in average DNA yield for fresh (before freeze-drying) and dry (after freeze-drying) samples is shown in the table below.

Table 3.2: Extraction yield for small samples

Sample size (mm)	DNA conc. (ng/µL)	Total DNA (ng)	Mean fresh weight (mg)	Yield (ng/mg FW) Mean± SD	Mean dry weight (mg)	Yield (ng/mg DW) Mean± SD	n	PCR
30	167.8	3356.8	10.6	321 ± 124.9	4.5	772 ± 356.3	6	++
10	24.2	484.7	3.2	149 ± 98.8	1.7	300 ± 227.5	3	++
3	17.9	358	1.3	272 ± 47.1	0.8	470 ± 58.1	3	++

Both intermediate and lesion size samples gave adequate yields of DNA that could be amplified reliably using *P. radiata* CAD primers (indicated as ++ in table). The yield of DNA was variable, but did not change greatly between samples of different size. This shows that the method was able to be successfully scaled down for smaller samples. The comparatively lower yield in 10 mm samples may indicate that further buffer volume optimization is required for this sample size. While variation in sample yield was high in the larger samples, the 3 mm sample size showed lower variation. This may be due to more consistent grinding of smaller needle sections, or greater control over temperature, and therefore enzyme activity, in smaller buffer volumes. This sample size was used for all further quantitative work.

3.2.3 Extraction from needles infected with *D. septosporum*

To ensure that the final method was capable of obtaining PCR quality *D. septosporum* DNA from needle lesions, DNA was extracted from 3 mm long needle sections centred on a *D. septosporum* lesion identified by microscopy (methods 2.1.2). These samples were expected to contain both pine and fungal DNA in varying amounts, meaning that this was a qualitative test only. Because the fungal DNA component was expected to contain a mix of both *D. septosporum* and other non-target DNA from fungal endophytes residing in the needle, PCR amplification was tested with *D. septosporum*-specific pksA primers and ITS nested primers (methods 2.1.11). The

ability to extract fungal DNA from surface-sterilised needles was also tested (sterilisation as per Ganley and Newcombe 2006, reproduced in methods 2.1.12). Because of the extremely low weight of infected needle samples, sets of three were weighed together and an average weight taken. Dry weights of these samples were too low to measure accurately.

Table 3.3: Extraction yield for *Dothistroma* lesions

Surface sterilised	DNA conc. (ng/µL)	Total DNA (ng)	Abs $_{260/280}$	Mean weight (mg)	Yield (ng/mg) Mean± SD	n	PCR (pksA)	Nested PCR (ITS)
-	13.4	267.3	1.45	0.3	827.8 ± 520	3	++	++
+	29.0	579.5	1.34	0.5	1091 ± 418	8	-	+

Both surface sterilised and unsterilised lesion samples gave greater yields than uninfected samples. This may be due to the lesion compromising the physical integrity of the needle, allowing for more effective lysis, or due to the presence of fungal DNA. Surface-sterilised needle samples gave similar yields to unsterilised samples, but did not give reliable PCR amplification. The use of nested PCR was required to give a product visible on an agarose gel. Subsequent work by Md. Shahjahan Kabir has shown that removal of the bleaching step in the surface sterilisation protocol improves PCR reliability, but does not give complete sterilisation (unpublished). High variation in yield between samples was expected since the biomass of fungal lesions was not normalized.

3.2.4 Extraction from herbarium specimens

DNA extractions were carried out on herbarium specimens to test the ability of the developed method to extract PCR amplifiable DNA from dried infected needle samples which had been stored. Lesions were taken from herbarium needle specimens provided by Scion (Rotorua, New Zealand) and surface sterilised (as per Ganley and Newcombe 2006) to reduce the possibility of contamination. As with the single lesion extractions, yield should not be taken as a reliable measurement and dry weights were not able to be accurately measured. The average DNA yield from 12 samples was 1438± 1072 ng DNA per mg fresh weight, which is similar to that of recently harvested lesions. The DNA was able to be amplified using nested PCR. As indicated by the high standard deviation, yield varied more than that of new lesions.

3.2.5 Fungal DNA extractions

The ability of the final modified method to be used to extract DNA from fungal mycelia was compared with Qiagen DNeasy and Phytopure methods (methods 2.1.4 and 2.1.5, respectively).

Table 3.4: Extraction yield from fungal mycelia

Extraction Method	DNA conc. (ng/µL)	Total DNA (ng)	Mean fresh weight (mg)	Yield (ng/mg FW) Mean± SD	n
Final	1014	20280	9.4	2104 ± 430	3
DNeasy	84	4190	6	710 ± 133	3
Phytopure	217	4339	8.8	531 ± 294	3

Table 3.4 shows a greatly increased yield when using the final method (Fig. 2.1 lane 12) over previously used Qiagen DNeasy and GE Healthcare Phytopure protocols (Fig. 2.1 lanes 3 and 5 respectively). The fungal material is not as resistant to disruption as pine needle tissue, and the difference in yields seen is most likely due to the Glucanex enzyme incubation in the final method.

3.3 Discussion

The development of a yield-focused DNA extraction method suitable for performing an *in vivo* time course of dothistromin production was successful. The method developed gives higher DNA yield from single lesion samples than the previously used Qiagen DNeasy method, and products were found to be PCR amplifiable.

The use of uninfected *P. radiata* needle section as a standard for DNA extraction comparisons relies on several assumptions. Firstly, it is assumed that the amount of DNA per weight of needle in each sample is used is consistent, and that this DNA is equally extractable. Since the needles used were collected from a single plantation containing trees of identical age exposed to nearly identical conditions, and needles were selected to be similar and free from defects, this can be considered a valid assumption. A second assumption is that extraction from uninfected pine tissue is representative of extraction from fungi within necrotic lesions. Extractions from *D. septosporum* mycelia have shown that the developed method is effective on fungi, which do not require the level of intensive physical tissue disruption that pine requires (Bradshaw 2006). This is an indication that the principal difficulty in extracting DNA from lesions may be due to the tough pine tissue. If this is true then the extent of fungal

lysis during DNA extraction would be increased by greater lysis of surrounding pine tissue. Of greater concern is the potential presence of PCR inhibitors in the *Dothistroma* infected lesions which are not present in uninfected pine. One potential source of inhibition is benzoic acid, which has been found to accumulate in lesions (Franich, Carson et al. 1986). PCR inhibitors from infected lesions are discussed further in chapter 5. Unfortunately, because of the variability in fungal biomass between lesions a plant DNA standard had to be used which may not have been completely representative of extraction efficiency.

The predicted causes of low yield with previous methods appear to be accurate: yield was improved by using more intense tissue breakdown and lysis techniques (freeze drying, Glucanex incubation, and Fastprep), and by the use of a chloroform purification step, indicating that previously used techniques are inadequate in these areas. The use of freeze drying prior to needle grinding enables samples to be ground more finely, and this may allow greater cell lysis by letting lysis buffer penetrate further into the tissue. Without freeze drying it was found to be more difficult to grind samples to a fine powder, with grinding taking longer and small fibrous sections still remaining in the samples even after grinding. Incubation with Glucanex enzyme gave a large increase in yield compared to a buffer-only incubation for *P. radiata* uninfected needle samples, despite being sold as a fungal lysing enzyme. This may be due to it being a crude enzyme mix, containing a mixture of β-glucanase, chitinase and cellulase (Petit, Boisseau et al. 1994). Since cellulose is a major component of the plant cell wall, this may explain the increase in yield seen in Glucanex treated pine samples. The use of bead beating in addition to manual grinding would further break down the pine tissue, but the high shearing forces that this exposes samples to may degrade DNA from cells which have already been lysed. This would explain the reduction in PCR reliability from these samples. Alternatively, the additional time taken to run bead beating on samples may allow DNA degradation by enzymes released from lysed cells.

The increase in yield seen with the use of a chloroform-based purification indicates that some loss of DNA is occuring with use of the DNeasy column purification steps. This may be due to an amount of DNA being retained on the membranes, and is likely to be proportionally greater in lower concentration samples. Since the samples run in these tests are considerably smaller than the protocols recommended maximum sample size (100 mg for Qiagen DNeasy), this yield loss may be unacceptably high depending on the concentration requirements of the application.

Use of a chloroform extraction would avoid loss of DNA by membrane adsorption, but also appears to decrease the purity of the final DNA product, as it removes fewer contaminants. While the aim of this work was to increase yield, and decrease in purity was considered an acceptable loss as long as samples still showed reliable PCR amplification, contamination with PCR inhibiting compounds could have a subtle effect on amplification that is not seen in non-quantitative PCR. Testing based on quantitative real time PCR could enable accurate comparisons to be made between methods based on the end result rather than just yield, and should be considered essential future work in the optimization of DNA extraction from single lesions.

The loss of DNA yield in samples where neither Phytopure resin or 5x TE buffer was added may be due to reduced DNA solubility, meaning that a larger amount of DNA was discarded with the chloroform layer. Another possibility is that the lack of a chelating agent allowed nuclease enzymes still present in the sample to degrade DNA, whereas with the addition of EDTA in TE buffer removes metal ion cofactors required for the function of these enzymes.

While the final method showed considerably higher yields from fungal mycelia than Qiagen DNeasy or GE Healthcare Phytopure methods, the use of this method for fungal mycelia extraction is most likely not necessary. While sampling single lesion samples places low limits on the extractable quantity of DNA, broth culture is generally made up in much larger batches, in which *D. septosporum* is present in at much greater concentrations. Therefore, sacrificing DNA purity for yield by using a yield-focused method would not be necessary. Additionally, because of the greater available sample and secretion of dothistromin into culture, dual extraction of DNA and dothistromin is not required. Use of a Glucanex enzyme incubation step in the method used would likely increase yield, but even the marginal increase in time and complexity may not be worth it when the option of simply taking a larger initial sample is available.

In conclusion, a method has been developed which allows the high yield extraction of DNA from single *Dothistroma* lesions. Used in conjunction with the *D. septosporum*-specific quantitative real-time PCR method developed by Dr Rebecca McDougal, this will enable the rapid and sensitive quantification of *Dothistroma* biomass *in planta.*

Chapter 4: Development of Dothistromin Extraction and Quantification Methods

4.1 Introduction

A robust method for the quantification of dothistromin has been required since investigation into *Dothistroma* species began. While methods such as ELISA and TLC have proved adequate for previous study, new methods have had to be developed to allow quantification *in planta*.

Previous quantification work using ELISA has shown high levels of variability between replicates (Schwelm, Barron et al. 2008). Additionally, the ELISA method used relies on an enyzme-linked anti-dothistromin antibody, which cannot be easily replenished when current stocks become depleted. TLC methods appear more reliable, but based on previously detailed sensitivity it was uncertain whether TLC would allow quantification of dothistromin from early stage lesions (Franich 1981). HPLC systems have not been used extensively for quantification of dothistromin, but potentially offer greater sensitivity and accuracy than TLC-based methods. Therefore, work focused on optimizing TLC- and HPLC-based quantification methods to determine the most effective means of quantifying dothistromin in in needle samples.

Both TLC and HPLC techniques require solvent extraction of the toxin from needles or broth. Extraction solvents must be acidified to prevent ionisation of dothistromin, which alters its mobility on TLC and HPLC, complicating its separation from other compounds (Zhang, personal communication; Franich, personal communication). Optimization of the TLC method required the comparison of several mobile phases (50:3 chloroform:methanol, 1:1 ethyl acetate:dichloromethane, and 2:1 methanol:water), each varying in their ability to resolve dothistromin from other compounds (Franich 1981). Conversely, selection of an HPLC solvent scheme was restricted by the lack of published methods (Debnam and Quach, unpublished). The fluorescent properties of the dothistromin molecule meant that detection and

quantification testing was primarily focused on fluorescence-detection, though other methods were investigated.

While research has already been done on quantification of dothistromin by TLC and HPLC methods, this work has not been updated for over twenty years, and no direct comparisons between these methods have been made. Hands on testing of both these systems allowed not only quantitative comparisons of their sensitivity and accuracy, but also qualitative judgements on their relative strengths and weaknesses as routine techniques, using modern equipment.

4.2 Results

4.2.1 Extraction

Since both TLC and HPLC methods require crude extration of dothistromin from broth, optimization of the extraction protocol was undertaken first. Solvent extractions were performed on broth cultures of *D. septosporum* using ethyl acetate (methods 2.2.2). Ethyl acetate was used as the extraction solvent based on previous work (Gallagher 1971), and the advice of chemist Dr. Robert Franich (personal communication). The extraction solvent was acidified to prevent dothistromin ionisation. Several solvent acidification methods were tested to determine the most effective method of suppressing dothistromin ionisation. Initially 1% acetic acid was used, but when samples were run on TLC using this concentration, visible streaking occurred due to ionised dothistromin (Fig 4.1, left lane). Increasing the acetic acid concentration to 5% reduced streaking (Fig 4.1, right lane), but made evaporation of the solvent much slower. Later tests with HPLC showed that 1% formic acid was just as effective at preventing ionisation. The use of 1% formic acid had the advantage of considerably faster evaporation of solvent and, in light of concerns about solvent volatility for ESI-MS, 1% formic acid was used in all further quantitative comparisons.

Fig 4.1: Effect of increased acidification on dothistromin ionisation

UV fluorescence of TLC using mobile phase of 50:3 chloroform:methanol acidified with 5% acetic acid, left lane showing sample extracted with 1% acetic acid and visible streaking from ionised dothistromin, right showing sample extracted with 5% acetic acid and reduction of streaking.

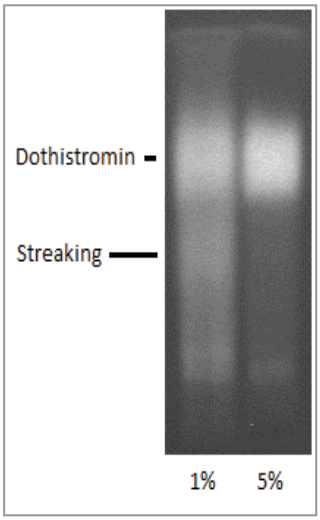

Because of the potential photodegradation of dothistromin (Franich, Carson et al. 1986), extractions vessels were covered with foil to reduce light exposure to a minimum. Preliminary trials showed that increasing extraction time from 24 hours to 48 or 72 hours resulted in higher extraction efficiency. To give the highest yield of dothistromin 72 hours was used for all further extractions.

4.2.2 TLC

The solvent system for TLC quantification was chosen based on tests of previously published protocols. To compare solvent schemes for separation of compounds from *D. septosporum*, crude broth extract samples were run on aluminium-backed silica analytical TLC plates cut into 100 mm by 20 mm strips (methods 2.2.5). Separation was compared for three solvent systems; 1:1 ethyl acetate:dichloromethane, 2:1 methanol:water (Franich 1981), and 50:3 chloroform:methanol (Debnam and Quach, unpublished). These mobile phases were chosen based on previous success in separating dothistromin from other *D. septosporum* secondary metabolites. All mobile phases were acidified with 1% formic acid.

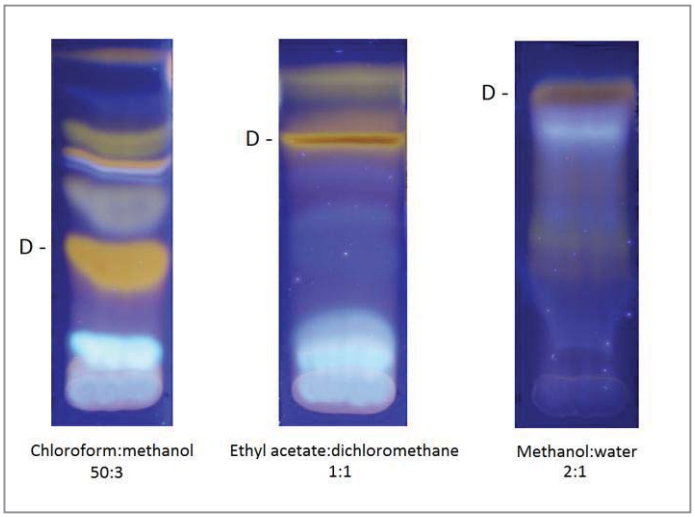

Fig 4.2: Separation of TLC solvent systems

Illumination of TLC strips with UV and photography with a colour camera shows the separation of dothistromin from other fluorescent compounds extracted from D. septosporum *broth culture. The direction of solvent flow is from the bottom of image to top, where cropping of image indicates the position of the solvent front. Bands identified as dothistromin are marked D. The bright blue fluorescent band is formed by caffeic acid (low mobility in left and middle strips, high mobility in right strip), see section 4.2.4 for details.*

Normal phase chloroform:methanol (Fig 4.2; left) showed the greatest separation of all sample components, but the dothistromin band was relatively diffuse. Ethyl acetate:dichloromethane mobile phase (Fig 4.2; centre) gave fewer distinct bands for minor components, but gave a very sharp dothistromin band. Methanol/water did not give adequate separation of any of the sample components, and had an extremely long run time (more than 40 minutes for a 10 cm TLC strip). Dothistromin bands were identified by retention factor (Rf) values and band colouration. Expected Rf values of dothistromin were based on a combination of published values (Franich 1981), previous work (Debnam and Quach, unpublished), and the mobility of a purified dothistromin standard.

Because of problems with quantification of nanogram levels of dothistromin by TLC, such as photodegradation and high background noise (Gallagher, personal communication), ethyl acetate:dichloromethane was thought to be a better solvent system than chloroform:methanol. While chloroform:methanol gave slightly better separation of dothistromin from other compounds, initial testing found the diffuse dothistromin bands hard to quantify at low levels. Because of the diffuse peak shape, amounts lower than 1 ug were found difficult to distinguish from background noise. The sharp dothistromin band formed by the ethyl acetate:dichloromethane mobile phase was easier to distinguish above background noise (Appendix 8.5).

To determine the sensitivity and consistency of the ethyl acetate:dichloromethane normal-phase TLC assay, a dilution series of purified

dothistromin was run. The dilution series was performed in triplicate, using serial 10-fold dilutions of a purified dothistromin sample between 10 ug and 1 pg. For maximum consistency between replicates, images were captured using a BioRad Gel Doc imager as per methods 2.2.5.

Fig 4.3: TLC dilution series.

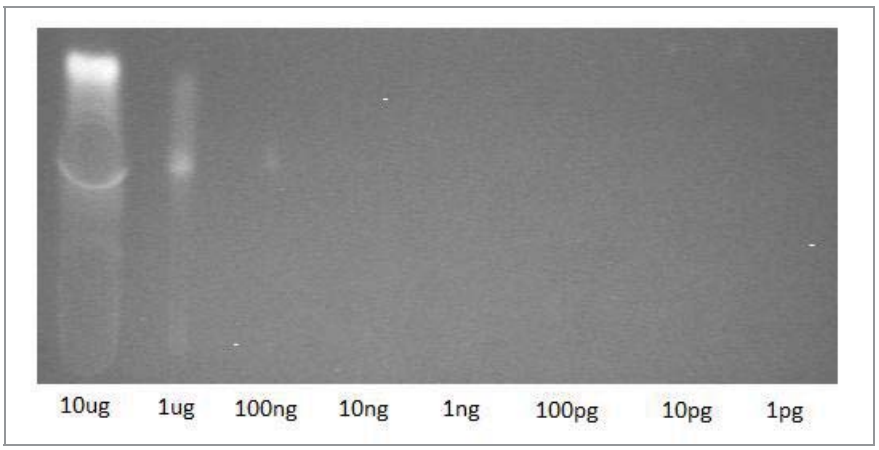

A 10x dilution series of purified dothistromin on TLC shows self-quenching at higher levels, and a lower limit of detection of between 10 and 100 ng. An unidentified band of higher mobility is seen despite an apparently pure sample; this may be a degradation product or low concentration contaminant of higher fluorescent response.

Quantification of the dilution series by fluorescence densitometry showed the minimum detectable level of dothistromin to be between 10 and 100 ng. Detection of dothistromin bands at levels below 100 ng was hampered by background noise. The 10 ug samples showed significant self-quenching, indicating that the upper level of quanitification is between 10 and 1 ug. Measured values for samples within the quantifiable range are shown in table 4.1.

Table 4.1: TLC dilution series

Replicate	Standard	IOD	Relative difference from 100 ng
A	1 µg	143.12	0.0640
	100 ng	134.51	
	Background	135.08	
B	1 µg	136.16	0.0613
	100 ng	128.30	
	Background	128.19	
C	1 µg	129.97	0.0391
	100 ng	125.07	
	Background	127.38	

TLC integrated optical density for three replicates.

As expected, TLC background was high, with two of the three replicates showing background integrated optical density (IOD) values higher than the lowest visible standard. Because the narrow range of quantification prevented calculation of a standard curve, and variable exposure prevented direct comparison, variation between replicates was measured using the relative difference between the two measurable standards. Over the three standards variation was high, with the integrated optical density of the 1 ug standard proportional to that of the 100 ng standard showing a relative standard deviation of 25% over the three replicates (average 0.0548, SD 0.0137). However the relative standard deviation of the two closest standards was much lower, at 3% (average 0.0627, SD 0.0019). The elevated background IOD values and high standard deviation may have been caused by variations in background noise levels between lanes the plate. Lower background was seen in plates imaged with a Canon 20D camera and separate UV illuminator (methods 2.2.5), however it was difficult to keep experimental conditions consistent with this method.

4.2.3 HPLC

The previously used method for HPLC separation of dothistromin from other *D. septosporum* metabolites is based on an acetonitrile:water gradient acidified with 1% acetic acid (Debnam and Quach, unpublished). Use of 1% formic acid was found to be preferable for LC-MS use because of its greater volatility. The gradient used by Debnam and Quach was extended in range to 5-95% acetonitrile (from the original from 15-75%) to help with removal of low mobility compounds associated with reverse

phase separation of *Dothistroma* lesions (Franich 1981), and to allow later identification of other metabolites from the same samples. Initial testing was performed using scanning UV-VIS absorption, which showed dothistromin eluting at 23.1±0.05 minutes.

Fig 4.4: Scanning UV-VIS absorbance HPLC

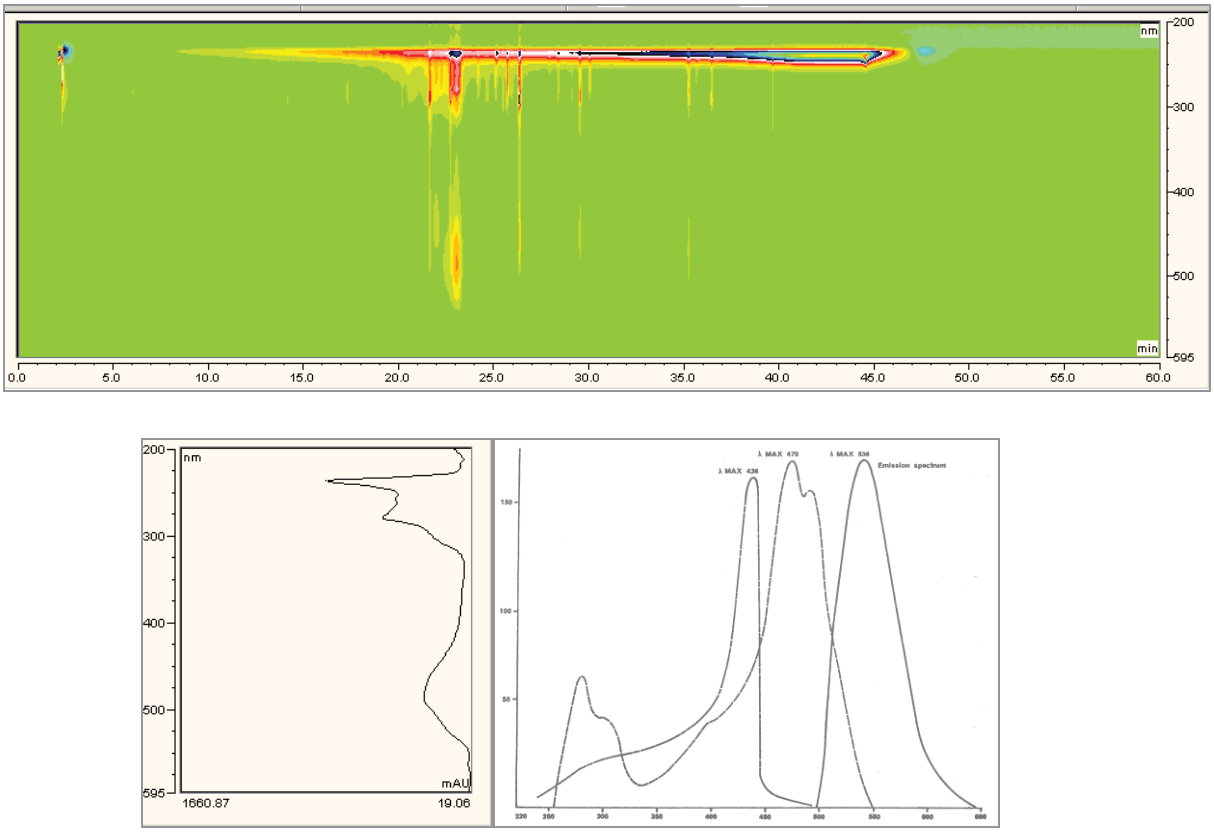

Top: Chromatogram of D. septosporum *broth extract showing a peak corresponding to dothistromin at 23.1 minutes. Bottom left: UV Spectrum of 23.1 minute peak. Bottom right: Previously determined UV absorbance, fluorescence excitation, and fluorescence emission spectra of dothistromin, from 220 to 650 nm (Reproduced from Franich, 1981).*

The dothistromin peak was identified by comparison of elution time with that of a purified dothistromin sample. Further confirmation was made by comparison of the 23.1 minute peak's UV-VIS spectrum with known spectra for dothistromin (Franich 1981).

For fluorescence detection, excitation and emission peaks of dothistromin were established using a broth extract sample in which the principle component had been established by TLC as dothistromin (as per methods 2.2.5, see Fig 4.1). This gave a peak excitation wavelength of 470 nm and and a peak emission wavelenth of 545 nm. These values agree with previously published spectra (Franich 1981). Initial testing

found fluorescence detection was able to detect dothistromin at lower levels than UV-VIS absorbance, and showed a lower noise floor. Trials also showed that fluorescence was able to accurately detect dothistromin from single lesion samples, whereas UV-VIS was not (see Fig 4.5).

Fig 4.5: HPLC detection

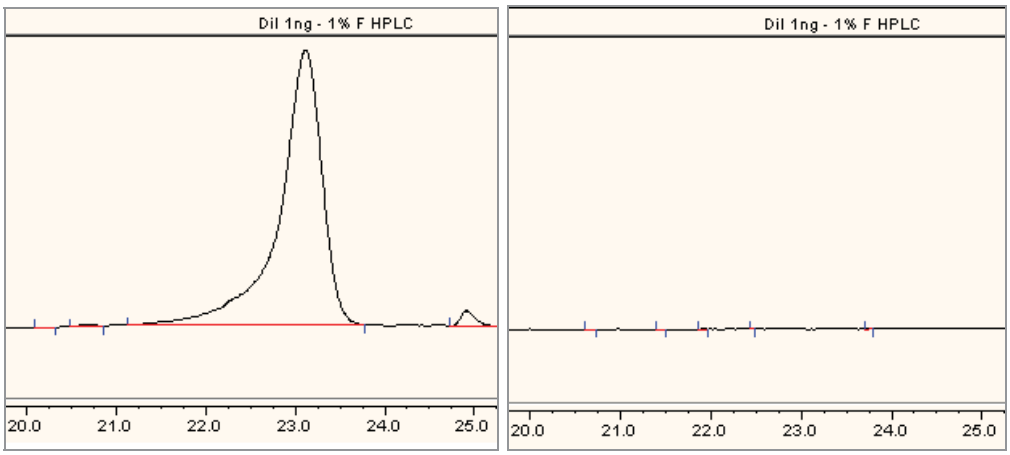

Left: The 23.1 minute dothistromin peak from a Dothistroma *lesion visualised by fluorescence. Right: UV-VIS chromatogram of the same sample (310 nm).*

Because of this increased sensitivity fluorescence detection was the HPLC quantification method of choice. The sensitivity and consistency of dothistromin detection and quantification by fluorescence was tested using a dilution series. The dilution series was performed using eight serial 10-fold dilutions of a purified sample to give standards of between 10 µg and 1 pg, allowing comparison of sensitivity to that of TLC.

Fig 4.6: Fluorescence detection dothistromin dilution series

A

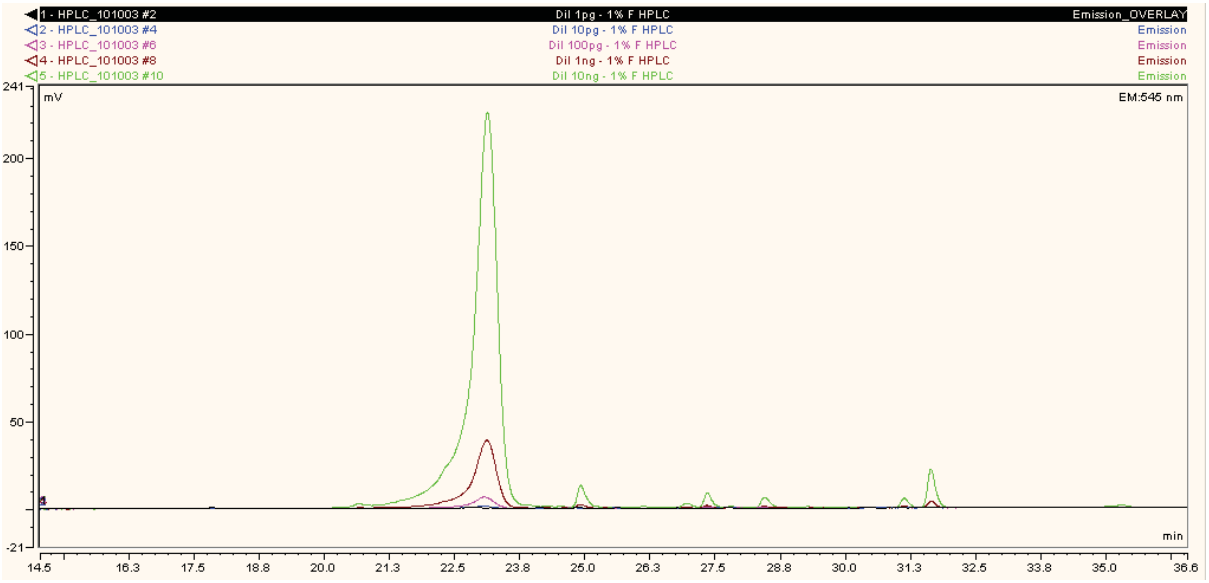

B

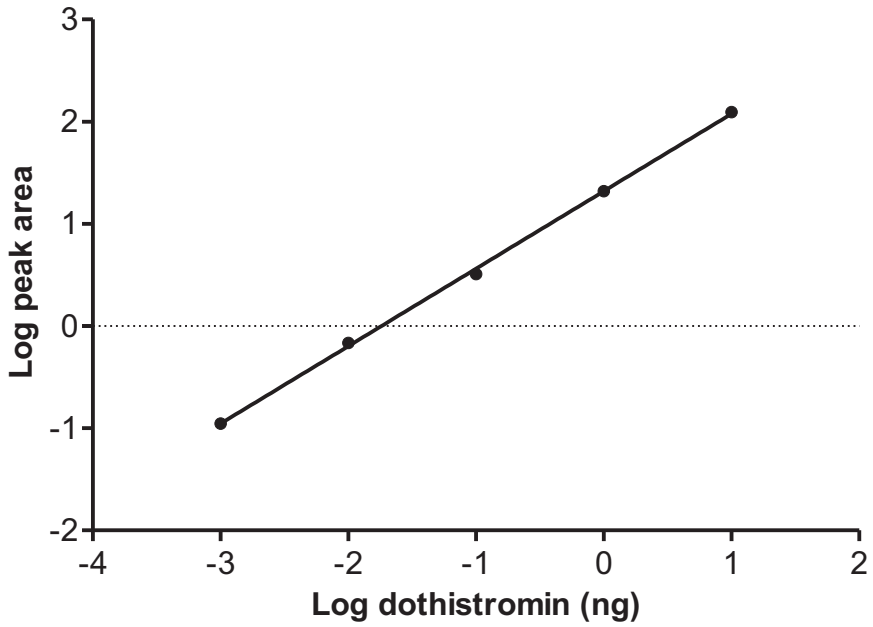

A) Chromatogram overlay of standards from 10 ng to 1 pg.

B) Graph of quantifiable standard peak area (10ng to 10 pg). Despite low standard deviation between samples and high R^2 value of the linear regression (0.9993), peak area is not directly proportional to dothistromin weight. This was also seen for UV-VIS (results not shown) and may indicate error in the standard dilution series.

Table 4.2: Fluorescence peak area of dothistromin HPLC standards

Standard	10 ug	1 ug	100 ng	10 ng	1 ng	100 pg	10 pg	1 pg
Peak area (av.)	OVER	OVER	OVER	124.171	20.902	3.218	0.683	0.111
SD	-	-	-	6.440	0.481	0.076	0.086	0.122

Peak area of dothistromin standards 10 ug to 1 pg. Fluorescence response from some samples was greater than the upper limit of quantification, peak area for these samples is shown as OVER. Standard deviation (SD) is shown for two replicates.

As little as 10 pg of dothistromin per injection was detectable by fluorescence, and peak area per dothistromin weight was linear down to this level (See Fig 4.5 B). Peaks were not detectable above background noise in the 1 pg sample (see SD figures, Table 4.2). Sample repeats showed an average standard deviation of 5.6%, though this figure was skewed by the higher standard deviation of the 10 pg sample, at 12.6%. The range of quantification using this methods was between 10 ng and 10 pg, although the standard curve suggests that the upper limit is closer to 800 ng. This range could be extended considerably by using UV-VIS to quantify high concentration samples, as UV-VIS and fluorescence readings can be taken concurrently. Tests with *Dothistroma* lesion extracts showed that this HPLC method was capable of separation adequate to give quantification of dothistromin in lesion samples (see appendix 8.7).

To confirm the identity of the 23.1 minute peak, samples of purified dothistromin, *Dothistroma* broth extract, and needle lesion extract samples were subjected to LC-MS by AgResearch (methods 2.2.7). Formic acid concentration was reduced to 0.3% to increase solvent volatility, but this did not have a noticeable effect on peak shape (results not shown). The dothistromin peak was seen at 24.5 minutes, and its identity confirmed by UV-VIS spectrum, fluorescence, and MS fragmentation. This variation in retention time is due to the different equipment used (methods 2.2.7).

Fig 4.7: Mass spectrum of dothistromin peak

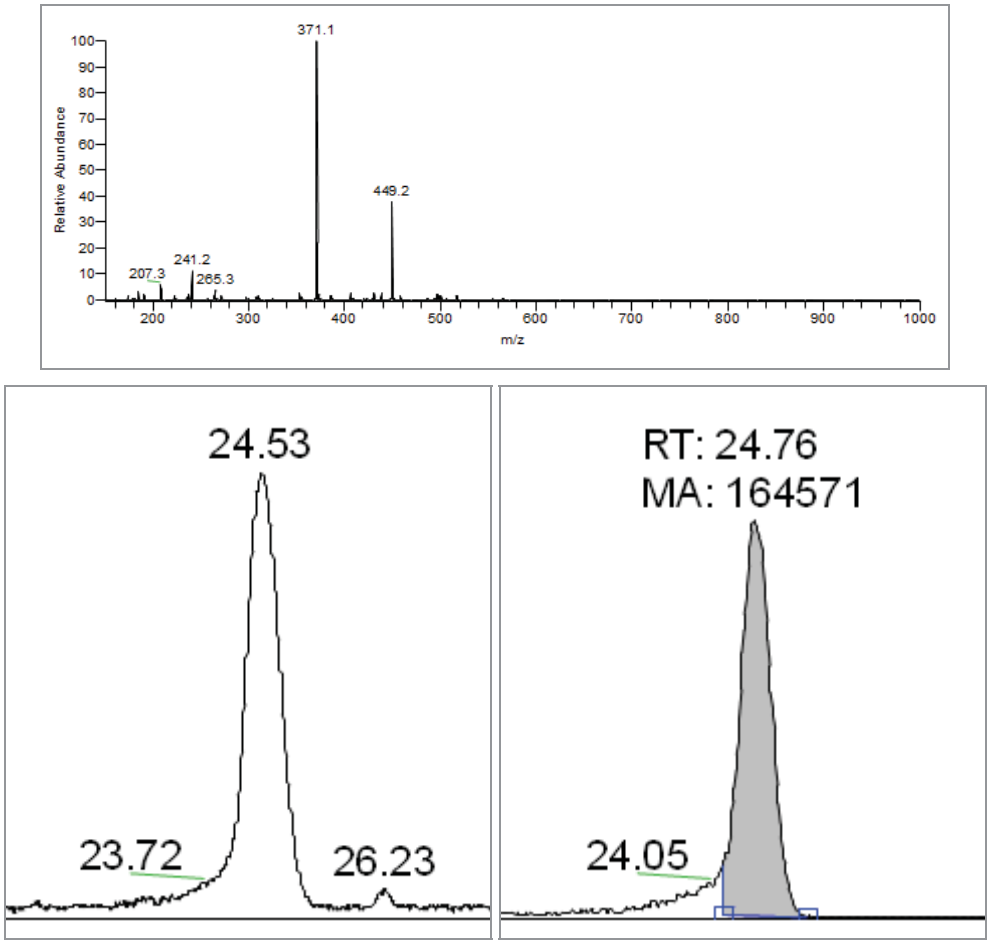

Top: MS1 spectrum of HPLC peak in purified dothistromin sample, m/z 371 is dothistromin. Other ions present were also found in a water blank, indicating that they are background contaminants possibly resulting from column bleed. Bottom left: Fluorescence peak. Bottom right: Targeted MS peak.

MS did not show unexplained contaminating compounds in the peak, confirming peak identity in samples tested. This work also concurred with the conclusion that UV-VIS was a much less sensitive detection technique for dothistromin than fluorescence.

4.2.4 Internal standard

The original plan of research called for the use of an internal standard to enable the calculation of dothistromin extraction losses. Caffeic acid was tested based on the suggestion of Robert Franich (personal communication), and was found to adequately separate under the final TLC and HPLC protocols (seen as bright blue fluorescence of lower Rf in TLC, figure 4.2, HPLC separation appendix 8.6). Detection was found to be possible with UV-VIS, and its absorbance spectrum matched published spectra (Cornard, Caudron et al. 2006; Cornard and Lapouge 2006). However, quantification

based on fluorescence in tandem with dothistromin fluorescence quantification was not possible within a single run due to limitations of the instrumentation used. The emission and excitation peaks of caffeic acid have little overlap with dothistromin, and only a single emission/excitation was able to be measured per run. TLC quantification is not limited in this way since the measurement equipment uses broad-spectrum illumination and detection.

4.2.5 ELISA

Sensitivity of the previously used ELISA protocol was compared with TLC and HPLC protocols by running the same 10x dilution series (10ug to 1pg) in triplicate. Limitations of the protocol meant that samples were diluted a total of 33.3×, final concentrations are shown in Fig 4.6 and Table 4.3 below.

Fig 4.8: ELISA dothistromin dilution series

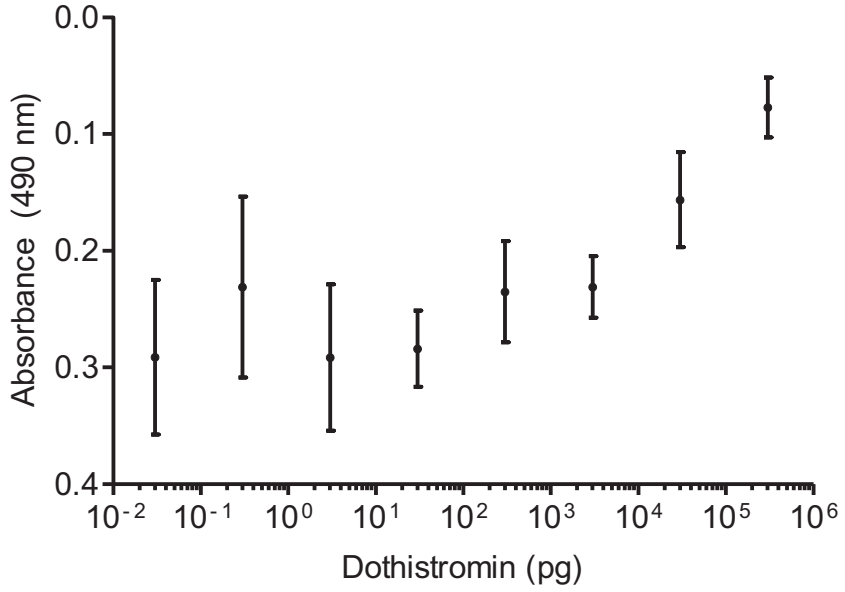

Average absorbance at 490 nm of ELISA assay wells for standards 30 fg – 300 ng (left to right, 9 replicates over 3 plates). Bars show standard deviation.

Table 4.3: Absorbance of ELISA Standards

Standard	300 ng	30 ng	3 ng	300 pg	30 pg	3 pg	300 fg	30 fg
Average	0.0773	0.1564	0.2311	0.2352	0.2840	0.2916	0.2312	0.2913
SD	0.0256	0.0407	0.0264	0.0434	0.0326	0.0627	0.0775	0.0662

Average absorbance values for ELISA standard curve at 490 nm.

Plate readings for the ELISA dilution series showed higher standard deviation than was expected based on previous work, even over a large number of replicates. This may indicate that the accuracy of the assay is more dependent on the operator than other methods tested. While this high standard deviation would make accurate quantification difficult at dothistromin levels of less than 3 ng, Fig 4.8 indicates that as little as 300 pg and as much as 3 µg dothistromin could be quantified if sample variability could be decreased.

A major disadvantage of this assay is the large amount of time taken; over 10 hours of incubations alone (see methods 2.2.4). Including setup time, performing a set of ELISA assays takes a minimum of two full days. It does have the advantage of high-bandwidth; after a 10 point standard curve each plate can take 33 samples (assuming the assay is run in triplicate).

4.2.6 Summary of tested methods

A comparison of the methods tested in shown in the Table 4.4. Methods were judged based on their sensitivity, accuracy, and difficulty (both in time taken and dependence of results on the experience of the operator).

Table 4.4: Dothistromin quantification methods summary

Method	Lower limit	%SD	Time taken (hours)	Operator dependence
TLC	100 ng	25%	2 (1.5)	+
HPLC	10 pg	5.6%	2 + 1 per sample (2)	-
ELISA	300 pg	22%	16 (5.5)	++

Lower limit shows the lowest quantifiable amount tested, actual lower limit may be lower. Percentage Standard deviation (SD) values are an average over all samples in the quantiifiable range. Time taken shows total time taken to run the assay, not including solvent extraction (72 hours). Time in brackets indicates the amount of this time which is 'hands on', as opposed to incubation or unattended.

Overall, HPLC using fluorescence-detection was considered the most effective technique for quantification of dothistromin at low levels. Both the range and lower limit of quantification was much improved over that which was seen using the TLC method, and variability between results was considerably lower than that seen for TLC or ELISA methods. Despite this, TLC and column chromatography based on TLC-

methods were found to be useful for preparative separation of dothistromin from other secondary metabolites of *Dothistroma* (results not shown, separation as per Fig 4.2).

4.3 Discussion

Testing of solvent extraction methods showed that insufficient acidification was responsible for the TLC streaking and accumulation of oily compounds seen in previous work (Zhang, unpublished). This streaking is caused by the ionisation of the dothistromin molecule. Ionised dothistromin has a lower TLC mobility on the system tested, and can also bind cell wall components (i.e. lipids), leading to the formation of the oily compounds (Franich, personal communication). Because streaking and formation of oily compounds inhibits accurate and repeatable separation and quantification, dothistromin ionisation must therefore be kept to a minimum by acidifying both extraction solvents and mobile phases. The initially used 1% acetic acid was shown to be insufficient, and while increasing acetic acid concentration to 5% decreased streaking (Fig 4.1), this concentration gave an unacceptable reduction in solvent volatility. The use of 1% formic acid (as previously used by Debnam and Quach) allowed faster evaporation and gave comparable reductions in dothistromin ionisation. The formic acid content of the HPLC mobile phase was dropped to 0.3% for MS work because solvent volatility was still considered too low for the ElectroSpray Ionisation (ESI) system used. This reduction in acidity does not appear to have affected the MS results, as comparison of dothistromin peaks in purified samples show little difference whether 1% and 0.3% formic acid is used (results not shown). The fluorescence and MS dothistromin peaks obtained by AgResearch are considerably more symmetrical than peaks obtained with our equipment (compare Figures 4.6 and 4.7). This may be due to their use of a UHPLC (Ultra High Performance Chromatography) system. UHPLC systems use finer particles in the stationary phase, giving better resolution. Because this increases the pressure required, UHPLC columns are narrower and consequently require a smaller injection volume. Column condition may also play a role in peak shape.

The selection of a TLC method for comparison to HPLC represented a compromise between resolution and sensitivity. A mobile phase of 1:1 ethyl acetate:dichloromethane was chosen because the focus of TLC testing was on detection of low levels of dothistromin. It is likely that quantification of higher quantities of

dothistromin by TLC would be better performed by a 50:3 chloroform:methanol system, as this gives better separation of dothistromin from other *D. septosporum* metabolites. At higher dothistromin concentrations the diffuse band is an advantage rather than a disadvantage, as it reduces self-quenching of fluorescence. Self quenching occurs where the concentration of the fluorescent molecule is high enough that molecules can interact to form a non-fluorescent complex. This self quenching is seen as a dark interior of dothistromin bands in Figs 4.2 and 4.3. The chloroform:methanol strip does not show visible self-quenching at this concentration. This could give the chloroform:methanol system a greater range of detection, even if it is less sensitive. Although TLC can be very sensitive under the right conditions (Franich, personal communication), specialised equipment for the sensitive and accurate detection of TLC fluorescence is unavailable in many laboratories. The equipment used for imaging of TLC plates in these experiments does not allow fluorescence detection based on specific excitation and emission wavelengths, and it was shown that the use of a modern digital camera and separate UV illuminator gave lower background (4.2.2). While this method could improve sensitivity, it was difficult to keep experimental conditions consistent, and results were therefore unreliable. The Biorad Geldoc equipment gives much greater consistency in imaging conditions, and was used for all quantitative TLC imaging. Even with the Biorad Geldoc, relative standard deviation was high. This may be due to the high level of background noise (seen in Fig 4.3), which was not seen to as great an extent on images taken with the Canon 20D. This may be due to weaker illumination; irrespective of lamp power, the Biorad Geldoc illuminates from behind the plate, whereas for imaging with the Canon 20D the plate was illuminated from above.

HPLC was found to give greater sensitivity than TLC with the equipment used. As little as 10 pg of purified dothistromin was able to be detected by the HPLC fluorescence detection, giving a lower limit than with previous fluorescence work (Briggs 1985). This may be due to the more modern equipment used. Compared with TLC, HPLC equipment is relatively abundant, as it is a more commonly used quantitative technique. This allows the use of more sophisticated equipment for detection, which likely accounts for some of the difference in sensitivity between the HPLC and TLC methods tested. HPLC also has the advantage that results are more operator independent. TLC is largely a manual process, involving spotting samples, drawing solvent fronts, and imaging plates. These manual processes allow for variation in results based on differences in operator skill and preference. HPLC is almost entirely

automated after the determination of a separation and quantification method. While there is still operator involvement in quantification, such as manual peak adjustment, there is far less possibility of operator-based variance in results. HPLC could also be considered less time consuming than TLC. While TLC gives faster results for multiple samples, since samples can be run in parallel, the automation of HPLC means that after the initial setup operator input is minimal. Additionally, the gradient used in the final method could be shortened greatly if it is to be used solely for quantification of dothistromin. This could involve sharply increasing the gradient after dothistromin elution, reducing equilibration time, starting the gradient at a higher percentage acetonitrile, and possibly decreasing the time over which the gradient is run. The latter two modifications may affect separation of dothistromin from other compounds, and any time optimization of the method should involve testing

The advantages of the HPLC methods over TLC methods for separation and quantification were not unexpected. HPLC is a much more modern technique, and has all but replaced TLC for quantification of dothistromin-related compounds. A search of current literature reveals a great number of publications on HPLC aflatoxin quantification schemes in the last decade, but only a handful using TLC methods. While the sensitivity of TLC-based fluorescence quantification of dothistromin could be improved by the use of High Performance TLC (HPTLC) type plates of smaller particle size, mechanical dosimeters for TLC spotting, and improved detection systems, this would eliminate the main advantage of the TLC system; that it can give quick and cost effective results.

Using ELISA for quantification of dothistromin has advantages and disadvantages; key among the latter being the impracticality of obtaining more dothistromin antibody. As with previous work (Schwelm, Barron et al. 2008), the ELISA method was found to give highly variable results. Despite this it is very sensitive, and the specificity of the dothistromin antibody means that extraction of dothistromin from broth is not necessary. While the extraction process is required for quantification by both HPLC and TLC methods, the time taken is very 'hands off', and could be reduced through further testing. Quantification of dothistromin in *Dothistroma* needle lesions would require solvent extraction, but this has not been tested. While standard deviation of results was high in tests of this assay, this may be due to higher dependence on the operator.

The accuracy of all of these methods is dependent on the accuracy of the standards used. The 'pure' dothistromin standard used shows some minor impurities under HPLC using fluorescence (see Fig 4.5) or UV-VIS absorbance. The presence of these impurities would lead to higher standard weight per dothistromin response, and therefore to higher than actual results in dothistromin quantification based on these standards. While the effect is likely to be minimal, preparative TLC or column chromatography could be used to create a dothistromin standard of higher purity. Peak area was not directly proportional to in the HPLC standard curve under fluorescence or UV-VIS. This may be due to additive inaccuracy in the dilution series. While calibrated pipettes were used for all dilutions, the sort if additive error may be difficult to avoid over a long dilution series. For future work, accuracy of low level quantification could be improved by the use of a single standard produced by one dilution as opposed to a standard curve.

The use of an internal standard was proposed as a way of determining extraction losses of dothistromin and as a replacement for an external purified dothistromin standard in regular testing. Caffeic acid was not able to be used for this purpose in the final HPLC-fluorescence method because of limitations of the equipment used, but it could be used as a standard for TLC-fluorescence or HPLC-absorbance quantification. The lack of an internal standard in the final method means that extraction losses are not compensated for. However, an internal standard would not be able to fully quantify loss of dothistromin during extraction from needle tissue. It is possible that caffeic acid could be 'spiked' into the needle tissue, but this is likely to be more easily extractable than dothistromin produced by *Dothistroma* within the plant tissue, and would therefore not be completely representative of extraction efficiency.

In conclusion, the HPLC-fluorescence quantification method developed gives the most accurate quantification of dothistromin at levels seen *Dothistroma* lesions. While this method is currently time consuming, automation of the method means that the majority of the time taken is 'hands off', and further development of the method will make it not only quicker, but potentially more accurate.

Chapter 5: Dothistromin *In Planta*

5.1 Introduction

Establishing the stage of infection at which dothistromin is produced is a crucial step in determining its role *in planta*. In broth culture dothistromin production is highest during the early logarithmic phase (Schwelm, Barron et al. 2008). However, a definitive relationship between dothistromin production and needle lesion development has not been determined. The production of dothistromin mainly during early lesion formation would be consistent with studies of broth culture, and would fit well with the hypothesised role of dothistromin as a competition factor.

Dothistroma septosporum shows an extremely low infection rate with artificial innoculation systems (generally less than 10%, (Barron 2006)). While improvements are being made to inoculation methods (Kabir, unpublished), the low number of initial lesions formed meant that it was not possible to establish a synchronised infection. Furthermore, since lesion size and rate of development can be highly variable (Bulman, Ganley et al. 2008), time since inoculation was not considered a reliable measure of disease progression. Instead, time since the appearance of the lesion was used.

Correlation of dothistromin levels with *Dothistroma* biomass required extraction of both dothistromin and DNA from a single lesions. DNA extraction and HPLC-fluorescence quantification techniques previously developed (chapters 3 and 4) were employed to determine the relationship between these factors *in planta*.

5.2 Results

5.2.1 Lesion Development and Categorization

A *Pinus radiata* seedling, which had been inoculated with *D. septosporum* NZE10 spores (as per material and methods 2.3.1), was used to develop a time course of

D. septosporum symptom development. Needles thought to be showing early symptoms of *D. septosporum* infection were labelled with the date of the first visual symptom occurrence, with the intent of using the time since first disease symptoms as representative of lesion development. However, development of symptoms in these lesions appeared highly variable, and this plan was abandoned in favor of quantitative real time PCR determination of biomass (methods 2.3.3). At 42 days post inoculation both labelled needles and needles with visible lesions at any stage of infection were cut from the plant and examined by light microscopy. When examined under the microscope many samples identified as *Dothistroma* lesions by the naked eye were found to be due to physical damage to the needle, infection by other microorganisms, or inconclusive (examples in Fig 5.1). Early stage infection was particularly difficult to identify visually due to the absence of the characteristic red band at this stage.

Fig 5.1: Variation in microscopic appearance of samples

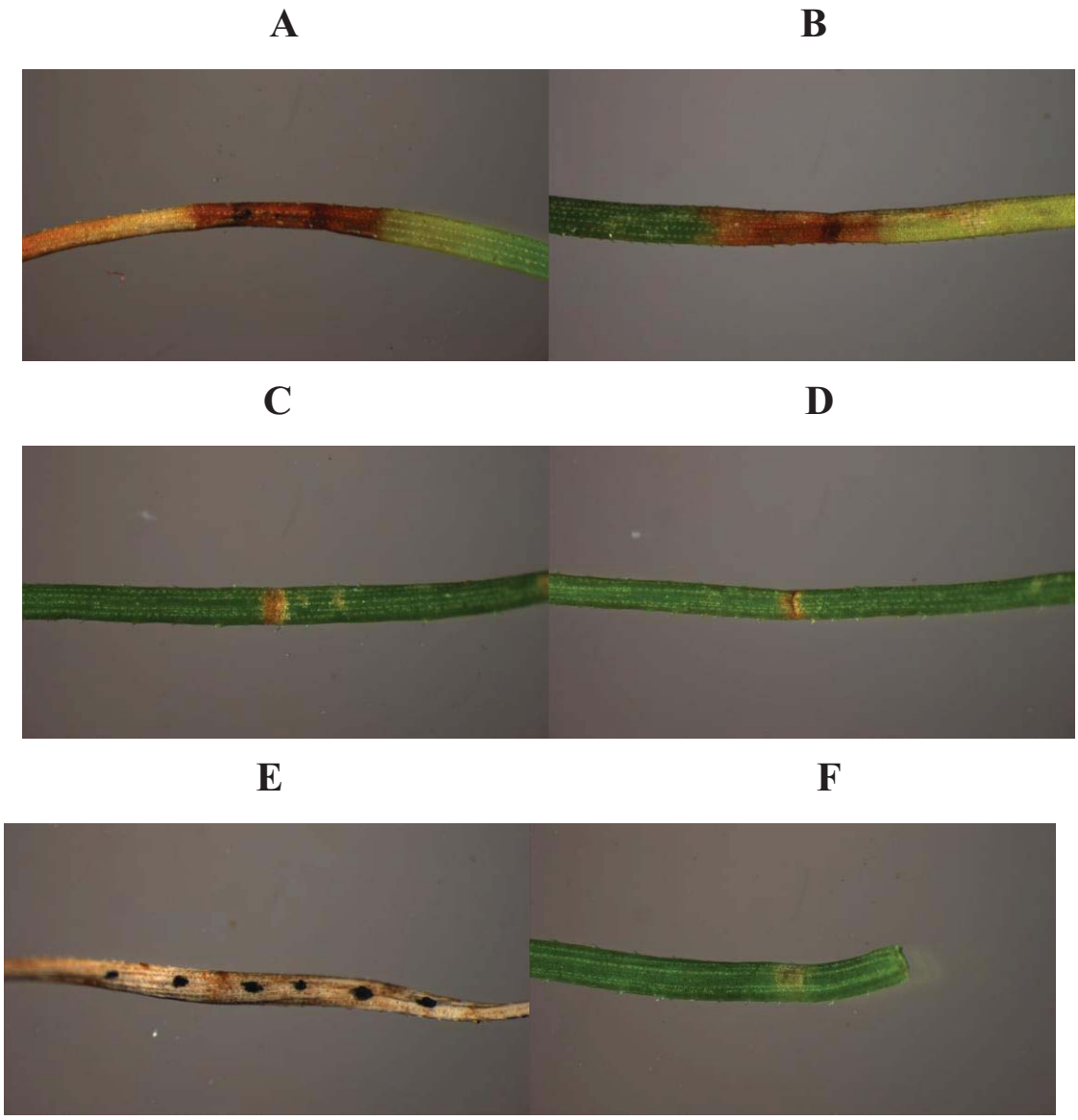

A) Image of sample 42, showing a large lesion containing fruiting bodies. B) sample 1, showed a large lesion, but no visible fruiting bodies. C, D) Samples 24 and 14, respectively, showing a similar small discolourations. The latter shows signs of physical damage to the needle. E) Sample 69, in which a band is not visible and fruiting bodies appear different to those seen in D. septosporum lesions (i.e. sample 42). F) Sample 8, showing light discolouration consistent with early stage lesion formation.

Samples were categorized based on visual features identifiable under the microscope. Features identified were; the presence of a red band consistent with *Dothistroma* infection, appearance of fruiting bodies in this band, physical damage to the needle (ie bends), and signs of infection by other fungi. This gave six main groups:

1) Discoloured, showing light discolouration consistent with early lesion formation (Fig 5.1F, sample 8).

2) Small-band (less than 5 mm), showing a darker but unextended band (Fig 5.1C, sample 24).

3) Large-band (greater than 5 mm), with a full size red band (Fig 5.1B, sample 1).

4) Large-band w/ fruiting bodies, showing a large band with protruding fruiting bodies (Fig 5.1A, sample 42).

5) Other Fungi, which show evidence of fungal infection other than *Dothistroma* (Fig 5.1E, sample 69).

6) Physical Damage, where banding is centred on needle damage such as a bend (Fig 5.1D, sample 14).

Based on their appearance, lesion samples were also classified as probably being caused by *Dothistroma* (groups 3 and 4), probably not being caused by *Dothistroma* (groups 5 and 6), or uncertain (groups 1 and 2). Unfortunately, visual classification did not end up giving much in the way of useful information. This is clarified further in the discussion.

5.2.2 PCR Biomass Quantification

Fifty of 107 needle samples were selected based on their likelihood of being *Dothistroma* lesions, but including a representative sample from each of groups 1-6. DNA was extracted from these needle samples using the method developed in chapter 3 (methods 2.1.6). Precipitated cell debris and chloroform waste were saved for dothistromin extraction. Extracted *D. septosporum* and *P. radiata* DNA was quantified by quantitative real-time PCR developed and run by Dr Rebecca McDougal (methods 2.3.3). Nearly all samples showed amplification under this scheme, though mostly at very low levels (below the range of the standard curve). This low level amplification was likely due to the presence of fungal material on the needle surface. Using *D. septosporum* specific primers, *Dothistroma* DNA concentration was determined based on a standard curve. In general, samples which had been categorized as probable

Dothistroma lesions after light microscopy (groups 3-4) were found to amplify more strongly than those classified as physical damage or other infection (groups 1, 5, and 6). This indicated greater *D. septosporum* biomass in samples from groups 3-4.

Fig. 5.2: Amplification of sample sets

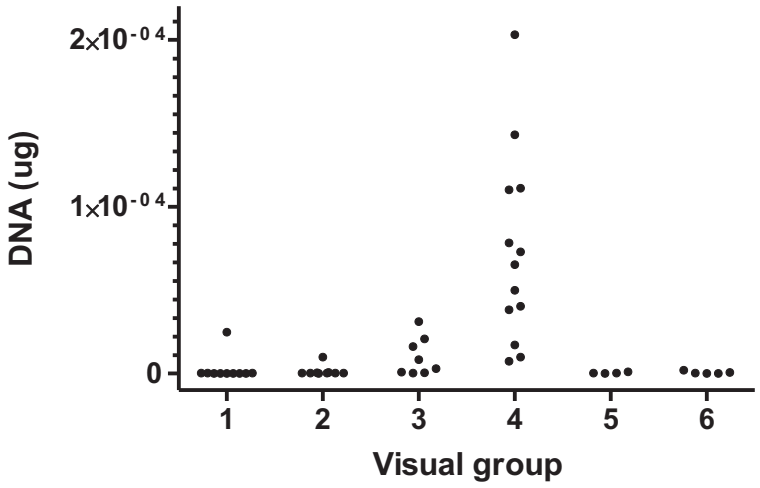

D. septosporum *DNA concentration is shown for samples from different visual groups. DNA concentration was determined by qPCR based on a standard curve, and should be representative of* Dothistroma *biomass in these samples. Because distribution was over several orders of magnitude, low values are shown clustered around zero. Very few samples did not show a detectable level of amplification.*

On average, more DNA was extracted from needle samples with well defined lesions that showed fruiting bodies. Samples with well defined lesions but without fruiting bodies generally showed less DNA, but were mostly within the range of quantification (1 ng - 1 pg). Samples from the other groups were mostly below the range of reliable quantification. Values below 1 pg were considered likely to be caused by contamination on the needle surface, and values lower than 0.1 pg were below the lower limit of the standard curve.

5.2.3 Dothistromin-biomass relationship

To obtain both DNA and dothistromin from the same samples, dothistromin had to be extracted from the otherwise discarded components of DNA extraction; precipitated cell debris and chloroform from DNA purification. A solvent extraction

similar to that used for broth was found to be successful, involving the same incubation with acidified ethyl acetate. Following this the extraction solvent from precipitated cell debris and from chloroform was pooled and evaporated, allowing resuspension of individual samples for HPLC-fluorescence quantification (methods 2.2.6). Dothistromin from individual lesions was found at levels close to and below the limit of quantification determined by a standard curve, ranging from 0.62 ng to 377 ng. While dothistromin levels were generally elevated in lesions with more obvious disease symptoms, a number of lesions with high PCR-biomass showed little to no dothistromin. This may be due to unseen errors in dothistromin quantification, such as unexpected retention time variation, and analysis of additional samples is required before any definite conclusions can be made. The presence and size of other fluorescence peaks varied greatly between samples, something not seen in methods development (Appendix 8.7). This may indicate changing metabolic conditions in the needle or fungus during lesion development. While none of these peaks prevented dothistromin quantification, their presence could have contributed to masking of any unexpected variation in retention time. Dothistromin content by visual group was otherwise similar to that for PCR-biomass.

Fig. 5.3: Dothistromin content of samples by group

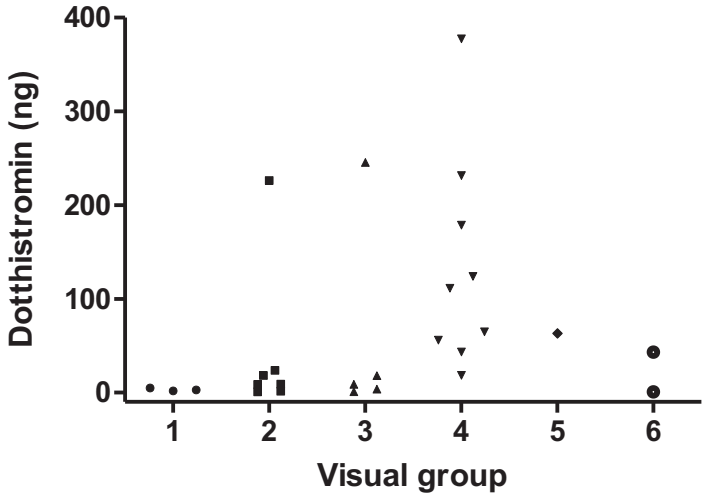

Dothistromin content of non-zero samples, organised by visual groups.

The similar grouping of PCR-biomass and dothistromin levels was expected, and indicates that the correlation between *Dothistroma* biomass and dothistromin seen

in broth culture (Schwelm, Barron et al. 2008) may also be seen *in planta*. This was investigated further by direct comparison of PCR-biomass with dothistromin content. Because the DNA and dothistromin content of samples varied over several orders of magnitude, a logarithmic plot of the two values was found to give the best representation of the results. While plotting logarithmically did not allow incorporation of zero-values into the data, a linear plot gave little in the way of useful information.

Fig. 5.4: DNA vs. Dothistromin

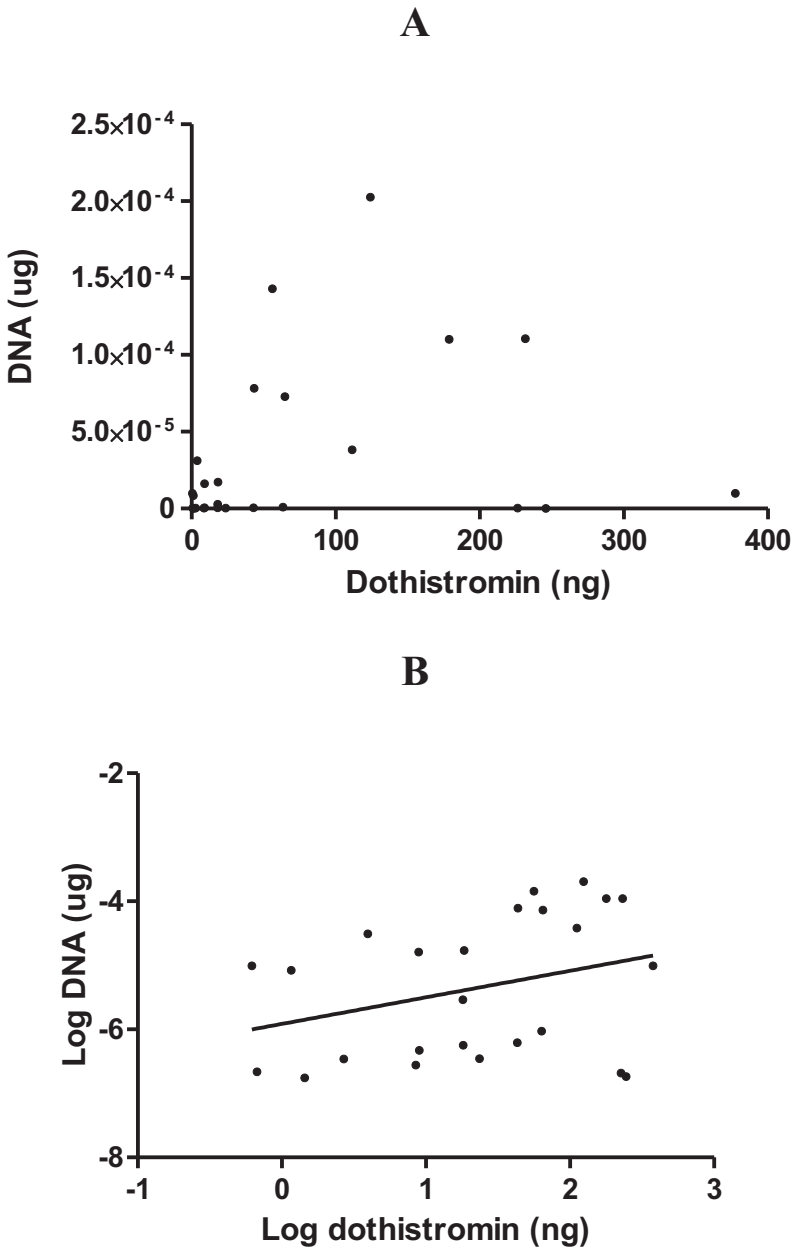

A) Linear plot. B) Log plot. Plotting the log of sample DNA against the log of sample dothistromin shows a possible correlation, but the trend-line shown was not found to be statistically significant.

A least-squares trend line was mapped to the log-transformed data, but was not found to be statistically significant (R^2 = 0.1013). The lack of statistical significance means that a greater sample size will be required for real conclusions to be made on the presence or absence this correlation.

5.3 Discussion

While the groundwork has been set for further work on characterising the production of dothistromin *in planta,* due to unexpected complications this experiment proceeded very differently from how it was initially planned. The original plan was for a time course of *Dothistroma* biomass and dothistromin during secondary infection, whereby infected needles were identified at an early stage and tagged to establish the time since appearance of first symptoms. This would have enabled an assessment of disease development over time and allowed the comparison of *in planta* results with those obtained from broth work. By tagging newly developed lesions as they appeared during an infection cycle, then harvesting and analysing all samples at the same time, it was hoped that a complete picture of lesion development over time could be established. While synchronized infection would be preferable from a logistical and experimental standpoint, current methods offer an extremely low infection rate (Barron 2006), making synchronized infection of large numbers of samples extremely difficult. Current work by PhD student Md. Shahjahan Kabir is aimed at increasing the infection rate of *D. septosporum* in assay systems, and this may allow synchronized infection in future experiments. With the system used, initial tagging appeared to be successful, however many tagged 'lesions' did not develop further, and a large proportion of these were later found to not actually be *Dothistroma.* Even when examined under a light microscope, a large number of early stage lesions could not be confidently distinguished from physical damage or needle discolouration (and vice versa), even by experienced examiners. This is one of the key problems which must be addressed before an accurate *Dothistroma* time course can be established. Unless a high-percentage infection system can be developed, the most effective way of overcoming this problem in future research would be to take a large number of samples and establish the presence or absence of *Dothistroma* by quantitative real time PCR.

While PCR-based identification of infected lesions would greatly simplify the establishment of a time course, the potential presence of *Dothistroma* on the needle

surface could lead to false positives. The dispersal of spores between needles by water, and the initial spore inoculation would leave large amounts of *Dothistroma* DNA on the needle surface. While surface sterilisation has been used to remove *Dothistroma* from the needle surface (Ganley and Newcombe 2006), the use of bleach as a sterilising agent is problematic, as it can rapidly degrade dothistromin. Sterilisation with only ethanol has been found ineffective (Kabir, unpublished), but with further testing it is likely that an effective sterilising agent can be found which is not destructive to dothistromin. Surface sterilisation of time course samples with such a technique would allow much more robust conclusions to be made on the *Dothistroma* content of possible early stage lesions. Equally, the accuracy of low level dothistromin quantification could be improved if an effective surface sterilisation technique could be developed. The presence of *Dothistroma* on the surface of needles means that dothistromin is also likely to be present there; work by Briggs showed that detectable levels of dothistromin or dothistromin containing matter can be deposited on surfaces near *Dothistroma* infection while forestry work is taking place (Briggs 1985). Whether this would occur under the experimental conditions used is unknown. While surface sterilisation is important in preventing low-level false positives, any incorporation of surface sterilisation into a future method should ensure that quantification remains both representative, in that sterilisation does not change levels of quantifiable DNA, and consistent with varying lesion development, in that sterilisation does not affect some stages of lesion more than others. For example, later stage lesions, especially those showing fruiting bodies, may allow greater access of sterilisation chemicals to fungal DNA within the needle because of the physical breakdown of needle tissue.

The changing conditions in the needle may also be responsible for the unexpected and variable appearance of various fluorescence peaks in lesion samples (see appendix 8.7). The varied presence and size of these peaks may indicate changing levels of fluorescent compounds within the needle during lesion development or simply variation in metabolite presence between needles due to unrelated factors (i.e. needle age). While these other peaks are numerous, comparison of retention times with those from *Dothistroma* broth samples may allow their origin to be determined. The use of MS peak data collected from these samples (see chapter 4) could allow their identification. Whether any of these peaks would obscure the presence of dothistromin is uncertain. While some showed overlap with the dothistromin peak (see appendix 8.7), any masking of the dothistromin peak would require a larger variation in retention time

than the ±0.05 minutes seen. Another potential problem is incomplete injection, where less than the full 50 µL is injected. To give maximum sensitivity, the assay was performed using the smallest possible resuspension volume with the equipment available (200 µL). While testing was performed to ensure that this volume was adequate to give a full 50 µL injection, variation in filtration losses could have potentially reduced this volume to below the threshold value required. While the 600-fold variation in dothistromin concentration over the samples tested means that this would have little effect on the overall correlation, future work would be well advised to take a more cautious approach and sacrifice a small amount of sensitivity for increased confidence in results. Additionally, optimization of the protocol to use small volume sample vials would reduce the likelihood of incomplete injection.

Despite these problems, the experiment provided enough data to show that it is possible to correlate *Dothistroma* biomass with dothistromin using single needle lesions. Furthermore, it has given an indication as to the nature of this correlation. While contamination with DNA and dothistromin from needle surfaces may have introduced false positives, these would most likely be found towards the lower end of detection. If this is the case, then any error in the quantification of actual lesions would be minimal, due to the exponential increase in DNA concentration. The lack of a time course makes it difficult to compare results to those obtained from broth culture, but some observations can be made on the relationship between the PCR-biomass and dothistromin content of samples (Fig 5.4). The trend line fit to these results shows an increase in sample dothistromin of approximately 260 fold over a 10 fold increase in DNA amount (i.e. a sample with 1 pg of DNA would have roughly 0.62 ng dothistromin, whereas a sample with 10 pg would have 161 ng). This is far more than could be accounted for by simple accumulation at a constant rate of production (per unit of biomass). If *Dothistroma* biomass can be considered a rough indicator of lesion development, then this indicates that dothistromin production is increasing over time. Since the samples towards the top end of the DNA curve are almost exclusively late stage lesions (see appendix 8.8), this indicates that dothistromin production per unit biomass is highest in these late stage lesions (by approximately 26 fold, not accounting for accumulation). While this does not necessarily discount dothistromin acting as a competition factor, production to inhibit competition would be expected to occur mainly as the necrotic lesion was being established, to prevent colonisation by competing species. However, since the relationship between these factors is not statistically

supported by current data, any conclusions drawn are purely speculative. Further research, either by establishing a time course or by examination of further samples to give statistically significant results, would allow a more solid conclusion to be drawn.

In conclusion, while this work does not support the hypothesis that dothistromin production is highest in early stage lesions, the lack of statistical significance means that neither can it be conclusively disproved without further investigation. To ensure that statistically valid conclusions can be drawn from further work, a greatly increased sample size should be used.

Chapter 6: Bioinformatic Investigation of Related Organisms

6.1 Introduction

Dothistroma septosporum is closely related to the wheat pathogen *Mycosphaerella graminicola*, and it is hypothesised that *D. septosporum* is similar to *M. graminicola* in having a latent phase followed by a necrotrophic phase. While the evolutionary origin of dothistromin production is unknown, finding homologs or related genes in *M. graminicola* could give insight into how dothistromin gene clusters evolved, and possibly even into its function *in planta*. The wealth of genome sequence available for plant pathogens means that bioinformatic location of dothistromin biosynthesis related genes can be attempted in a number of related organisms. Those chosen for analysis are *M. graminicola, M. fijiensis, Cochliobolus heterostrophus, Stagonospora nodorum,* and *Alternaria brassicola*, which are all pathogenic fungi in the dothideomycete class. These organisms are closely related to *D. septosporum,* and have their genome sequences available from the Joint Genome Institute.

6.2 Results

6.2.1 Bioinformatics

The dothistromin *pksA* gene was chosen as the starting point for this analysis. Biosynthesis of polyketide-based secondary metabolites requires a polyketide synthase (PKS) enzyme as an integral part of the biosynthetic pathway, whereas other pathway genes have a less specific function, making them less suitable for cluster location (Keller 2005). Potential homologs of the dothistromin *pksA* polyketide synthase gene were identified by BLASTP against gene models in the target genomes (methods 2.4.1). This gave a large number of hits, most likely due to sequence conservation of the polyketide synthase functional domains. The search was narrowed down by discarding hits with a BLASTP E-value of higher than e^{-50}. It was thought that hits with higher similarity to the *Dothistroma* PksA (and therefore lower E-value) would be more likely

to be part of a related biosynthetic cluster. The numbers of BLASTP hits in each genome with an E-value lower than e^{-50} are shown in table 6.1.

To determine whether these PKS genes were part of a secondary metabolite biosynthesis cluster related to the dothistromin, aflatoxin, or sterigmatocystin biosynthetic clusters, the genomes were examined to find potential pathway genes (i.e. aflR/J homologs) close to selected PksA BLASTP hits. By the proximity and number of these pathway genes, it was hoped that the PksA matches most likely to be part of clusters related to those involved in dothistromin biosynthesis could be selected.

Preliminary investigation with the *M. graminicola* genome determined that the most effective way of finding potential toxin biosynthesis gene homologs in the areas around these genes was a 'brute force' method. All genes within 35 kb of low E-value pkaA hits were aligned against the NCBI database by BLASTP, and hits against known toxin biosynthesis genes from *D. septosporum, A. parasiticus,* and *A. nidulans* were recorded. Thirty-five kb in each direction was chosen as the search area, as this gave 70 kb total, approximately equal to the size of the aflatoxin and sterigmatocystin clusters in *A. parasiticus* and *A. nidulans*, respectively. Based on the number, proximity, and clustering of these hits, one PKS gene from each genome was selected as the most likely to be part of a toxin-biosynthesis gene cluster related to dothistromin, aflatoxin, or sterigmatocystin production.

Table 6.1: Biosynthesis gene matches surrounding potential PKS homologs

Genome	Total PksA BLASTP hits (E-value < e^{-50})	Selected PksA hit	E-value	Toxin gene hits (in area)
A. brassicola	7	AB06180.1	$9e^{-57}$	3
C. heterostrophus	17	PKS19	0	4
M. fijiensis	8	Mycfi1.e_gw1.7.973.1	0	6
M. graminicola	11	PKS7	$1e^{-84}$	4
S. nodorum	13	SNOG_06682.1	$4e^{-74}$	3

The number of PksA BLASTP hits against selected genomes under the threshold value, and the hit selected. The E-value is given for this hit, and the number of potential toxin biosynthesis genes found in the surrounding area (±35 kb) based on BLASTP of gene models against the NCBI database (methods 2.4.2). Other PksA hits and the toxin gene hits around them are not shown.

Examination of predicted domains in gene models in the area around selected PKS genes identified a number of additional gene models with predicted protein domains found in dothistromin, aflatoxin, or sterigmatocystin biosynthesis genes (Yu, Chang et al. 2004; Ehrlich, Yu et al. 2005; Zhang, Schwelm et al. 2007). The selected clusters are shown in Fig. 6.1-6.5. The full protein sequences of gene models within these clusters were aligned with sequences of known toxin biosynthesis genes from *A. parasiticus, A. nidulans,* and *D. septosporum* (methods 2.4.2). The results of these comparisons are shown in tables 6.2-6.6. Cluster genes which have over 15% full protein sequence identity to the gene models shown are shown, along with the copy number of these genes. *Afl** genes are from *A. parasiticus, stc** genes are from *A. nidulans*, and other genes are from *D. septosporum*. Gene copy number in *A. nidulans* is shown in brackets (Carbone, Ramirez-Prado et al. 2007).

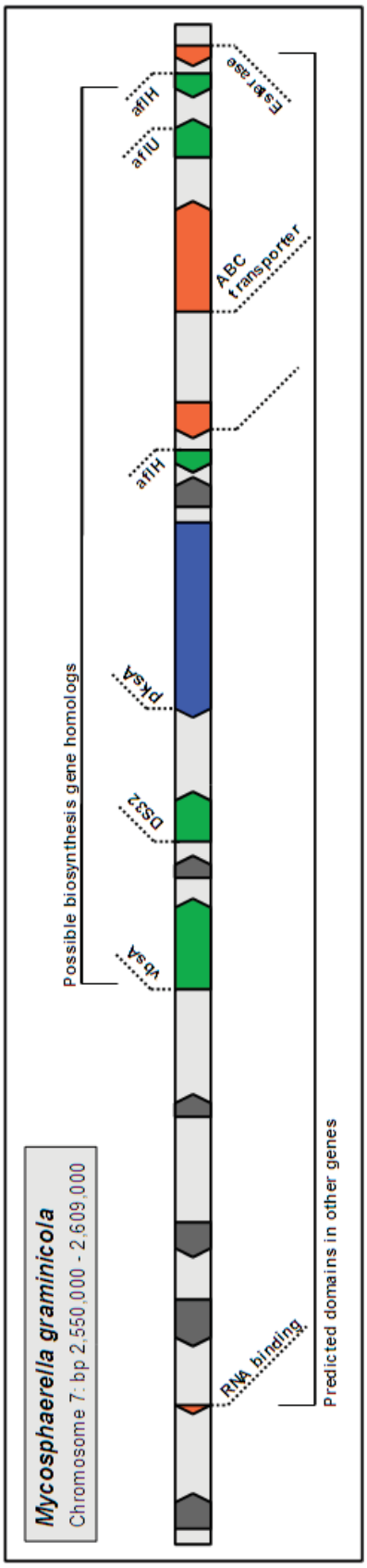

Fig. 6.1: *M. graminicola* PKS7 cluster

Scale representation of gene models in the region surrounding M. graminicola *PKS7, shown in blue. Genes identified based on similarity to toxin biosynthesis genes are shown in green, with potential homologs shown above. Other genes in the area with predicted functional protein domains are shown in orange, with predicted domains below. Genes with no predicted protein domains are shown in grey. This potential gene cluster is located at the end of chromosome 7; secondary metabolite biosynthesis gene clusters are often found in telomeric regions (Keller, Turner et al. 2005).*

The area around *M. graminicola* PKS7 shows a number of gene models with domains similar to those in toxin biosynthesis genes (e.g. Epoxide hydrolase). Despite this, gene identity was mostly either below the 15% cut-off or much lower than that seen between known toxin biosynthesis genes.

Of the genes which showed notable amino acid identity (>15% over the entire sequence), most were from genes whose equivalents show a high copy number in *A. nidulans.* An oxidoreductase showed 35% identity to *vbsA* and 34% identity to *aflK*, but their *A. nidulans* equivalent (*stcN*) has seven copies in the genome. This makes it likely that the gene has a different function, even if it is similar in sequence.

Some gene models showed similarity to genes with low copy number (i.e. *aflH* and *aflM*, whose *A. nidulans* equivalents have no duplicates). In these cases identity was considerably lower than that seen between these genes in known toxin producers (66 and 80 between *D. septosporum* and *A. parasiticus* for *aflH* and *aflM*, respectively; Bradshaw, unpublished).

It is therefore unlikely that this putative cluster produces a secondary metabolite chemically similar to dothistromin, but may have another biosynthetic function.

Table 6.2: *M. graminicola* PKS7 cluster gene models

Gene model name	Predicted domains	BLASTP Hits	Notable AA Identities (> 15%)
fgenesh1_pg.C_chr_7000654	-	-	-
gw1.7.1046.1	RNA-binding region RNP-1	-	-
fgenesh1_pg.C_chr_7000656	-	-	-
estExt_fgenesh1_pg.C_chr_70650	-	-	-
estExt_fgenesh1_pg.C_chr_70651	-	-	-
estExt_fgenesh1_pm.C_chr_70294	Glucose-methanol-choline oxidoreductase	*vbsA*	*vbsA* 35% *aflK* 34%
gw1.7.361.1	-	-	-
e_gw1.7.675.1	Amino acid/polyamine transporter	*DS32*	-
e_gw1.7.2.1 / PKS7	n/a	n/a	None
e_gw1.7.248.1	Taurine catabolism dioxygenase TauD/TfdA	-	-
e_gw1.7.311.1	Short-chain dehydrogenase/reductase SDR	*aflH*	*aflH* 17% *aflM* 21% *stcU* 21% (2) *stcE* 16% (1) *dotA* 21%
e_gw1.7.886.1	Epoxide hydrolase	-	-
estExt_fgenesh1_pm.C_chr_70300	ABC Transporter	-	-
e_gw1.7.194.1	Cytochrome P450	*aflU*	*aflU* 28% *stcL* 21% (2) *aflL* 22% *aflG* 21% *stcF* 22% (4) *aflV* 19% *stcB* 18% (2) *cypA* 18%
e_gw1.7.870.1	Short chain dehydrogenase/reductase SDR	*aflH*	*aflH* 25%
e_gw1.7.928.1	Esterase/lipase/thioesterase	-	-

Gene models in Fig. 6.1, from left to right.

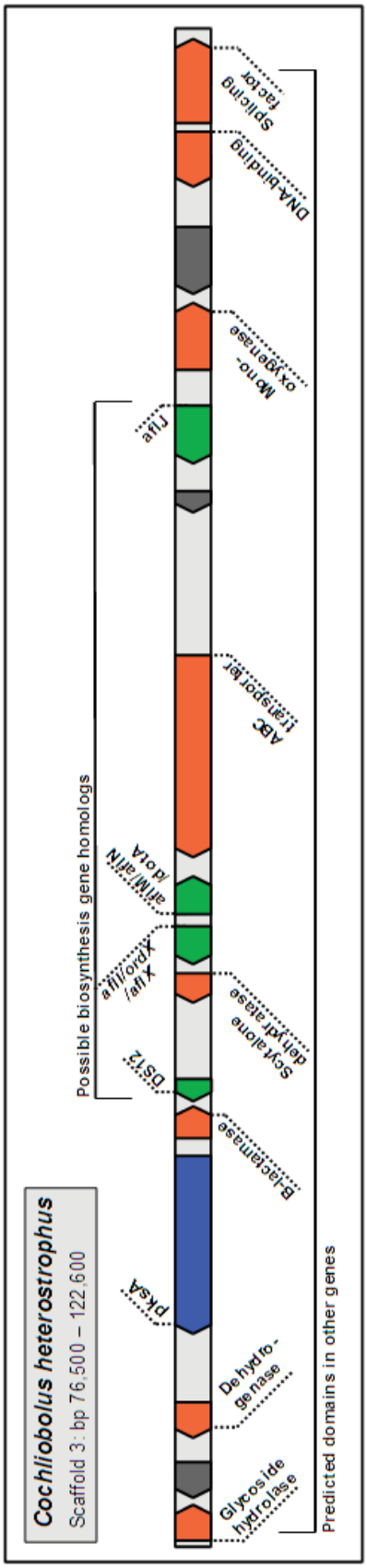

Fig. 6.2: *C. heterostrophus* PKS19 cluster

Scale representation of gene models in the region surrounding C. heterostrophus PKS19. Gene model colours are as per Fig 6.1.

Three gene models from the putative *C. heterostrophus* PKS19 cluster show notable identity to a number of low copy number toxin biosynthesis genes, including the regulatory gene *aflS*. Additionally, the polyketide synthase PKS19 shows higher identity to *D. septosporum pksA* than the PKS genes in the other potential clusters examined, but considerably lower than that seen between PKS genes in known toxin clusters. Other notable amino acid identities are not much lower than between known toxin cluster genes (Mostly around 10%; Bradshaw, unpublished).

While this may indicate that these genes are orthologs of those in *D. septosporum*, the low PKS identity makes it unlikely that this cluster produces dothistromin or a chemically similar compound.

Table 6.3: *C. heterostrophus* PKS19 cluster gene models

Gene model name	Main predicted domains	BLASTP Hits	Notable AA Identities (> 15%)
estExt_fgenesh1_pg.C_30018	Glycoside hydrolase, family 38	-	-
fgenesh1_pg.C_scaffold_3000019	-	-	-
estExt_Genewise1Plus.C_30034	Short-chain dehydrogenase/reductase SDR	-	-
estExt_Genewise1.C_30036 / PKS19	n/a	n/a	*aflC* 28% *stcA* 25% (27) *pksA* 26%
estExt_Genewise1.C_30037	Beta-lactamase like	-	-
estExt_fgenesh1_pg.C_30023	-	*DS12*	-
estExt_Genewise1Plus.C_30042	Scytalone dehydratase	-	-
estExt_fgenesh1_pg.C_30025	-	*ordX*, *aflX*, *avfA*	*aflX* 36% *stcQ* 35% (2) *avfA* 21% *aflI* 21% *stcO* 19% (1)
estExt_fgenesh1_kg.C_30006	Short-chain dehydrogenase/reductase SDR	*aflM*, *aflN*, *dotA*	*dotA* 60% *aflM* 64% *stcU* 63% (2)
e_gw1.3.1026.1	ABC transporter	-	-
fgenesh1_pg.C_scaffold_3000029	-	-	-
estExt_fgenesh1_kg.C_30008	Bacterial regulatory protein, LacI	*aflS*	*aflS* 31%
estExt_fgenesh1_pg.C_30030	Monooxygenase	-	-
fgenesh1_pg.C_scaffold_3000032	Ankyrin	-	-
fgenesh1_pg.C_scaffold_3000033	DNA-glycosylase	-	-
estExt_Genewise1.C_30059	RNA recognition, region 1	-	-

Gene models in Fig. 6.2, from left to right.

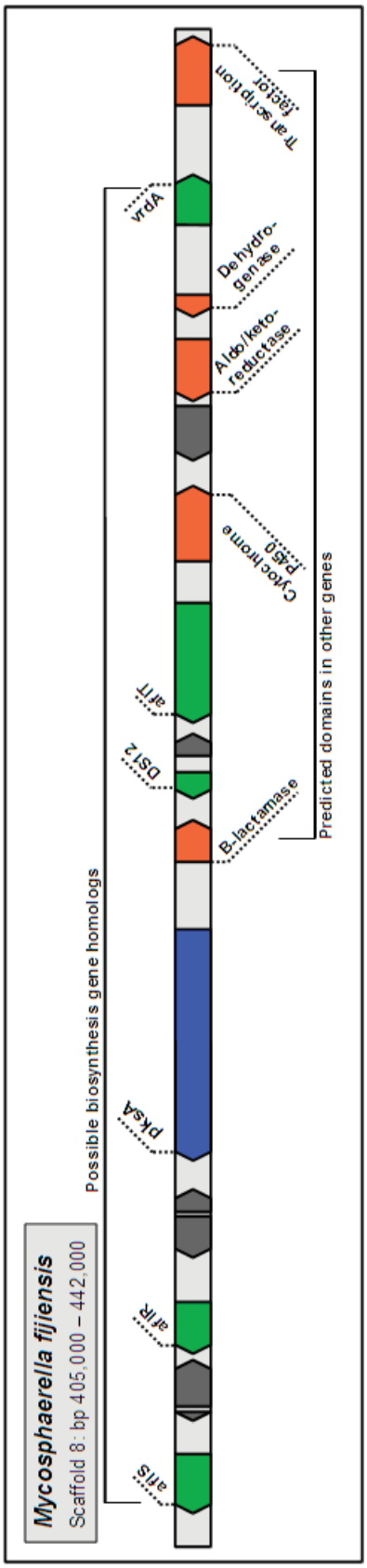

Fig. 6.3: *M. fijiensis* Mycfi1.e_gw1.7.973.1 cluster

Scale representation of gene models in the region surrounding M. fijiensis *Mycfi1.e_gw1.7.973.1. Gene model colours are as per Fig 6.1.*

The putative *M. fijiensis* cluster shows a number of gene models with notable amino acid identity. While not all of the notable identities are to low copy number genes, matches to both toxin regulatory genes (*aflS* and *aflR*) are seen. Additionally, the predicted domains in other gene models are similar to those required for synthesis of polyketide toxins. This indicates that this area is likely part of a secondary metabolite biosynthetic cluster, which may be related to those responsible for polyketide toxin biosynthesis.

Table 6.4: *M. fijiensis* Mycfi1.e_gw1.7.973.1 cluster gene models

Gene model name	Predicted domains	BLASTP Hits	Notable AA Identities (> 15%)
fgenesh1_pm.8_#_59	-	*aflS*	*aflS* 33%
Genemark.8735_g	-	-	-
Genemark.8734_g	-	-	-
fgenesh1_pg.8_#_73	Aflatoxin biosynthesis regulatory protein	*aflR*	*aflR* 27%
Genemark.8738_g	-	-	-
Genemark.8737_g	-	-	-
Mycfi1.e_gw1.7.973.1 / PKS	n/a	n/a	*stcA* 25% (27) *aflC* 28% *pksA* 24%
fgenesh1_pm.8_#_61	Aldehyde dehydrogenase	-	-
Mycfi1.e_gw1.7.445.1	-	*DS12*	-
Mycfi1.e_gw1.7.551.1	-	-	-
fgenesh1_pm.8_#_63	MFS transporter	*aflT*	*aflT* 41% *dotC* 26%
estExt_fgenesh1_pm.C_80063	Cytochrome P450	-	-
estExt_fgenesh1_kg.C_80032	-	-	-
estExt_Genewise1Plus.C_80170	Aflatoxin keto-reductase	-	*aflE* 17%
Mycfi1.gw1.7.397.1	Short-chain dehydrogenase/reductase SDR	-	*aflH* 19% *aflM* 20% *stcU* 21% (2) *aflD* 20% *dotA* 20%
Mycfi1.estExt_fgenesh1_pg.C_70406	Acetate reductase	*vrdA*	*aflE* 23% *stcV* 25% (4)
estExt_Genewise1.C_80178	Transcription factor	-	-

Gene models in Fig. 6.3, from left to right.

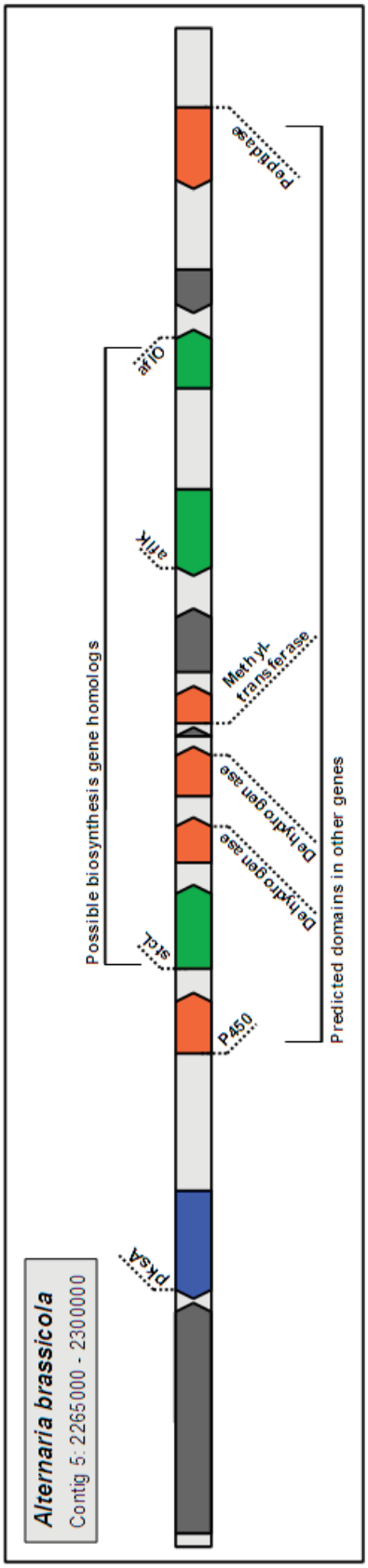

Fig. 6.4: *A. brassicola* AB06180.1 gene cluster

Scale representation of gene models in the region surrounding A. brassicola *AB6180.1. Gene model colours are as per Fig 6.1.*

While some gene models from the *A. brassicola* putative gene cluster showed over 25% amino acid identity to known toxin genes, these were mostly to genes with high copy number in *A. nidulans.* Additionally, predicted domains in other gene models were mostly unrelated to secondary metabolite biosynthesis, making it unlikely that this area forms part of a biosynthetic cluster.

Table 6.5: *A. brassicola* AB06180.1 gene cluster models

Gene model name	Predicted domains	BLASTP Hits	Notable AA Identities (> 15%)
AB06179.1	von Willebrand factor and related coagulation proteins	-	-
AB06180.1 / PKS	n/a	n/a	-
AB06181.1	Cytochrome P450	-	*aflG* 16% *cypA* 16%
AB06182.1	Cytochrome P450	*stcL*	*stcL* 33% (2) *aflL* 33% *aflG* 31% *stcF* 32% (4) *aflU* 20% *aflV* 20% *stcB* 22% (2) *cypA* 23%
AB06183.1	Short-chain dehydrogenase/reductase SDR	-	*stcU* 16% (2)
AB06184.1	Short-chain dehydrogenase/reductase SDR	-	-
AB06185.1	-	-	-
AB06186.1	O-methyltransferase	-	*aflO* 16%
AB06187.1	-	-	-
AB06188.1	GMC oxidoreductase	*aflK*	*aflK* 28%
AB06189.1	O-methyltransferase	*aflO*	-
AB06190.1	Aminoacyl-tRNA synthetase	-	-
AB06191.1	Aminoacyl-tRNA synthetase	-	-

Gene models in Fig. 6.4, from left to right.

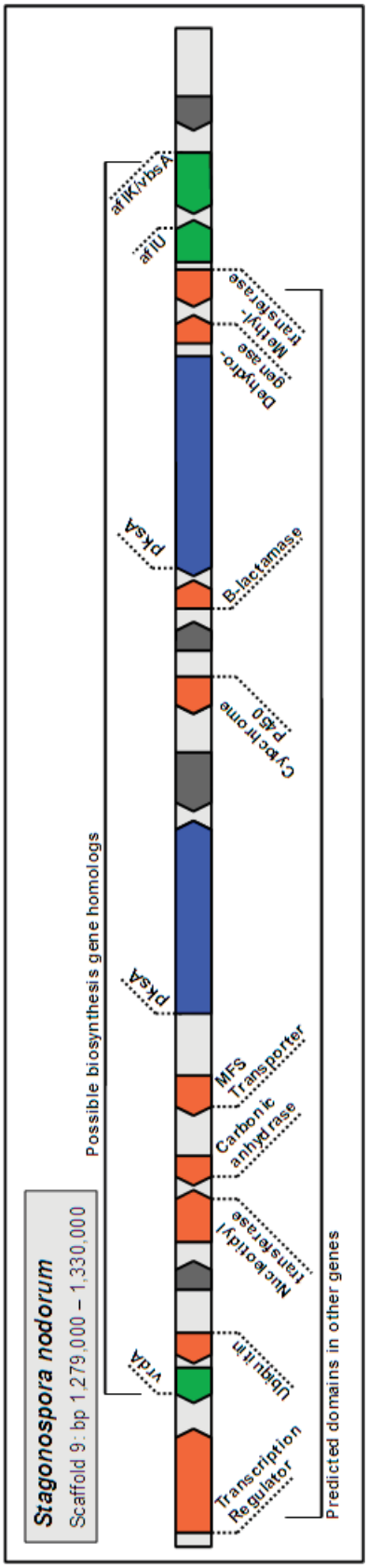

Fig. 6.5: *S. nodorum* JAM_SNOG_06672/ JAM_SNOG_06682 cluster

Scale representation of gene models in the region surrounding S. nodorum *SNOG_06676.2 (left) and SNOG_06682.1 (right). Gene model colours are as per Fig 6.1.*

While the area examined in *S. nodorum* contains a number of gene models with predicted domains similar to those in toxin biosynthetic genes, and showed a number of notable identities, these identities were generally low, or to genes with a high copy number. While this area is likely part of a biosynthetic cluster, any relation to known toxin biosynthesis clusters would be distant.

Table. 6.6: *S. nodorum* JAM_SNOG_06672/ JAM_SNOG_06682 cluster gene models

Gene model name	Predicted domains	BLASTP Hits	Notable AA Identities (> 15%)
SNOG_06665.2	Fungal transcriptional regulatory protein	-	-
SNOG_06666.2	Aldo/Keto reductase	*vrdA*	*aflE* 22% *stcV* 26% (4)
SNOG_06667.2	Ubiquitin	-	-
SNOG_06668.1	-	-	-
SNOG_06669.2	Nucleotidyl transferase	-	-
SNOG_06670.1	Carbonic anhydrase	-	-
SNOG_06672.2	MFS transporter	-	-
JAM_SNOG_06676 / PKS	n/a	n/a	-
SNOG_06678.1	-	-	-
SNOG_06679.2	Cytochrome P450	-	*stcL* 16% (2) *stcB* 16% (2)
SNOG_06680.2	-	-	-
SNOG_06681.1	Beta-lactamase	-	-
JAM_SNOG_06682 / PKS	n/a	n/a	*pksA* 17% *aflC* 16% *stcA* 17% (27)
SNOG_06683.2	Short-chain dehydrogenase/reductase SDR	-	*aflM* 20% *stcU* 19% (2) *aflD* 18% *stcE* 16% (1) *dotA* 18%
SNOG_06684.1	O-methyltransferase	-	*aflO* 25% *aflP* 21%
SNOG_06685.1	Cytochrome P450	*aflS*	*stcL* 21% (2) *aflL* 21% *aflG* 20% *stcF* 20% (4) *aflU* 25% *aflV* 21% *stcB* 22% (2) *cypA* 20%
SNOG_06686.1	GMC oxidoreductase	*aflK*, *vbsA*	*aflK* 33%
SNOG_06687.1	-	-	-

Gene models in Fig. 6.5, from left to right.

While many gene models showed sequence similarity over the threshold value (15%), most were between 15 and 35% over the entire sequence. This is considerably lower than the amino acid identity of known dothistromin biosynthesis genes to aflatoxin and sterigmatocystin genes from *A. parasiticus* and *A. nidulans*, which can be as high as 80% (Bradshaw, unpublished). None of the models examined showed a full complement of toxin biosynthesis genes. This indicates that they are unlikely to synthesize dothistromin unless the biosynthesis genes are distributed more widely, as is seen in *D. septosporum*.

6.2.2 Toxin assay

While none of the putative clusters showed a full complement of dothistromin biosynthetic genes, these genes are not necessarily clustered, and may still be present in the genome. Therefore, a dothistromin assay was performed to determine if *M. graminicola* was a dothistromin producer in broth culture.

M. graminicola was grown as a broth cultures as per methods 2.2.1, which were pooled, then extracted as per methods 2.2.2. The extract was assayed for the presence of dothistromin using the previously developed HPLC method (chapter 4, methods 2.2.6). Dothistromin was not found to be present; however other fluorescing compounds were visible. These compounds were not analysed further.

Fig. 6.6: *M. graminicola* HPLC lacking dothistromin

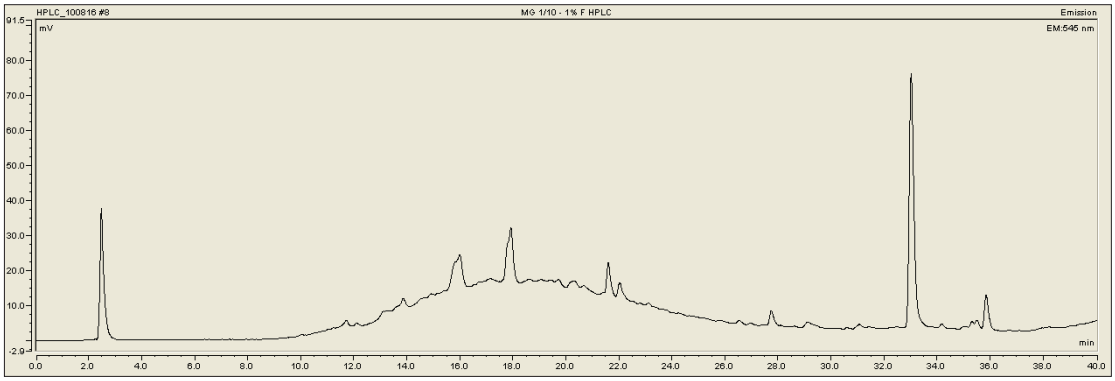

HPLC-fluorescence chromatogram of 1/10 diluted M. graminicola *extract. No dothistromin was detected (absence of a 23.1 minute peak), even at much higher concentrations. Some baseline drift can be seen, this could be due to incomplete evaporation of the ethyl acetate extraction solvent.*

Mass spectroscopy was performed by AgResearch on a sample of *M. graminicola* broth extract as per materials and methods 2.2.7. As per HPLC results, no detectable amounts of dothistromin were found in the sample.

6.3 Discussion

While many matches were found to polyketide biosynthesis genes based on BLAST hits, the low amino acid identity of most hits and lack of other toxin biosynthesis-associated genes clustered alongside indicates that these are not likely to be functional homologs to the dothistromin biosynthesis genes. The genes found in putative clusters do not match up to those found in dothistromin mini-clusters, and are much more likely to be responsible for production of other types of polyketides. None of the potential gene clusters identified show a complete set of the genes required for dothistromin, aflatoxin, or sterigmatocystin biosynthesis. This does not discount the possibility that biosynthesis genes are spread over a wider area, similar to dothistromin genes in *D. septosporum*. While only *M. graminicola* was tested for production of dothistromin, it seems likely that the other organisms investigated are not dothistromin producers either. None of these organisms are known to produce dothistromin, and this work has not turned up any evidence of genes with high sequence identity to those involved in dothistromin biosynthesis.

More difficult to ascertain is the genetic relationship, or lack thereof, between dothistromin biosynthesis genes and those identified bioinformatically. While many score highly as BLAST matches, overall amino acid identity between these genes is mostly low. This may indicate that similarity is more due to conservation of functional domains, as opposed to a close genetic relationship. This could be determined by matching conserved areas with predicted functional protein domains. This will be possible through the JGI browser once the *D. septosporum* sequence is publicly released. The mapping of polyketide enzyme sequences from the selected genomes into one or more phylogenetic trees would offer the best visualisation of any relationships. While fungal genomes contain a large number of polyketide synthase enzymes, the organisation of these by computational phylogenetics (both per organism and between organisms) could show the way in which these genes have evolved. The construction of a tree showing these relationships would be a key step in any extension of this work.

While the putative clusters identified are most likely not responsible for production of dothistromin, they may be responsible for producing chemically related metabolites (e.g. averufin). That the *M. graminicola* broth extract did not show the presence of dothistromin by HPLC-fluorescence and MS is strong evidence that it is not a dothistromin producer. While it is possible that dothistromin is present in quantities too low to detect by these methods, or that dothistromin is produced under different growth conditions to those used, this seems unlikely. Dothistromin was not present even in very concentrated extracts of *M. graminicola*, whereas in contrast *D. septosporum* is a strong producer of dothistromin in broth culture.

The lack of detected dothistromin does not discount the production of related metabolites by *M. graminicola;* both HPLC and MS techniques are relatively specific, and a number of other peaks were seen by HPLC-fluorescence (Fig. 6.6). If the metabolites produced are chemically similar to dothistromin in polarity they should be separated into the extraction solvent, and could be quantified by the current HPLC gradient. However, if they are chemically different it is possible that they would separate differently; very polar metabolites would be eluted immediately after injection and very non-polar metabolites would be retained on the column, rather than eluted during the gradient. This would make quantification and subsequent identification of these metabolites impossible under the current HPLC protocol.

This problem could be avoided by the use of electrospray MS on a crude extract without prior LC separation. Combined with the use of MS databases, this technique can be used to give a relatively rapid indication of the diverse range of secondary metabolites produced by an organism (Smedsgaard 1995). However, it is likely that more chemically similar metabolites would be of greater interest, and therefore an HPLC-fluorescence or HPLC-absorbance method would most likely give acceptable (and more financially justifiable) results. While fluorescence detection was required for quantification of dothistromin produced in infected needles, quantification from broth culture is simplified by the larger quantities available for assay. Large volume extracts from broth can be concentrated to give metabolite levels high enough to allow UV detection. This could allow related metabolites to be tentatively identified by their UV-VIS absorbance spectrum.

In conclusion, while the related organisms examined are unlikely to be toxin producers and contain homologs of dothistromin biosynthesis genes, it is possible that they contain gene orthologs responsible for production of polyketides similar to

dothistromin. Potential polyketide biosynthetic clusters have been found in these organisms, and one cluster from each organism has been shown to contain genes with sequence similarity to toxin biosynthesis genes. While their amino acid identities with toxin biosynthesis genes are mostly too low for them to be considered homologs, they may have similar functions.

Chapter 7: Summary

The aims of this work were to develop the methods required for quantification of *Dothistroma* biomass and dothistromin levels in the lesion, and to use the developed methods to determine their relationship *in planta*. An additional component of the research was the bioinformatic investigation of related organisms for the presence of dothistromin biosynthesis gene homologs.

Development of DNA extraction and dothistromin quantification gave final methods which, used together, allowed extraction and quantification of both DNA and dothistromin from a single lesion. Further development of these methods should focus on optimization of the protocols. This could include development of a surface sterilization technique which can be used with dothistromin, and the time optimization of the HPLC gradient solely for dothistromin quantification.

While first two hypotheses of this research were validated, success in proving or disproving the second two was limited. While the developed methods allowed a correlation to be made between *Dothistroma* biomass and dothistromin *in planta*, this correlation was not statistically significant, most likely due to inadequate sample size. Increasing the number of lesions sampled and carrying out the suggested modifications to the method would allow the hypothesis that dothistromin levels relative to *D. septosporum* biomass are highest in early stage lesions to be conclusively proven or disproven. This would in turn allow conclusions to be made on the hypothesis that dothistromin acts as a competition factor.

It was hoped that investigation into related dothideomycete fungi would give insight into the role of dothistromin. While some potential gene homologs were found, no definite conclusions could be drawn on their relationship based on the results. Construction of a phylogenetic tree of PKS genes in these species and toxin producer species may give a better picture of dothistromin biosynthesis evolution.

In conclusion, while no firm conclusions on dothistromins role *in planta* can be drawn based on the results given, this work sets a firm basis for future study.

Chapter 8: Appendix

8.1 Gel electrophoresis

TBE Buffer

10.8 g/L Tris (Carl Roth GmbH, Karlsruher, Germany), 0.93 g/L EDTA (Sigma-Aldrich Chemie GmbH), and 5.5 g/L boric acid (BDH), adjusted to pH 8.2 with HCl (BDH)

Bromophenol blue loading dye

20% w/v sucrose (BDH), 1% w/v SDS (BDH), 0.2% xylene cyanol (BDH), 5 mM EDTA (Sigma-Aldrich Chemie GmbH), and 0.2% w/v bromophenol blue (J.T. Baker Chemical Co., Phillipsburg, New Jersey, USA)

8.2 ELISA Buffers

PBS (10×)

8% NaCl (Pure Science Ltd., Wellington, New Zealand), 2.9% Na_2HPO_4 (BDH, Poole, England), 0.2% KH_2PO_4 (BDH), adjusted to pH 7.4 with HCl (BDH)

PBST

1× PBS with 0.1% Tween 20 (Sigma-Aldrich Chemie GmbH, Steinheim, Germany)

Blocking solution

1% skim milk powder, 1× PBS, and 0.01% thiomersal (BDH)

Dilution buffer

8 mL 10× PBS, 32 mL MilliQ, 0.8g skim milk powder, and 80 µL Tween 20 (Sigma-Aldrich Chemie GmbH).

Substrate

50 mL 0.2 M Na_2HPO_4 (BDH), 1 tablet (20 mg) o-phenylene diamine (Sigma-Aldrich Chemie GmbH), 0.25 g citric acid (BDH), and 20 µL of 30% H_2O_2.

8.3 List of compared genes

Full length amino acid identity of genes in potential clusters to known toxin biosynthesis genes containing similar domains.

Table 8.1: ***Alternaria brassicola*** **gene comparisons**

Gene model	Compared genes	Gene model	Compared genes
AB06179.1	-	AB06186.1	*aflO* 16% *aflP* 14%
AB06180.1	*pksA* 9% *aflC* 10% *stcA* 10%	AB06187.1	-
AB06181.1	*aflG* 16% *stcF* 15% *aflU* 15% *aflV* 14% *stcB* 15% *cypA* 16%	AB06188.1	*aflK* 28% *aflQ* 12%
AB06182.1	*stcL* 33% *aflL* 33% *aflG* 31% *stcF* 32% *aflU* 20% *aflV* 20% *stcB* 22% *cypA* 23%	AB06189.1	*aflO* 11% *aflP* 10%
AB06183.1	*aflE* 13% *stcV* 11% *aflF* 9% *aflH* 13% *aflM* 15% *stcU* 16% *aflD* 10% *stcE* 14% *dotA* 15%	AB06190.1	-
AB06184.1	*aflE* 11% *stcV* 8% *aflF* 11% *aflH* 13% *aflM* 14% *stcU* 13% *aflD* 11% *stcE* 10%	AB06191.1	-
AB06185.1	-		

Table 8.2: *Cochliobolus heterostrophus* gene comparisons

Gene model	Compared genes	Gene model	Compared genes
estExt_fgenesh1_pg.C_30018	-	estExt_fgenesh1_kg.C_30006	*dotA* 60% *aflM* 64% *stcU* 63% *aflN* 11% *stcS* 10%
fgenesh1_pg.C_scaffold_3000019	-	e_gw1.3.1026.1	*dotC* 6% *aflT* 6%
estExt_Genewise1Plus.C_30034	*aflF* 11% *aflH* 11% *aflM* 9% *stcU* 9% *aflE* 11% *stcV* 10% *aflD* 12% *stcE* 12% *dotA* 10%	fgenesh1_pg.C_scaffold_3000029	-
estExt_Genewise1.C_30036	*aflC* 28% *stcA* 25% *pksA* 26%	estExt_fgenesh1_kg.C_30008	*aflS* 31%
estExt_Genewise1.C_30037	-	estExt_fgenesh1_pg.C_30030	*aflG* 13% *stcF* 13% *cypA* 10% *aflN* 13% *stcS* 13% *aflQ* 13% *aflU* 11% *aflV* 9%
estExt_fgenesh1_pg.C_30023	-	fgenesh1_pg.C_scaffold_3000032	-
estExt_Genewise1Plus.C_30042	-	fgenesh1_pg.C_scaffold_3000033	*aflR* 11% *aflS* 9%
estExt_fgenesh1_pg.C_30025	*aflX* 36% *stcQ* 35% *avfA* 21% *aflI* 21% *stcO* 19%	estExt_Genewise1.C_30059	*aflR* 13% *aflS* 10%

Table 8.3: *Mycosphaerella fijiensis* gene comparisons

Gene model	Compared genes	Gene model	Compared genes
fgenesh1_pm.8_#_54	-	Mycfi1.e_gw1.7.973.1	*stcA* 25% *aflC* 28% *pksA* 24%
estExt_fgenesh1_kg.C_80028	-	fgenesh1_pm.8_#_61	*aflE* 12% *stcV* 14% *aflF* 13% *aflH* 11% *aflM* 13% *stcU* 12% *aflD* 13% *stcE* 12% *dotA* 11%
e_gw1.8.525.1	-	Mycfi1.e_gw1.7.445.1	-
Mycfi1.gw1.7.459.1	-	Mycfi1.e_gw1.7.551.1	-
e_gw1.8.1861.1	-	fgenesh1_pm.8_#_63	*aflT 41%* *dotC* 26%
Mycfi1.e_gw1.7.46.1	-	estExt_fgenesh1_pm.C_80063	*stcL* 15% *aflL* 15% *aflG* 14% *stcF* 12% *aflU* 13% *aflV* 11% *stcB* 11% *cypA* 12%
fgenesh1_pm.8_#_59	*aflS 33%* *aflR* 12%	estExt_fgenesh1_kg.C_80032	-
Genemark.8735_g	-	estExt_Genewise1Plus.C_80170	-
Genemark.8734_g	-	Mycfi1.gw1.7.397.1	*aflE* 8% *stcV* 10% *aflF* 10% *aflH* 19% *aflM* 20% *stcU* 21% *aflD* 20% *stcE* 14% *dotA* 20%
fgenesh1_pg.8_#_73	*aflR 27%* *aflS* 10%	Mycfi1.estExt_fgenesh1_pg.C_70406	*aflD* 10% *stcE* 11% *aflE* 23% *stcV* 25% *aflM* 13% *stcU* 11% *dotA* 13%
Genemark.8738_g Genemark.8737_g	-	estExt_Genewise1.C_80178	-

Table 8.4: *Mycosphaerella graminicola* gene comparisons

Gene model	Compared genes	Gene model	Compared genes
fgenesh1_pg.C_chr_7000654	-	e_gw1.7.2.1	*pksA* 11% *StcA* 10% *AflC* 11%
gw1.7.1046.1	*aflR* 3% *aflS* 3%	e_gw1.7.248.1	*aflG* 13% *stcF* 13% *cypA* 12% *aflN* 12% *stcS* 10% *aflQ* 12% *aflU* 11% *aflV* 11%
fgenesh1_pg.C_chr_7000656	-	e_gw1.7.311.1	*aflH 17%* *aflE* 9% *stcV* 13% *aflF* 12% *aflM* 21% *stcU* 21% *aflD* 12% *stcE* 16% *dotA* 21%
estExt_fgenesh1_pg.C_chr_70650	-	e_gw1.7.886.1	*epoA* 12% *aflJ* 13% *stcI* 13%
estExt_fgenesh1_pg.C_chr_70651	-	estExt_fgenesh1_pm.C_chr_70300	dotC 8% aflT 7%
estExt_fgenesh1_pm.C_chr_70294	*vbsA 35%* *aflK* 34% *aflQ* 10%	e_gw1.7.194.1	*aflU 28%* *stcL* 21% *aflL* 22% *aflG* 21% *stcF* 22% *aflV* 19% *stcB* 18% *cypA* 18%
gw1.7.361.1	-	e_gw1.7.870.1	*aflH 25%* *aflE* 13% *stcV* 12% *aflF* 12% *aflM* 15% *stcU* 14% *aflD* 12% *stcE* 12% *dotA* 15%
e_gw1.7.675.1	*dotC* 13% *aflT* 11%	e_gw1.7.928.1	*epoA* 11% *aflJ* 15% *stcI* 10%

Table 8.5: *Stagonospora nodorum* gene comparisons

Gene model	Compared genes	Gene model	Compared genes
SNOG_06665.2	*aflR* 8% *aflS* 9%	SNOG_06679.2	*stcL* 16% *aflL* 14% *aflG* 13% *stcF* 13% *aflU* 14% *aflV* 12% *stcB* 16% *cypA* 13%
SNOG_06666.2	*aflD* 12% *stcE* 11% *aflE* 22% *stcV* 26% *aflM* 11% *stcU* 11% *dotA* 11%	SNOG_06680.2	-
SNOG_06667.2	-	SNOG_06681.1	-
SNOG_06668.1	-	JAM_SNOG_06682	*pksA* 17% *aflC* 16% *stcA* 17%
SNOG_06669.2	-	SNOG_06683.2	*aflE* 10% *stcV* 12% *aflF* 10% *aflH* 15% *aflM* 20% *stcU* 19% *aflD* 18% *stcE* 16% *dotA* 18%
SNOG_06670.1	-	SNOG_06684.1	*aflO* 25% *aflP* 21%
SNOG_06672.2	*dotC* 11% *aflT* 12%	SNOG_06685.1	stcL 21% *aflL* 21% *aflG* 20% *stcF* 20% *aflU* 25% *aflV* 21% *stcB* 22% *cypA* 20%
JAM_SNOG_06676	*pksA* 10% *aflC* 10% *stcA* 10%	SNOG_06686.1	*aflK* 33% *aflQ* 12%
SNOG_06678.1	-	SNOG_06687.1	-

8.4 Alternative Buffers Tested

Lysis buffer A

2.5% w/v EDTA (Sigma), 2.5% w/v SDS (BDH).

Precipitation buffer A

12.5% v/v acetic acid (Merck), adjusted to pH 5.5 with NaOH.

Lysis buffer B

2.5% w/v EDTA (Sigma), 2.5% w/v SDS (BDH), 50 mM Tris (Carl Roth GmbH), adjusted to pH 7.0 with NaOH.

Precipitation buffer B

5M NaCl (Pure Science Ltd.)

Lysis buffer C (Doyle and Doyle 1990)

2% w/v CTAB, 1% w/v PVP40 (Sigma), 1.4 M NaCl (Pure Science Ltd.), 20 mM EDTA, 0.1 M Tris-HCl (Carl Roth GmbH; BDH), adjusted to pH 8.0.

Lysis buffer D (Al-Samarrai and Schmid 2000)

40 mM Tris (Carl Roth GmbH), 20 mM sodium acetate (Ajax Finechem, Auckland, New Zealand), 1 mM EDTA (Sigma), 1% w/v SDS, adjusted to pH 7.8.

Lysis buffer E

2% w/v CTAB, 1% w/v PVP40 (Sigma), 20 mM EDTA (Sigma), 0.1 M Tris-HCl (Carl Roth GmbH; BDH), adjusted to pH 8.0.

Lysis buffer F

2.5% w/v SDS (BDH), 2% w/v PVP40 (Sigma), 20 mM EDTA (Sigma), 20 mM sodium acetate (Ajax Finechem), 110 mM acetic acid (Merck), 100 mM 2-mercaptoethanol (Riedel-de Haen AG, Buchs, Switzerland), adjusted to pH 5.5.

Lysis buffer G

2.5% w/v SDS (BDH), 2% w/v PVP40 (Sigma), 20 mM EDTA (Sigma), 5 M sodium acetate (Ajax Finechem), 5 M acetic acid (Merck), 100 mM 2-mercaptoethanol (Riedel-de Haen AG), adjusted to pH 5.5.

8.5 TLC Background

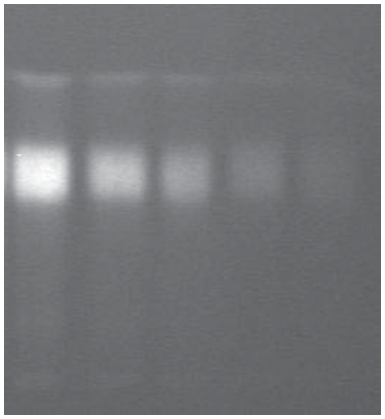

Fig. 8.1: Chloroform:methanol TLC background

A 2× dilution series of a dothistromin standard from 50 μL to 3.125 μL on a preparative TLC plate, separated using a 50:3 chloroform:methanol mobile phase. The diffuse peak is of much lower intensity relative to other components than that seen with a 1:1 ethyl acetate:dichloromethane mobile phase (see Fig. 4.3), making it difficult to distinguish from background noise.

8.6 Caffeic acid HPLC

Fig. 8.2: Caffeic acid HPLC chromatogram

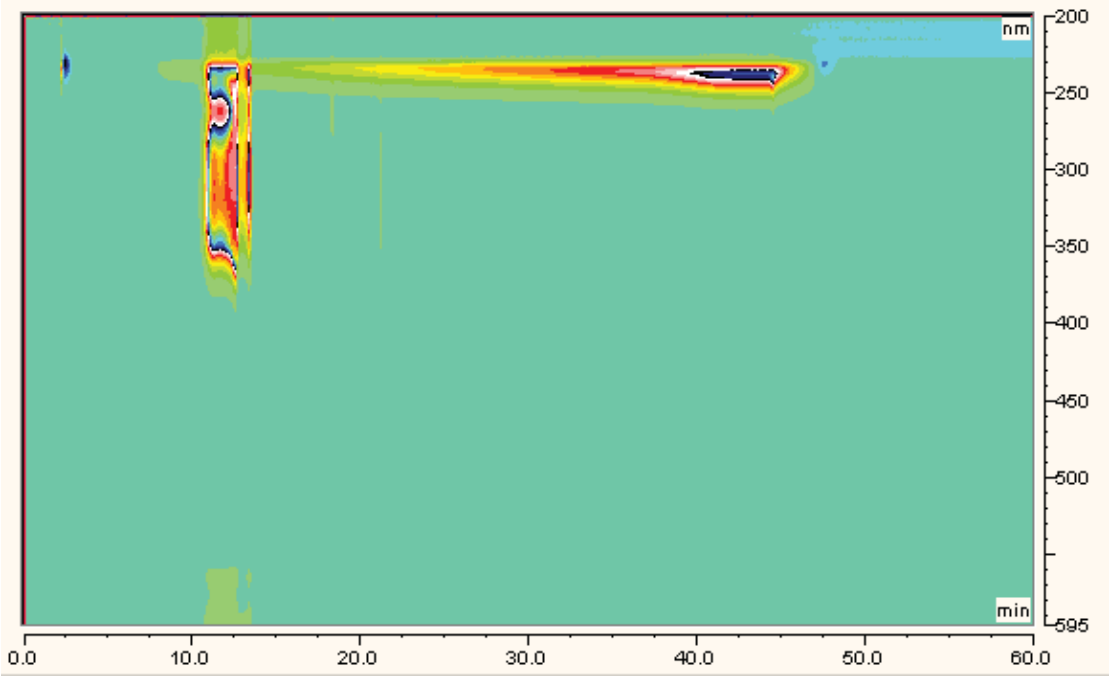

UV-VIS spectrum of caffeic acid run through the HPLC protocol. A heavily fronted caffeic acid peak can be seen after 10 minutes. Analysis of the absorbance spectrum change across the front indicates that fronting may be due to ionisation (Cornard, Caudron et al. 2006; Cornard and Lapouge 2006).

8.7 Lesion component variation

Fig. 8.3: Variation in HPLC fluorescence peaks

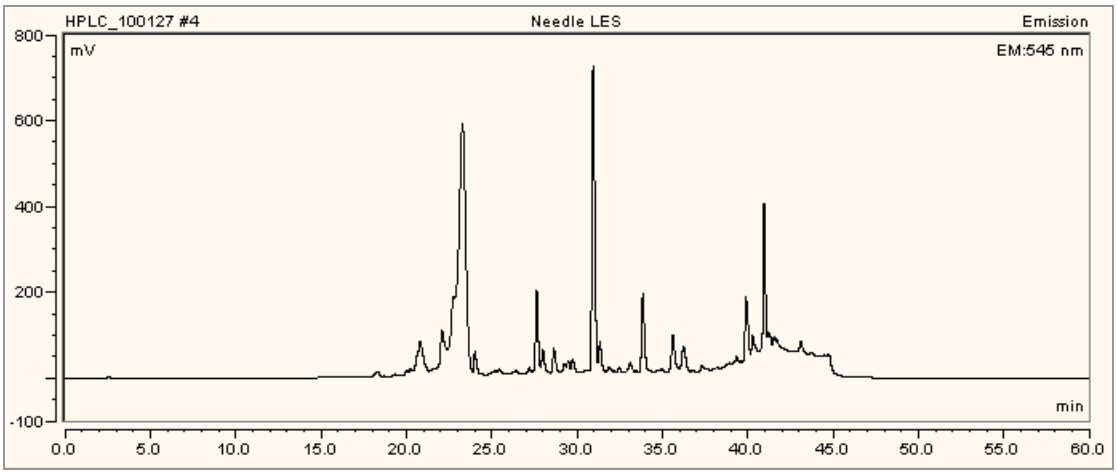

Fluorescence chromatogram of pooled infected needle samples.

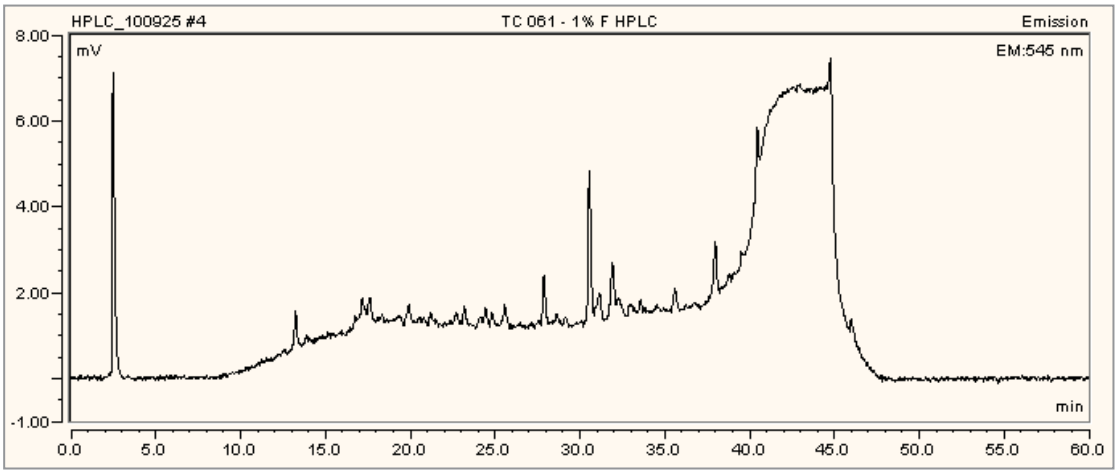

Time course sample 61, showing a different set of fluorescence peaks.

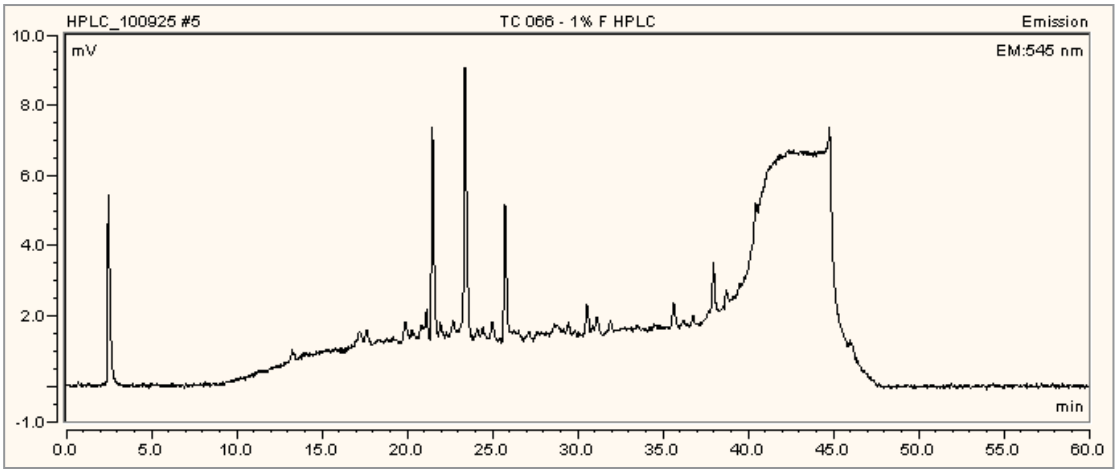

Time course sample 66, showing a different set of fluorescence peaks to both pooled lesions and sample 61.

8.8 Sample group distribution

Fig. 8.4: DNA vs. dothistromin, by sample group

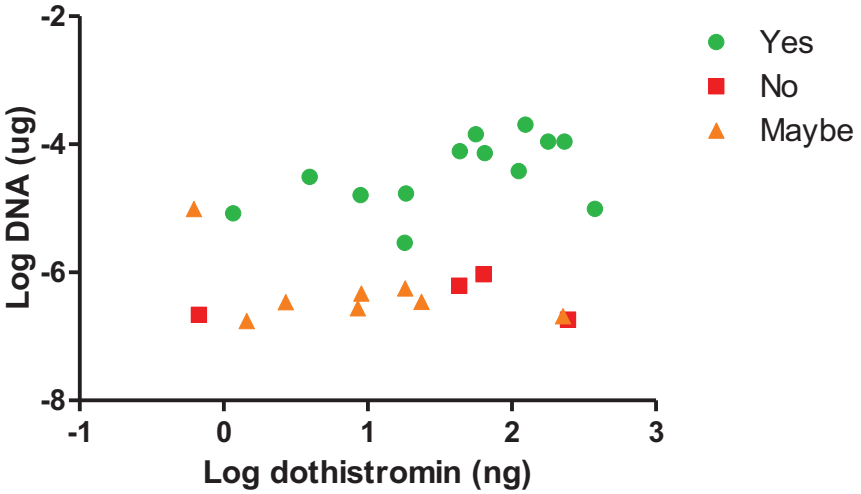

DNA vs. dothistromin classified by sample group, as per 5.2.1. Yes: probably caused by D. Septosporum. *No: probably not caused by* D. Septosporum. *Maybe: uncertain.*

Chapter 9: Bibliography

Al-Samarrai, T. H., & Schmid, J. (2000). *A simple method for extraction of fungal genomic DNA*. Letters in Applied Microbiology, 30, 53-56.

Barnes, I., Crous, P. W., Wingfield, B. D., & Wingfield, M. J. (2004). *Multigene phylogenies reveal that red band needle blight of* Pinus *is caused by two distinct species of* Dothistroma, D. septosporum *and* D. pini. Studies in Mycology, 50, 551-565.

Barnes, I., Kirisits, T., Akulov, A., Chhetri, D.B., Wingfield, B. D., Bulgakov, T. S., & Wingfield, M. J. (2008). *New host and country records of the* Dothistroma *needle blight pathogens from Europe and Asia*. Forest Pathology, 38(3), 178-195.

Barron, N. J. (2006). *Optimizing* Dothistroma septosporum *infection of* Pinus radiata *and the development of red-band disease* (Master's thesis). Palmerston North, New Zealand: Massey University.

Bassett, C., Buchanan, M., Gallagher, R. T., & Hodges, R. (1970). *Toxic difuroanthraquinone from* Dothistroma pini. Chemistry & Industry, 52, 1659-1660.

Bearchell, S. J., Fraaije, B. A., Shaw, M. W., & Fitt, B. D. L. (2005). *Wheat archive links long-term fungal pathogen population dynamics to air pollution*. Proceedings of the National Academy of Sciences of the United States of America, **102**(15), 5438-5442.

Bradshaw, R. E., Bhatnagar, D., Ganley, R. J., Gillman, C. J., Monahan, B. J., & Sconi, J. M. (2002). Dothistroma pini, *a forest pathogen, contains homologs of aflatoxin biosynthetic pathway genes*. Applied and Environmental Microbiology, **68**(6), 2885-2892.

Bradshaw, R. E., Foster, S. J., & Monahan, B. J. (2006). Molecular Diagnostic Tools for Detection of Plant Pathogenic Fungi. In Rao, J. R., Fleming, C. C., & Moore, J. E. (Eds.), *Molecular diagnostics: current technology and applications* (47-70). Norwich, United Kingdom: Horizon Scientific Press.

Bradshaw, R. E., Ganley, R. J., Jones, W. T., & Dyer, P. S. (2000). *High levels of dothistromin toxin produced by the forest pathogen* Dothistroma pini. Mycological Research, 104, 325-332.

Bradshaw, R. E., Jin, H. P., Morgan, B. S., Scwelm, A., Teddy, O. R., Young, C. A., & Zhang, S. G. (2006). *A polyketide synthase gene required for biosynthesis of the aflatoxin-like toxin, dothistromin*. Mycopathologia, 161(5), 283-294.

Briggs, J. K. (1985). *The exposure of forestry workers to the toxic fungal metabolite*

dothistromin. Report W/3/85. Wellington, NZ: Occupational Health and Toxicology Branch, Department of Health.

Bulman, L., Ganley, R., & Dick, M. (2008). *Needle diseases of radiata pine in New Zealand: A review* (Report 13010). Rotorua, New Zealand: Scion.

Carbone, I., Ramirez-Prado, J. H., Jakobek, J. L., & Horn, B. W. (2007). *Gene duplication, modularity and adaptation in the evolution of the aflatoxin gene cluster*. BMC Evolutionary Biology, 7, 111.

Chiavaro, E., Dall'Asta, C., Galaverna, G., Biancardi, A., Gambarelli, E., Dossena, A., & Marchelli, R. (2001). *New reversed-phase liquid chromatographic method to detect aflatoxins in food and feed with cyclodextrins as fluorescence enhancers added to the eluent.* Journal of Chromatography A, 937(1-2), 31-40.

Cornard, J. P., Caudron, A., & Merlin, J. C. (2006). *UV-visible and synchronous fluorescence spectroscopic investigations of the complexation of Al(III) with caffeic acid, in aqueous low acidic medium*. Polyhedron, 25(11), 2215-2222.

Cornard, J. P., & Lapouge, C. (2006). *Absorption spectra of caffeic acid, caffeate and their 1 : 1 complex with Al(III): Density functional theory and time-dependent density functional theory investigations*. Journal of Physical Chemistry A, 110(22), 7159-7166.

Debnam, P. M., & Quach, H. L. *Separation and identification of dothistromin and other anthraquinones from* Dothistroma pini *culture filtrates* (Internal report). Rotorua, New Zealand: Forest Research Institute.

Doyle, J. J., & Doyle, J. L. (1990). *Isolation of plant DNA from fresh tissue*. Focus, 12, 13-15.

Dunn, J. J., Lee, L. S., & Ciegler, A. (1982). *Mutagenicity and toxicity of aflatoxin precursors.* Environmental Mutagenesis, 4(1), 19-26.

Ehrlich, K. C., Yu, J., & Cotty, P. J. (2005). *Aflatoxin biosynthesis gene clusters and flanking regions*. Journal of Applied Microbiology, 99(3), 518-527.

Ferguson, L. R., Parslow, M. I., & McLarin, J. A. (1986). *Chromosome-damage by dothistromin in human peripheral-blood lymphocyte cultures - A comparison with aflatoxin B-1*. Mutation Research, 170(1-2), 47-53.

Franich, R. A. (1981). *Determination of dothistromin by quantitative reversed-phase thin-layer chromatography*. Journal of Chromatography, 209(1), 117-120.

Franich, R. A., Carson,M. J., & Carson, S. D. (1986). *Synthesis and accumulation of benzoic-acid in* Pinus radiata *needles in response to tissue-injury by dothistromin, and correlation with resistance of* Pinus radiata *families to* Dothistroma pini.

Physiological and Molecular Plant Pathology, 28(2), 267-286.

Frisvad, J., & Thrane, U. (1987). *Standardized high-performance liquid chromatography of 182 mycotoxins and other fungal metabolites based on alkylphenone retention indices and UV-VIS spectra(diode array detection).* Journal of Chromatography, 404(1), 195-214.

Gallagher, R. T. (1971). *The Structure Of Dothistromin* (Doctoral dissertation). Palmerston North, New Zealand: Massey University.

Ganley, R. J., & Newcombe, G. (2006). *Fungal endophytes in seeds and needles of* Pinus monticola. Mycological Research, 110, 318-327.

Gibson, I. A. S. (1972). Dothistroma *blight of* Pinus radiata. Annual Review of Phytopathology, 10, 51-72.

Heiser, I., Osswald, W., & Elstner, E. F. (1998). *The formation of reactive oxygen species by fungal and bacterial phytotoxins*. Plant Physiology and Biochemistry, 36(10), 703-713.

Hesseltine, C. W., Shotwell,O. L, Ellis, J. J., & Stubblef, R. D. (1966). *Aflatoxin Formation by* Aspergillus flavus. American Society for Microbiology, 30(4), 795-805.

Ioos, R., Fabre, B., Saurat, C., Rourrier, C., Frey, P., & Marcais, B. (2010). *Development, Comparison, and Validation of Real-Time and Conventional PCR Tools for the Detection of the Fungal Pathogens Causing Brown Spot and Red Band Needle Blights of Pine*. Phytopathology, 100(1), 105-114.

Jones, W., Harvey, D., Jones, S. D., Fielder, S., Debnam, P., & Reynolds, P. H. S. (1993). *Competitive ELISA employing monoclonal antibodies specific for dothistromin*. Food and Agricultural Immunology, 5(4), 187-197.

Jones, W. T., Harvey, D., Jones, S. D., Sutherland, P. W., Nicol, M. J., Sergejew, N., Debnam, P. M., Cranshaw, N., & Reynolds, O. H. S. (1995). *Interaction between the phytotoxin dothistromin and Pinus radiata embryos*. Phytopathology, 85(10), 1099-1104.

Keller, N. P., & Hohn, T. M. (1997). *Metabolic pathway gene clusters in filamentous fungi*. Fungal Genetics and Biology, 21(1), 17-29.

Keon, J., Antoniw, J., Carzaniga, R., Deller, S., Ward, J. L., Baker, J. M., Beale, M. H., Hammond-Kosack. K., & Rudd, J. J. (2007). *Transcriptional adaptation of* Mycosphaerella graminicola *to programmed cell death (PCD) of its susceptible wheat host*. Molecular Plant-Microbe Interactions, 20(2), 178-193.

Park, K. Y., & Bullerman, L. B. (1981). *Increased Aflatoxin Production by* Aspergillus parasiticus *under Conditions of Cycling Temperatures*. Journal of Food Science, 46, 1147-1151.

Petit, J., Boisseau, P., & Arvelier, B. (1994). *Glucanex - A cost effective yeast lytic enzyme.*

Trends in Genetics, 10(1), 4-5.

Reverberi, M., Ricelli, A., Zjalic, S., Fabbri, A. A., & Fanelli, C. (2010). *Natural functions of mycotoxins and control of their biosynthesis in fungi*. Applied Microbiology and Biotechnology, 87(3), 899-911.

Schuster, R., Marx, G., & Rothaupt, M. (1992). *Analysis of Mycotoxins by HPLC with Automated Confirmation by Spectral Library* (Application Note 12-5091-8692). Santa Clara, CA: Aglient Technologies. Retrieved from http://www.chem.agilent.com/Library/applications/50918692_000327.pdf

Schwelm, A., N. J. Barron, Baker, J., Dick, M., Long, P. G., Zhang, S., & Bradshaw, R. E. (2009). *Dothistromin toxin is not required for* dothistroma *needle blight in* Pinus radiata. Plant Pathology, 58(2), 293-304.

Schwelm, A., N. J. Barron, Zhang, S., & Bradshaw, R. E. (2008). *Early expression of aflatoxin-like dothistromin genes in the forest pathogen* Dothistroma septosporum. Mycological Research, 112, 138-146.

Senyuva, H., & Gilbert, J. (2010). *Rapid Analysis of Crude Fungal Extracts for Secondary Metabolites by LC/TOF-MS–A New Approach to Fungal Characterization* (Application note 5980-6820EN). Santa Clara, CA: Agilent Technologies. Retrieved from https://www.chem.agilent.com/Library/applications/5989-6820EN.pdf

Shain, L., & Franich, R. A. (1981). *Induction of* Dothistroma *blight symptoms with dothistromin*. Physiological Plant Pathology, 19(1), 49.

Shaw, G. J., Chick, M., & Hodges, R. (1978). *C-13 NMR-study of biosynthesis of anthraquinone dothistromin by* Dothistroma pini. Phytochemistry, 17(10), 1743-1745.

Stoessl, A. (1984). *Dothistromin as a metabolite of* Cercospora arachidicola. Mycopathologia, 86(3), 165-168.

Stoessl, A., Abramowski, Z., Lester, H. H., Rock, G. L., & Towers, G. H. N. (1990). *Further toxic properties of the fungal metabolite dothistromin*. Mycopathologia, 112(3), 179-186.

Takino, M., & Tanaka, T. (2008). *Determination of Aflatoxins in Food by LC/MS/MS* (Application note 5989-7615EN). Santa Clara, CA: Agilent Technologies. Retrieved from http://www.chem.agilent.com/Library/applications/5989-7615EN.pdf

Tsumura, Y., & Ohba, K. (1993). *Genetic-structure of geographical marginal populations of* Cryptomeria japonica. Canadian Journal of Forest Research, 23(5), 859-863.

Watt, M. S., Kriticos, D. J., Alcaraz, S., Brown, A. V., & Leriche, A. (2009). *The hosts and potential geographic range of* Dothistroma *needle blight*. Forest Ecology and

Management, 257(6), 1505-1519.

Weissman, K. J. (2008). *Anatomy of a fungal polyketide synthase*. Science, 320(5873), 186-187.

West, P. J. (2004). *Development of a pathogenicity testing system for* Dothistroma pini *infection of* Pinus radiata (Master's thesis). Palmerston North, New Zealand: Massey University.

Woods, A., Coates, K. D., & Hamann, A. (2005). *Is an unprecedented* dothistroma *needle blight epidemic related to climate change*? Bioscience, 55(9), 761-769.

Youngman, R. J. & Elstner, E. F. (1984). Photodynamic and reductive mechanisms of oxygen activation by the fungal phytotoxins, cercosporin and dothistromin. In Bors, W., & Saran, M. (Eds.), *Oxygen radicals in chemistry and biology* (501-508). Berlin, New York: W. de Gruyter.

Yu, J. J., Chang, P. K., Erlich, K. C., Cary, J. W., Bhatnagar, D., Cleveland, T. E., Payne, G. A., & Linz, J. E., Woloshuk, C. P., Bennett, J. W. (2004). *Clustered pathway genes in aflatoxin biosynthesis*. Applied and Environmental Microbiology, 70(3), 1253-1262.

Zhang, S. G., Schwelm, A., Jin, H. P., Collins, L. J., & Bradhsaw, R. E. (2007). *A fragmented aflatoxin-like gene cluster in the forest pathogen* Dothistroma septosporum. Fungal Genetics and Biology, 44(12), 1342-1354.